GEOLOGICA ULTRAIECTINA

Mededelingen van de
Faculteit Aardwetenschappen der
Rijksuniversiteit te Utrecht

No.69

HYDROTHERMAL ELEMENT DISTRIBUTIONS AT HIGH TEMPERATURES

AN EXPERIMENTAL STUDY ON THE PARTITIONING OF MAJOR AND TRACE ELEMENTS BETWEEN PHLOGOPITE, HAPLOGRANITIC MELT AND VAPOUR

ARIEJAN BOS

GEOLOGICA ULTRAIECTINA

Mededelingen van de
Faculteit Aardwetenschappen der
Rijksuniversiteit te Utrecht

No.69

HYDROTHERMAL ELEMENT DISTRIBUTIONS AT HIGH TEMPERATURES

AN EXPERIMENTAL STUDY ON THE PARTITIONING OF MAJOR AND TRACE ELEMENTS BETWEEN PHLOGOPITE, HAPLOGRANITIC MELT AND VAPOUR

CIP-DATA KONINKLIJKE BIBLIOTHEEK, DEN HAAG

Bos, Ariejan

Hydrothermal element distributions at high temperatures : an experimental study on the partitioning of major and trace elements between phlogopite, haplogranitic melt and vapour / Ariejan Bos. - [Utrecht: Instituut voor Aardwetenschappen der Rijksuniversiteit Utrecht]. - (Geologica Ultraiectina, ISSN 0072-1026 ; no. 69)
Thesis Utrecht. - With ref. - With summary in Dutch.
ISBN 90-71577-22-8
SISO 562 UDC 550.42(043.3)
Subject headings: element distributions ; experimental petrology

HYDROTHERMAL ELEMENT DISTRIBUTIONS AT HIGH TEMPERATURES

AN EXPERIMENTAL STUDY ON THE PARTITIONING OF MAJOR AND TRACE ELEMENTS BETWEEN PHLOGOPITE, HAPLOGRANITIC MELT AND VAPOUR

HYDROTHERMALE ELEMENTVERDELINGEN BIJ HOGE TEMPERATUREN

EEN EXPERIMENTELE STUDIE NAAR DE VERDELING VAN HOOFD- EN SPORE-ELEMENTEN TUSSEN PHLOGOPIET, HAPLOGRANITISCHE SMELT EN DAMP

(MET EEN SAMENVATTING IN HET NEDERLANDS)

PROEFSCHRIFT TER VERKRIJGING VAN DE GRAAD VAN DOCTOR
AAN DE RIJKSUNIVERSITEIT TE UTRECHT
OP GEZAG VAN DE RECTOR MAGNIFICUS, PROF. DR. J. A. VAN GINKEL,
INGEVOLGE HET BESLUIT VAN HET COLLEGE VAN DEKANEN
IN HET OPENBAAR TE VERDEDIGEN OP WOENSDAG
24 OKTOBER 1990 DES NAMIDDAGS OM 12.45 UUR

DOOR

ARIEJAN BOS

GEBOREN OP 2 JULI 1953, TE NIJMEGEN

PROMOTOR: PROF. DR. R. D. SCHUILING
CO-PROMOTOR: DR. J. B. H. JANSEN

aan mijn ouders
aan Hans, Dienke en Maartje
ter nagedachtenis aan Willem

Voorwoord

Het doet mij plezier, dat ik eindelijk de gelegenheid heb al diegenen te bedanken, die de afgelopen jaren op een of andere wijze hebben bijgedragen aan de voltooiing van dit proefschrift. Mijn oprechte dank gaat dan ook uit naar allen, die ik hieronder noem, maar ook naar allen, die ik hierbij heb vergeten.

Paul Anten, Frits Geelen, Geert Jan de Haas, Sjoerd Koster, Charles Laman, Jan Meesterburry, René Poorter, Nellie Slaats en alle medewerkers van Servicelab, Slijpkamer en Bibliotheek.

De medewerkers van HPT-lab en -werkplaats: Dirk Steenbeek, Eimert de Graaf, en vooral Ad van der Eerden en Gert Kastelein. Jullie bijdrage aan dit proefschrift is van onschatbare waarde geweest.

Mijn kamergenoten en collegae, die mij kortere of langere tijd van het werk hebben proberen te houden: Luc Bol, Ton de Nijs en Jack Voncken.

De petrologiestaf, Gé Hermans, Cees Maijer, Toni Senior, Alex Tobi, Rob Verschure en alle petrologiestudenten.

Mijn werkgever, het ECN te Petten, voor de faciliteiten, die zij voor de voltooiing van het proefschrift gegeven hebben.

Mijn promotor, Prof. R. D. Schuiling, voor de wijze waarop hij me de laatste klippen heeft helpen omzeilen.

Ben Jansen, die mij tijdens de jaren in Utrecht al op zijn gebruikelijke ongebruikelijke manier stimuleerde, maar er ook in de Enschedese jaren weer de vaart in bracht.

Het proefschrift draag ik in de eerste plaats op aan mijn ouders, die mij altijd onvoorwaardelijk gesteund hebben. Voorts natuurlijk aan Hans, die mij de moeilijke laatste jaren op gang heeft gehouden, en mijn kinderen Dienke en Maartje, voor wie ik hoop, dat ze er niet al te zeer onder geleden hebben. En tenslotte aan Willem, te kort mijn kamergenoot, wiens invloed op mijn onderzoek ik graag groter had gehad.

Table of contents

Samenvatting

In dit proefschrift wordt de experimentele verdeling van ertsvormende metaalelementen onderzocht tussen een graniet of in een graniet voorkomende mineralen, en een waterige oplossing, als bijdrage tot de oplossing van het probleem van ertsvorming. Deze verdelingsevenwichten worden bestudeerd bij drukken van 2000 to 5000 bar, overeenkomend met een gesteentediepte van ongeveer 6 tot 15 kilometer, en temperaturen van 550 to 850°C, onder welke kondities een graniet gewoonlijk in (deels) gesmolten toestand verkeert.

Binnen het proefschrift kan een onderscheid worden gemaakt tussen de Hoofdstukken 2 tot 5, waarin elementverdelingen worden bestudeerd tussen het mineraal phlogopiet en een chloride-houdende waterige oplossing, en de hoofdstukken 6 tot 8, waarin de elementverdelingen worden onderzocht tussen een silikaatsmelt van granitische samenstelling en een chloride- danwel fluoridehoudende waterige oplossing. Phlogopite, het magnesium-eindlid van het mineraal biotiet, werd gebruikt, omdat het een belangrijk mineraal is in de faserelaties van een smeltende of, omgekeerd, een kristallizerende graniet. Zijn kristalstruktuur biedt relatief veel plaats aan spore-elementen met verschillende valenties. Bovendien is zijn stabiliteit in oxiderend milieu aanzienlijk hoger dan van het ijzer-eindlid anniet.

Het proefschrift richt zich op dit stadium van het ertsvormende proces, waarbij het ertsvormende element wordt vrijgemaakt uit de granitische smelt of het mineraal, en in de hydrothermale oplossing terecht komt. De granieten, die de bron zijn voor deze elementen, kunnen ontstaan door fraktionele kristallizatie van een gabbroide of een basaltisch magma, maar ook door partiële opsmelting van metasedimentaire gesteenten. Onafhankelijk van deze oorsprong, zal het magma op zeker moment kristallizeren. Na verloop van tijd raakt het magma waterverzadigd en verdere kristallizatie zal leiden tot de vorming van een afzonderlijke waterige fase. Afhankelijk van hun geochemisch karakter zullen sommige elementen zich bij voorkeur in de kristallizerende mineralen of de resterende smelt verdelen, terwijl andere voornamelijk in de waterige fase fraktioneren. In het algemeen bepaalt de kompositie van zowel de vaste fasen, alswel van de waterige fase de mate van verdeling. Echter, binnen een graniet is de variatie in mineraalkompositie meestal gering, en derhalve wordt de mate van verdeling in sterke mate bepaald door de samenstelling van de waterige fase, met name door de aanwezigheid van chloor of fluor. Indien de waterdruk groter wordt dan de tegendruk van de omringende gesteenten, ontstaan breuken. Hierdoor kunnen de hydrothermale oplossingen ontsnappen, waarna de ertsvormende elementen zich kunnen afzetten door reaktie met het nevengesteente.

Eerdere experimentele onderzoekingen naar elementverdelingen tussen phlogopiet en een waterige oplossing richtten zich vooral op het uitwisselingsgedrag van de alkalielementen natrium, kalium, lithium en rubidium, van de tweewaardige hoofdelementen magnesium en ijzer, en van het fluoride ion, dat het hydroxide ion kan vervangen. Van de verdeling van tweewaardige spore-elementen zoals zink zijn geen gegevens bekend. Experimentele studies naar elementverdelingen tussen een silikaatsmelt van granitische kompositie en een waterige oplossing wijzen op het belang van chloor als komplexerend

ion in de hydrothermale oplossing. Behalve chloor heeft vermoedelijk de alkaliniteit van de smelt, bepaald door de molaire verhouding van aluminium tot het totaal van natrium en kalium, een belangrijke invloed op het verdelingsgedrag van de metaalelementen. Naast chloor wordt ook fluor vaak aangetroffen in associatie met ertsafzettingen. Fluor gedraagt zich echter sterk verschillend van chloor, doordat het in hoge mate oplosbaar is in een silikaatsmelt. Het verlaagt de viskositeit van de smelt en verhoogt de snelheid van iondiffusie. Experimenteel onderzoek naar fluor is echter vooral gericht op het effekt van fluor op de faserelaties van granieten. Er zijn weinig experimentele gegevens betreffende elementverdelingen, die elkaar bovendien lijken tegen te spreken.

Het proefschrift houdt zich bezig, zoals eerder aangegeven, met het gedrag van hoofd- en spore-elementen tijdens de kristallizatie van een graniet en de hiermee gepaardgaande vorming van een separate waterige fase. De resultaten van deze onderzoekingen worden, zoals gebruikelijk in vergelijkbare studies, gepresenteerd in de vorm van verdelingskoëfficiënten. Deze koëfficiënten zijn de verhoudingen van de elementkoncentraties in de betrokken fasen in de mineraal/oplossing- of smelt/oplossing-evenwichten. Hierbij is het belangrijk te weten, of en in welke mate zich chemisch evenwicht heeft ingesteld. Onder andere in Hoofdstuk 3 en Hoofdstuk 7 wordt aan de hand van de experimentele resultaten aangetoond, dat chemisch evenwicht niet altijd bereikt is ten gevolge van kinetische effekten.

Gelet op het werkgebied van het proefschrift, kan een tweedeling van de hoofdstukken gemaakt worden. Het eerste deel, van Hoofdstuk 2 tot Hoofdstuk 5, is gericht op de experimentele verdeling van ammonium (NH_4), kalium (K) en magnesium (Mg) als hoofdelementen, en van lithium (Li), rubidium (Rb) en zink (Zn) als spore-elementen tussen phlogopiet en een chloridehoudende waterige oplossing bij verschillende temperaturen en een druk van 2000 bar. Aan de rol van ammonium als ertstransporterend komplex werd tot voor kort weinig aandacht besteed ten gevolge van analytische problemen. De relatie van ammonium met sommige ertsafzettingen wijst er echter steeds meer op dat ammonium een belangrijk komplex bij ertsmineralizaties is. Na een beschrijving van de synthese van ammonium-phlogopiet in Hoofdstuk 2, volgen de experimentele resultaten van de ammonium/kalium uitwisselingen in Hoofdstuk 3 en 4. In Hoofdstuk 4 wordt tevens aandacht geschonken aan de stabiliteit van de ammonium- en kalium-eindleden van phlogopiet tijdens de experimentele kondities. De resultaten voor de uitwisselingsexperimenten geven aan, dat tussen 550 en 850°C bij een druk van 2000 bar ammonium ten opzichte van kalium preferent wordt gefraktioneerd in phlogopiet. De verdelingskoëfficiënt tussen phlogopiet en oplossing neemt bovendien toe met toenemende temperatuur. Tussen 700 en 750°C vindt echter ontleding plaats van de ammonium-phlogopiet. De experimenten geven aan dat in geologische systemen phlogopiet een belangrijke bron kan zijn voor stikstof of stikstofhoudende komplexen. In Hoofstuk 5 wordt de verdeling van de hoofdelementen kalium en magnesium, en de spore-elementen lithium, rubidium en zink onderzocht bij een temperatuur van 650°C en een druk van 2000 bar. De verdelingen voor kalium, lithium en magnesium geven een goed verband met de chloridekoncentratie. Voor rubidium en zink is dit verband onduidelijk: de verdeling is waarschijnlijk koncentratie-bepaald. De verdelingen van de elementen lithium, kalium en magnesium wijzen er bovendien op, dat kinetische faktoren niet-evenwichts-verdelingen hebben opgeleverd.

Het tweede deel, van Hoofdstuk 6 tot 8, behandelt de verdelingen van de hoofdelementen natrium, kalium en aluminium, en van de spore-elementen lithium, rubidium, zink, koper (Cu), lood (Pb) en tin (Sn) tussen een granitische smelt en een

chloride- of fluoridehoudende waterige oplossing bij temperaturen van 750 tot 850°C en drukken van 2000 en 5000 bar. De experimenten met de chloridehoudende oplossingen worden gepresenteerd in de Hoofdstukken 6 en 7. In deze hoofdstukken wordt het effekt van kompositie en temperatuur- en drukkondities op de elementverdelingen onderzocht. Om de komplexvormende eigenschappen van fluor te vergelijken met die van chloor, worden in Hoofdstuk 8 verdelingsexperimenten beschreven tussen een granitische smelt en een fluoridehoudende oplossing bij temperatuur- en drukkondities van 850°C en 2000 bar, gelijk aan die van Hoofdstuk 6. Voor alle geanalyzeerde éénwaardige ionen blijkt de verdeling tussen smelt en chloride- of fluoridehoudende oplossing een lineair verband op te leveren met de chloride- danwel fluoridekoncentratie, waarbij de voorkeur van de ionen voor de smelt afneemt in de volgorde rubidium, kalium, natrium. Het kleinste ion lithium heeft echter een verdelingskoëfficiënt, die in alle gevallen tussen die van natrium en kalium ligt, en verstoort deze volgorde naar iongrootte. Het verband van lithium met alkaliniteit van de smelt (Hoofdstuk 7) wijst op een sterke koppeling aan de smeltstruktuur. De verhouding tussen de verdelingskoëfficiënten van natrium en kalium is konstant en lijkt temperatuur- en drukafhankelijk te zijn. De verdeling van het tweewaardige ion zink vertoont een kwadratische relatie met de chloridekoncentratie (Hoofdstuk 6) en deze wordt vermoedelijk nog sterker dan lithium bepaald door de alkaliniteit van de smelt. De aluminiumkoncentraties van de waterige oplossingen zijn meestal zeer laag, met uitzondering van enkele chloride-experimenten in Hoofdstuk 6, en van de fluoride-experimenten. In het laatste geval vertoont de verdelingskoëfficiënt voor aluminium een verband met de derde macht van de fluoridekoncentratie.

Toepassingen van de resultaten van de verschillende onderzoekingen liggen vooral op het gebied van de elementmodellering. Met de verdelingskoëfficiënten kan de samenstelling van waterige oplossing in evenwicht met een phlogopiet of een granitische smelt geschat worden met inachtneming van de experimentele kondities. Kombinatie van mineraal/oplossing en smelt/oplossing-verdelingen bij gelijke kondities geeft een mineraal/smelt-verdelingskoëfficiënt. In de gewoonlijk gekompliceerde geologische systemen zijn deze koëfficiënten een belangrijk middel om de ontwikkeling van magmatische gesteenten te ontrafelen. Bij alle toepassingen dient men echter voor ogen te houden, dat de experimentele gegevens zijn verkregen bij vastgestelde kondities wat betreft temperatuur, druk en kompositie. Bij gebruik van deze gegevens voor welk geologisch probleem dan ook zal men ten allen tijde en in voldoende mate rekening moeten houden met deze beperkingen.

Chapter 1

Summary and introduction

This thesis deals with the distribution of ore-forming elements between granites or granite minerals and an aqueous solution, as a contribution in solving the problem of ore-formation. The distribution of elements between different phases can be investigated by direct observation in the field and subsequent chemical analysis of these phases. A second approach is the experimental study of distribution equilibria between minerals or rocks and aqueous solutions under conditions of pressure (2000 to 5000 bars) and temperature (550 to 850°C), which encompass the normal melting and solidification condition of granitic magmas.

This thesis follows the experimental approach, and the experiments reported here can be divided into the following groups:

1. Systems with phlogopite and a chloride-containing hydrothermal solution (Chapters 2 to 5).
2. Systems with a simplified granite and chlorine- (Chapters 6 and 7) or fluorine- (Chapter 8) containing hydrothermal solution.

Phlogopite was chosen for the following reasons. Biotite commonly is the first major mineral to crystallize from granitic melts, or, alternatively, the last mineral to melt during anatexis. Biotite can accomodate trace elements of different valencies in greater amounts than the other rock-forming minerals quartz and feldspars. Phlogopite was chosen as a model phase for biotite, because it has a larger stability field than the endmember annite in terms of temperature and oxygen fugacity.

Granites and ore-formation. Following Eugster (1985) the processes of ore formation in relation to granitic magmas can be subdivided as follows: 1. the acquisition of the ore-forming elements by the magma; 2. the distribution of these elements between the different phases of the magma during crystallization; 3. the release of the ore-forming elements to hydrothermal solutions and 4. the reactions of the solutions with the wall-rock, resulting in the formation of ore-deposits. This thesis aims at an experimental elucidation and quantification mainly of stage 3, the release of the ore-forming elements to the hydrothermal solutions.

The granites, which are the source for these ore-forming elements, may be produced by two fundamentally different processes. Winkler et al. (1975) distinguish granites as a late product of fractional crystallization of a gabbroic/basaltic magma from granites formed by partial melting of metasedimentary rocks. Similarly Chappell and White (1974) distinguish I-type granites with an igneous origin and S-type granites formed by anatexis of metasedimentary sequences on the basis of geochemical and mineralogical characteristics. Independent of the origin, at some stage the magma will start to crystallize. Sooner or later the composition of the granite will become H_2O-saturated by the crystallization of mainly anhydrous minerals (quartz and feldspars). Further crystallization will lead to the formation of a separate aqueous phase. Depending on their geochemical character, some elements will be fractionated into the crystallizing

minerals (the lithophile elements) or into the silicate melt (the 'magmatophile' elements) and others will mainly fractionate into the hydrothermal solution (the incompatible elements). Generally the degree of fractionation will depend equally on the composition of the solid phases and the hydrothermal solution. However, as the granite minerals quartz, feldspar and biotite do not vary greatly in composition, the degree of fractionation is largely determined by the composition of the hydrothermal fluid. Type and concentration of the anions, in particular Cl and F, are the determining factor. Once this separate fluid is formed, the fluid pressure may exceed the wall-rock strength, causing fracturing; the escaping fluids will enter the wall-rock system and deposit their ore-elements (Salemink, 1985; Salemink and Schuiling, 1987).

Previous experimental studies on element ion exchange in biotite were mainly focussed on the alkalis (Na, K, Li, Rb) in major and trace amounts (Beswick, 1973; Volfinger, 1976; Iiyama and Volfinger, 1976), the divalent ions Fe and Mg (Schulien, 1980) and the OH-substitute F (Munoz and Ludington, 1974). Exchange experiments on divalent trace elements in micas are absent in the literature. Experimental studies on the distribution of major and trace elements (like Zn and Pb) between granitic melts and hydrothermal solutions were initiated by Holland (1972). This study and the study of Flynn and Burnham (1978), who studied the distribution of rare earth elements between a chloride solution and a silicate melt, emphasize the importance of chlorine as a complexing ion in melt/solution equilibria. Urabe (1985) assumed, that, beside the chloride molality, the alkalinity of the melt has a large influence on the solution/melt element distributions. Beside chlorine, fluorine is an important ion in the evolution of granitic magmas and it is often associated with ore-deposits (Bailey, 1977). In contrast to chlorine, fluorine is very soluble in the melt. Like H_2O, it strongly depolymerizes the melt, decreasing the melt viscosity and increasing ionic diffusivities. Experimental studies are mainly directed to the effect of fluorine on the phase relations in granitic systems (Bailey, 1977; Manning, 1981). Relatively little is known on its complexing capacity in hydrothermal systems relative to chlorine. A major study on the exchange of elements in fluorine-bearing systems does not exist, whereas the scarce experimental data are controversial.

The experiments. As stated, the thesis deals with the behaviour of major and trace elements under conditions, where a magma solidifies and starts to segregate a hydrothermal aqueous phase, i.e. the beginning of the ore-forming cycle. In this perspective the thesis can be divided two parts.

The first part, ranging from the Chapters 2 to 5, focusses on the experimental determination of the distribution of NH_4, K and Mg as major cations, and of Li, Rb and Zn as trace ions between phlogopite and an aqueous chloride solution at a pressure of 2000 bars and a range of temperatures. The role of ammonium in ore transport has not been given much attention, probably on account of analytical difficulties. The studies of Volynets and Suschevskaya (1972), who detected measurable amounts of ammonium in fluid inclusions, related to tin deposits, of Sterne et al. (1982), who observed an increase in NH_4^+ towards stratiform Zn-Pb-Ag mineralizations, and of Kydd and Levinson (1986) and Krohn and Altaner (1987), who detected a relation of ammonium to gold mineralizations, show that ammonium complexes may play an important role in mineralization. After a description of the synthesis of a pure ammonium-phlogopite in Chapter 2, the exchange experiments are presented in the Chapters 3 and 4. In Chapter 4 some attention is given to the stability of ammonium- and potassium-phlogopite at the experimental conditions. In the Appendix a XRD characterization of the ammonium-

phlogopite is given.

Chapter 5 presents the results on the experimentally determined distributions of K, Mg, Li, Rb and Zn between phlogopite and solution at 650°C and 2000 bars. Lithium and rubidium are often strongly enriched in residual melts during the crystallization of a magma. On the partitioning the alkali ion between phlogopite and solution several studies exist, but on the partitioning of Mg, Li and the ore-forming elements few experimental data are available. Zn, and also Cu and Pb were added in trace amounts; as Cu and Pb suffered losses during experimentation, the results are only briefly mentioned.

The second part of the thesis, starting from Chapter 6, deals with the experimental determination of the distributions of the major elements Na, K and Al and of the trace elements Li, Rb, Zn, Cu, Pb and Sn between a granite melt and a hydrothermal solution. In the Chapters 6 and 7 the hydrothermal solution was again a chloride solution, whereas the experimental PT-conditions were 850°C and 5000 bars for the experiments of Chapter 6, and 750 or 800°C and 2000 bars for those of Chapter 7. The trace elements, studied in these two chapters, were Li, Rb (only Chapter 7), Zn, Cu, Pb and Sn (only Chapter 6). Experimental Li distributions between granitic melt and chloride solution were not presented before. In these chapters the effect of composition of the system and of the changing PT-conditions on the element distribution coefficients was investigated.

To compare the complexing capacity of fluorine with chlorine, Chapter 8 describes distribution experiments between granite and a fluorine-bearing hydrothermal solution at identical pressure and temperature conditions of the experiments of Chapter 6. In the exchange experiments between granite and fluoride solution, Li, Zn and Pb were chosen as trace elements. Also here Pb suffered losses during experimentation.

Summary of the results. In this thesis distribution coefficients are often used for the presentation of the experimental results, which is common practice in similar experimental studies. These coefficients are the element concentration ratios of the involved phases in the mineral/solution- and melt/solution-equilibria. The definition of the distribution coefficients in the different chapters of the thesis was chosen in a way, that the data can be compared with similar other studies.

An important issue for all exchange experiments is the attainment of chemical equilibrium. As demonstrated in several chapters, equilibrium often is not reached, due to kinetic constraints. For the mineral/solution exchange experiments, this is clearly shown in Chapter 3, where complete NH_4/K equilibrium between phlogopite and solution is not attained, even after 28 days. It is suggested, that complete equilibrium here is reached only by recrystallization of the phlogopite. For the melt/solution experiments, the kinetic factor is demonstrated in Chapter 7, where some elements (Na, K) are more close to equilibrium than others (Li, Rb), while the divalent elements are still very far from it. The reason for this is probably the polymerized state of the high-silica melt at these PT-conditions, which has a large effect on the diffusivities of the different ions.

The results for the **phlogopite/solution** equilibria can be summarized as follows. The distribution coefficient $K_D^{NH_4/K}$ between phlogopite and vapour was determined to be larger than 1 at the investigated temperatures and a pressure of 2000 bars. The K_D increases with temperature and between 550 and 850°C the temperature dependence of the K_D was calculated as: $\log K_D = -243/T + 0.533$. The preference of phlogopite for NH_4^+, also relative to other ammonium-containing minerals like feldspars, makes it an important possible source for nitrogen and nitrogen-containing complexes. At the

investigated temperatures of 750 and 850°C, the stability limit of the ammonium-phlogopite was exceeded and in the ammonium-rich experiments the phlogopite started to decompose. The stability experiments, described in Chapter 4, confirmed, that the potassium-phlogopite remains stable at the experimental conditions, whereas the ammonium-phlogopite decomposes at temperatures between 700 and 750°C, at a pressure of 2000 bars. For the exchange experiments of Chapter 5 the distribution coefficients for K and Li show a good linear relationship with chloride molality. The distribution coefficient for Mg between solution and phlogopite is low, if compared to the K_D^K. The distribution of the trace elements Rb and Zn, and probably also Li, appeared to be mainly concentration dependent. For Li it was not possible to decide, whether it substituted for K or for Mg, although Li behaves more like K than like Mg in its exchange behaviour. The results of this chapter seem, however, to be influenced by kinetic factors, which makes application of the results to geological problems difficult.

For the **melt/solution** exchange experiments the distribution coefficient K_D between solution and melt for all monovalent ions exhibit a linear relationship with chloride or fluoride molality. The highest K_D-values are obtained for Na, the lowest for Rb, with the K_D^K in between. This relation with ionic size is not obeyed by Li. The K_D^{Li} is intermediate between the K_D^{Na} and the K_D^K in all studies, suggesting a coupling to the structure of the melt. In Chapter 7 an increase of the K_D^{Li} with increasing Al/(Na+K)-ratio of the melt is observed, providing further evidence for this structural coupling. The $K_D^{Na/K}$-ratio, which is a constant, was determined to be 0.63 at 750°C and 2000 bars, and 0.65 at 850°C and 5000 bars. Combined with the $K_D^{Na/K}$-value of 0.74 of Holland (1972), this apparently PT-dependent ratio can be used to predict the composition of a hydrothermal solution with respect to Na and K. The divalent elements Zn and Pb exhibit a linear relation with the squared chloride molality. Urabe (1985) suggested, that the Al/(Na+K)-ratio of the melt has a large influence on the distribution coefficients of these elements. The K_D^{Zn}-values, obtained in Chapter 6, support this assumption. At the moment it is not possible to demonstrate, if the large variation of the distribution coefficients, due to the variation in alkalinity of the melt, are equilibrium variations, or variations in kinetics, partly caused by structural changes in the melt, which influences the diffusivities of the ions. The considerable increase of the K_D^{Zn} with increasing Al/(Na+K)-ratio of the melt provides an effective means for the release of ore elements, if during the evolution of a granitic body the composition of the melt changes from a peralkaline to a peraluminous composition. The other investigated ore-forming elements Cu and Sn, but partly also Pb, suffer from loss during experimentation, due to reaction with the capsule wall. The results for these elements indicate, that they normally behave like Zn. For the fluorine experiments, no relation is evident between the K_D^{Zn} or the K_D^{Pb}, and the fluorine molality. The Al-concentrations in the reacted chloride solutions are normally below the analytical detection limit. In the higher chlorinity runs of Chapter 6 its concentration becomes detectable, and may have a relation with $(Na+K)^3$ or $(mCl)^6$. In the fluorine runs the Al-concentration of the reacted solutions is considerably higher, as shown not only by the analytical results of the reaction solution, but also by the Al-rich quench phase chiolite. Compared to the solution/melt distribution coefficients, obtained for the chloride systems, the coefficients for the fluoride systems are generally lower for all elements except for Al.

Application of the results. The obtained distribution coefficients for phlogopite/solution and melt/solution equilibria can be used in element modelling studies. With the coefficients an estimate can be made of the fluid composition in

equilibrium with a phlogopite or a granitic melt at the investigated conditions. Combining the K_D of mineral/solution and melt/solution equilibria at identical pressure, temperature and solution composition conditions produces a mineral/melt distribution coefficient. In the usually complicated geological systems, the distribution coefficients between mineral and melt are an important tool in unravelling the evolution of magmatic bodies. In all applications to geological situations it has to be borne in mind, however, that the experimental data are obtained at fixed conditions regarding P, T, composition of the system and other experimental restrictions. Therefore all experimental data have to be applied with careful consideration to any geological problem.

References

Bailey D. K. (1977) Fluorine in granitic rocks and melts: A review. Chem. Geol. **19,** 1-42.

Beswick A. E. (1973) An experimental study of alkali metal distribution in feldspars and micas. Geochim. Cosmochim. Acta **37,** 183-208.

Chappell B. W. and White A. J. R. (1974) Two contasting granite types. Pacific Geology **8,** 173-174.

Eugster H. P. (1985) Granites and hydrothermal ore deposits: a geochemical framework. Mineral. Mag. **49,** 7-23.

Flynn T. R. and Burnham C. W. (1978) An experimental determination of rare earth partition coefficients between a chloride containing vapour phase and silicate melts. Geochim. Cosmochim. Acta **42,** 685-701.

Holland H. D. (1972) Granites, solutions and base-metal deposits. Econ. Geol. **67,** 281-301.

Iiyama J. T. and Volfinger M. (1976) A model for trace-element distribution in silicate structures. Mineral. Mag. **40,** 555-564.

Krohn M. D. and Altaner S. P. (1987) Near-infrared detection of ammonium minerals. Geophysics **52,** 924-930.

Kydd R. A. and Levinson A. A. (1986) Ammoniumhalos in lithogeochemical exploration for gold at the Horse Canyon carbonate-hosted deposit, Nevada, U.S.A.: use and limitations. Applied Geoch. **1,** 407-417.

Manning D. A. C. (1981) The effect of fluorine on liquidus phase relationships in the system qz-ab-or with excess water at 1 kb. Contrib. Mineral. Petrol. **76,** 206-215.

Munoz J. L. and Ludington S. (1974) Fluorine-hydroxyl exchange in biotite. Amer. J. Sci. **274,** 396-413.

Salemink J. (1985) Skarn and ore formation at Seriphos, Greece. Phd. Thesis, Geol. Ultr. 40. Utrecht, 232pp.

Salemink J. and Schuiling R. D. (1987) A two-stage, transient heat and mass transfer model for the granodiorite intrusion at Seriphos, Greece, and the associated formation of contact metasomatic skarn and Fe-ore deposits. In: Chemical transport in metasomatic processes (Ed. H. C. Helgeson). NATO ASI series C: Mathematical and Physical Sciences, vol. 218, 547-575.

Schulien S. (1980) Mg-Fe partitioning between biotite and a supercritical chloride solution. Contrib. Mineral. Petrol. **74,** 85-93.

Sterne E. J., Reynolds Jr. R. C. and Zantop H. (1982) Natural ammonium illites from black shales hosting a stratiform base metal deposit, Delong Mountains, Northern Alaska. Clays and Clay Minerals **30,** 161-166.

Urabe T. (1985) Aluminous granite as a source magma of hydrothermal ore deposits: an experimental study. Econ. Geol. **80,** 148-157.

Volfinger M. (1976) Effet de la température sur les distributions de Na, Rb et Cs entre la sanidine, la muscovite, la phlogopite et une solution hydrothermale sous une pression de 1 kbar. Geochim. Cosmochim. Acta **40,** 267-282.

Volynets V. F. and Sushchevskaya T. M. (1972) Nitrogen in hydrothermal processes (ammonium in fluid inclusions). Geokhimiya 1972 [1], 58-63.

Winkler H. G. F., Boese M. and Marcopoulos T. (1975) Low tempeature granitic melts. N. Jb. Miner. Mh., H. 6, 245-268.

Chapter 2

Hydrothermal synthesis of ammonium-phlogopite

Ariejan Bos, Geert Jan L.M. de Haas, Jack H.L. Voncken, Ad M.J. van der Eerden & J. Ben H. Jansen
Department of Experimental Geochemistry and Petrology, Institute of Earth Sciences, State University of Utrecht, Budapestlaan 4, 3584 CD Utrecht, The Netherlands

Received 23 March 1987; accepted in revised form 1 June 1987

Key words: ammonium-phlogopite, hydrothermal synthesis

Abstract

The hydrothermal synthesis of well-crystallized ammonium-phlogopite has been performed in our department's high pressure and temperature (HPT) laboratory. The experimental techniques are described. The experimental conditions for the synthesis of the mica were 550° C and 2000 bars. Scanning electron microscopy (SEM), infrared spectroscopy (IR), and X-ray diffraction (XRD) characteristics of the ammonium-phlogopite are discussed. Implications for the natural occurrence of the mineral are considered and potential environments for its discovery are suggested.

Introduction

Nitrogen is an important element in the biological and geological cycles. Estimates of the amount of nitrogen on earth are ca. $40*10^{20}$ g atomic N in the atmosphere, minimally $5*10^{20}$ g or 0.2 ppm in the crust and $100*10^{20}$ g or at least 2 ppm in the mantle. An estimate of $500*10^{20}$ g atomic N in the earth's core is based on the mean value of ca. 30 ppm nitrogen for iron-meteorites. The nitrogen in the mantle and in the core is probably present in nitrides and oxynitrides. Most of the nitrogen in the crust is found as organic nitrogen in sediments, as NH_4^+ in silicate minerals, and as a constituent of metamorphic fluids (Stevenson, 1962; Wlotzka, 1961; Hallam & Eugster, 1976; Norris & Schaeffer, 1982).

NH_4^+ commonly occurs as a major interlayer ion in alkali sites in clay minerals (Barrer & Dicks, 1966, 1967). Hydrothermal experiments on the formation of ammonium-rich clay minerals were performed by Tsunashima et al. (1975); to imitate realistic circumstances the NH_4^+ in these experiments was supplied by decompositon of amino acids. Records of metamorphic minerals containing NH_4^+ as a major ion occupying alkali sites are scarce. Erd et al. (1964) describe the ammonium-feldpar buddingtonite as a product of the interaction of sodium-plagioclase with ammonium-rich fluids from a volcanic hot spring system. Barker (1964) crystallized the ammonium-feldspar in a hydrothermal synthesis. Two decades later natural buddingtonite was discovered in a nitrogen-rich environment of oil shales (Loughnan et al., 1983). Ammonioleucite, the ammonium analogue of leucite, has recently been discovered by Hori et al. (1986). The latter mineral is supposed to have formed from leucite by exchange of K^+ for NH_4^+ during hydrothermal alteration related to hot springs, which are still active within 20 kilometres of the deposit. Ammonioleucite was synthesized already much earlier (Barrer, 1950; Barrer et al., 1953). Minor ammonium substitution for potassium in natural muscovites was reported by Vedder (1965), Yamamoto & Nakahira (1966), Honma & Itihara (1981) and Duit et al. (1986). Juster (1984) de-

scribed the occurrence of ammonium-bearing muscovite in low grade metamorphic, coal-associated pelites. The natural ammonium-muscovite tobelite was described for the first time by Higashi (1978, 1982). Ammonium-muscovite was synthesized hydrothermally by Eugster & Munoz (1966). Mineralogical characteristics of synthetic tobelite will be described in a forthcoming paper by Voncken et al. (1987; this issue, pp 259–269). Hallam & Eugster (1976) studied the stability relations of buddingtonite and tobelite as a function of temperature at 2000 bars under oxygen- and nitrogen-buffered conditions. They determined that tobelite is stable at much lower NH_3 fugacities than buddingtonite. Therefore, the conclusions seem reasonable that in nitrogen-rich geological environments tobelite should be a normal constituent, and of more common occurrence than buddingtonite (Voncken et al., 1987).

The ammonium content of natural biotite is generally low, but in most cases higher than in coexisting muscovite. Honma & Itihara (1981) determined a value of 2.38 for the average distribution coefficient of NH_4^+ between biotite and muscovite. A study by Duit et al. (1986) on the ammonium content of biotites and muscovites in the metamorphic complex of the Dôme de l'Agout (France) reported a concentration of upto 2000 ppm NH_4^+ in biotites, and an average NH_4^+ distribution coefficient between biotite and muscovite of about 2.63. recently found NH_4^+-concentration of 5000 ppm in the biotite fraction of a rock from the Belgian Ardennes (Wevers, personal communication) is significant as it provides the highest NH_4^+-concentration ever measured in a biotite untill now. A pure ammonium end-member of the biotite series has not been discovered in nature. Gruner (1939) synthesized an ammonium- and magnesium-containing dioctahedral mica by reactions with vermiculite. Synthetic ammonium-phlogopite is the Mg end-number of the biotite series, with NH_4^+ substituting for all K^+. It was synthesized by Eugster & Munoz (1966) for the first time.

The ammonium-phlogopite described in this article was produced for experiments on the partitioning of NH_4^+ and K^+ between phlogopite and a solution containing NH_4Cl and KCl (Bos et al., in prep.). The study was undertaken in order to obtain a better understanding of the behaviour of ammonium and nitrogen during medium grade metamorphic processes. It is a part of a geochemical research project on the behaviour of nitrogen and ammonium during metamorphism and on their origin in the earth's crust.

Experimental equipment

The synthesis of the ammonium-phlogopite was performed at the high pressure and temperature (HPT) laboratory of the Institute for Earth Sciences at Utrecht. The laboratory has extensive facilities for experimental studies at elevated pressures and temperatures. For the hydrothermal syntheses Tuttle type autoclaves (Tuttle, 1949) were used. An assembled vessel is illustrated in Fig. 1. The autoclaves are often referred to as externally-heated or cold-seal pressure vessels. The vessels are usually made of Stellite No. 25 (a cobalt-based alloy) or René No. 41 (a nickel-based alloy). The maximum conditions, to which these vessels can be subjected, are 6000 bars at 650° and 1000 bars at 750° C. The experimental set-up is depicted in Fig. 2 A and 2 B. Because of its inert behaviour argon gas is used as pressure medium in the vessels. The pressures are monitored by simple Bourdon-type pressure gauges, which are regularly calibrated against a Heise precision gauge. The accuracy is ± 10 bars within the pressure range to 6000 bars. Temperatures are measured by chromel-alumel thermocouples with an accuracy of ± 5° C.

The experimental charge is contained in a noble metal (gold, silver, silver-palladium or platinum) capsule, which is sealed on both sides with a graphite arc-welder. Platinum and silver-palladium capsules are used in hydrogen-buffered experiments, because hydrogen diffuses easily through these metals. By sealing the experimental charge in a platinum or silver-palladium capsule and placing it in another sealed capsule, containing an excess available hydrogen buffer, the buffer controls the hydrogen pressure within both capsules during the experiment, without being in contact with the experimental charge. The malleable properties of the

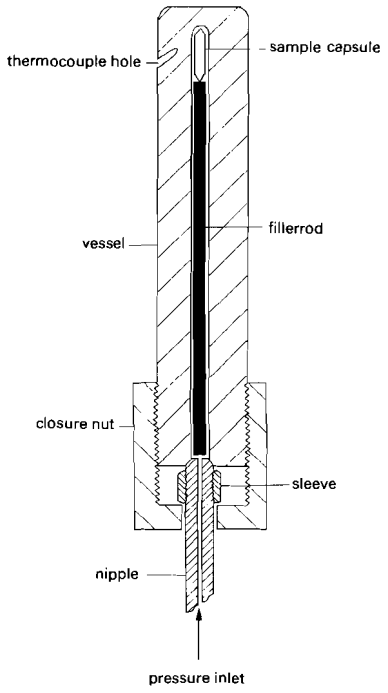

Fig. 1. Tuttle-type pressure vessel (Tuttle, 1949). The vessels are positioned vertically as depicted in this scheme. The hot spot of the furnace-vessel system is at the place of the charge capsule. The closure nut is cooled to prevent corrosion and failure of the thread by high temperature. The fillerrod has a three-fold function, it minimizes the gas content of the vessel, it minimizes argon gas convection during experimentation, and it keeps the capsule at the hotspot.

noble metal capsules ensure that the pressure is uniformly, hydrothermally exerted on the capsule contents, and that the internal pressure of the capsule is equal to the externally applied argon pressure. The noble metals are relatively inert, which explains their use as containers for the substances to be studied at high temperatures. However, the capsule metals may form alloys with metals used in the chemical experiment-system; e.g. iron, often required in hydrogen buffers, will dissolve in platinum, and gold, silver and silver-palladium may be attacked by sulfur, present in the capsule charge.

The experiments are terminated by removing the vessel from the furnace and cooling it down by blasting with compressed air. Room temperature is normally reached within 10 minutes. The quenching must be relatively rapid in order to freeze the chemical reaction. For fast cooling rates a special rapid quench vessel is designed, in which isobaric quenching to room temperature can be attained in approximately 5 seconds.

Experimental methods

The ammonium-phlogopite was crystallized from a mixture of oxide components and the ammonium salt sal volatile, which is a mixture of ammonium carbonate (NH_4HCO_3) and ammonium carbamate ($NH_4CO_2NH_2$). The sal volatile contains 30 to 33 weight percent ammonium and is added in excess to create an ammonia-rich atmosphere for the NH_4-phlogopite crystallization. The hygroscopic oxide components were treated specially to remove moisture and to enhance their reactivity. Amorphous $SiO_2.nH_2O$ was heated to 1200° C for 24 hours for conversion into cristobalite and MgO was heated to 1200° C for 2 hours to remove admixtures of H_2O and CO_2. The weighed oxide components were ground and mixed carefully in an agate mortar. An amount of doubly distilled water was put into a gold capsule, which had been welded on one side. The sal volatile was dissolved in the water, and the required amount of the oxide mixture added. Subsequently the top of the gold capsule was welded under continuous cooling in a water or ice-water bath. Welding has to be done with sufficient heat supply at the top, as the melting temperature of gold is 1064° C, while sufficient cooling is required at the bottom, as sal volatile decomposes already at 60° C. In special cases liquid nitrogen may be used for cooling purposes (Voncken et al., 1987).

The prepared capsule was placed in the pressure vessel and subjected to the experimental conditions of 550° C at 2000 bars for 5 to 14 days. A run time of 5 to 7 days produces sufficiently large crystals for the exchange experiments. Longer run times have only a small effect on the increase of crystal size. The ammonium-phlogopite is formed according to the reactions

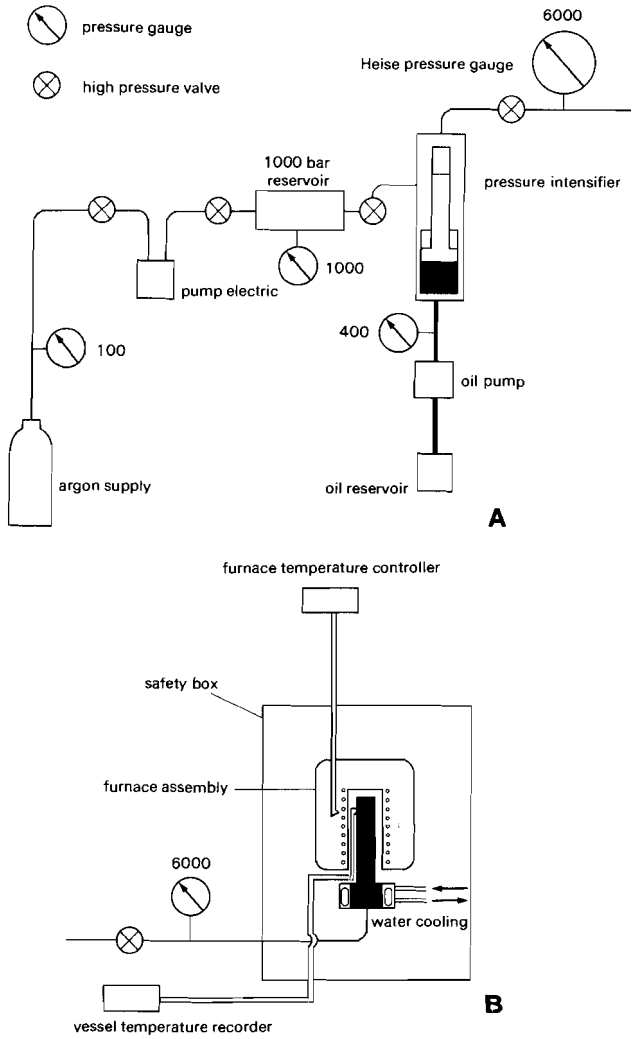

Fig. 2. Schematic P-T arrangement for the Tuttle-type vessels.

A: The pumping system for operation upto 6 kbar. The argon gas is brought to 6 kbar in two stages. The first-stage pump is an electric membrane pump and pressurizes the argon gas from ca 100 bars to 1000 bars. In the second stage a pressure intensifier driven by oil pressurizes the gas from 1000 to 6000 bars. The high pressure of the system is measured with a calibrated Heise gauge. The numbers at the pressure gauges indicate the maximum pressure in the specific part of the system. Low pressure parts of the system are separated from the high pressure parts by one-way safety valves.

B: The furnace and vessel (black) assembly. This assembly is surrounded by a safety box, which provides ample protection against a possible failure of the pressure vessel. The closure nut of the vessel is surrounded by a cooling block. The pressure valve separates the vessel from the rest of the high pressure system during experimentation.

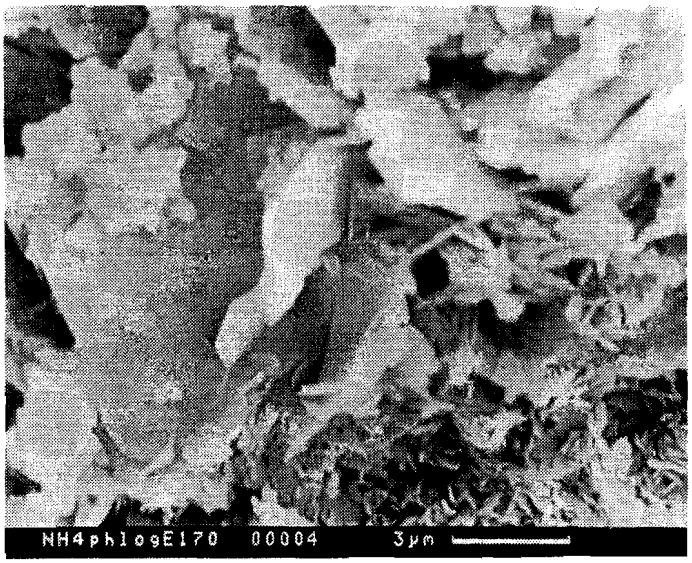

Fig. 3. Scanning electron microscope (SEM) photograph of an ammonium-phlogopite aggregate.

$$xNH_4HCO_3 + yNH_4CO_2NH_2 \rightarrow (x + 2y)NH_3 + (x + y)\,CO_2 + xH_2O \quad (1)$$

$$2NH_3 + 6MgO + Al_2O_3 + 6SiO_2 + 3H_2O \rightarrow 2NH_4Mg_3AlSi_3O_{10}(OH)_2 \quad (2)$$

The amount of phlogopite which can be crystallized in an experiment depends on the amount of oxide mixture added to the capsule. However, as one can see from reaction (1) a considerable amount of CO_2 is released during decomposition of the sal volatile. A welded gold capsule with a capsule wall thickness of 0.2 mm may withstand a maximum inner over-pressure of ca 20 atm. Therefore the amount of filling is restricted as otherwise the capsule will burst, when the pressure is released to atmospheric conditions after termination of the experiment. Normally 200 to 300 milligrams of phlogopite can be crystallized in a capsule with a volume of ca. 1 cm^3. If a homogeneous temperature is required over the total sample capsule, the length is restricted to 2 to 3 cm. If a temperature gradient over the capsule is required, e.g. for special crystal growth experiments, the length of the capsule can be several times greater.

Analytical techniques

The ammonium-phlogopite was checked on crystallinity and purity first optically with a microscope and next with X-ray diffraction (XRD). The obtained XRD-pattern was measured for a structure analysis to compute the cell parameters of the ammonium-phlogopite (Bos et al., in prep.) The calculated cell volume is 507.8 ± 0.3 (Å)^3, i.e. slightly larger than the cell volume of 504.19 (Å)^3 calculated by Eugster & Munoz (1966) for their ammonium-phlogopite. Normal phlogopite has a unit cell volume of 497.0 ± 0.6 (Å)^3 (Hazen & Wones, 1972), which is considerably smaller than the unit cell volume of the ammonium-phlogopite. The increase in cell volume is mainly attributed to a longer c-axis, caused by the incorporation of the relatively large ammonium-ion in the K-layers.

Normally the ammonium-phlogopite is well crystallized, although the grain dimensions are restricted and the flakes are very thin. The phlogopites were studied in more detail with a scanning electron microscope (SEM). A SEM photograph of a crystal aggregate is shown in Fig. 3. The size of

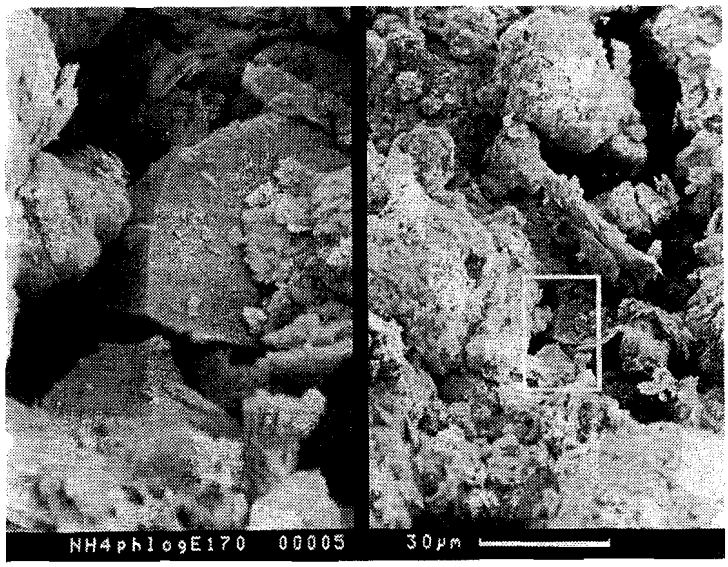

Fig. 4. SEM photograph of quartz, which is rarely detected in some runs.

the ammonium-phlogopite flakes seldomly exceeds 20–30 μm. Unreacted starting material, crystalline phases other than phlogopite, and quench products were absent in most runs. Only in a few runs a small amount of α-quartz was detected, which was probably caused by incomplete reaction of the starting materials, or by a slight inhomogeneity of the starting mixture. Figure 4 shows a SEM photograph of the euhedral quartz.

Wet-chemical analyses of the ammonium-phlogopite yield a lower NH_4-content (ca. 80–90 mole%) than expected on the basis of the ideal formula. This is confirmed by thermogravitational analysis (TGA). The ammonium-phlogopite was analyzed also with infrared spectroscopy (IR), a powerful and relatively simple technique for the qualitative analysis of ammonia incorporated in the crystal structure. Infrared spectroscopy is based on the absorption of infrared radiation by specific bending or stretching vibrations of atoms within a molecule. Various structural groups within a molecule can easily be identified. Figure 5 shows spectrograms of pure potassium-bromide (KBr), which is the usual material for the pressed carrier tablets, of synthetic potassium-phlogopite, and of synthetic ammonium-phlogopite. The positions of the OH-vibrations of absorbed atmospheric H_2O are shown by the spectrogram of the hygroscopic KBr tablet and appear detectable in all three spectra. The presence of ammonium in the ammonium-phlogopite is indicated by the bands at 3270, 3030 and 1430 cm^{-1}. The absorption peaks below 1100 cm^{-1} belong mainly to Si-O-Si and Si-O-Al^{IV} bending and stretching vibrations. Differences in the two spectrograms of the phlogopites are obvious at the frequencies near 3700 cm^{-1}, due to different octahedral OH-vibrations. The absorption bands at 3720 cm^{-1} for the K-phlogopite and at 3707 cm^{-1} for the NH_4-phlogopite are due to the octahedral Mg_3OH-vibrations. The small peak at 3680 cm^{-1} for the K-phlogopite and the larger peak at 3672 cm^{-1} for the NH_4-phlogopite may be attributed to a Mg_2Al-OH vibration. Stoichiometric considerations point at an alumina deficiency for the tetrahedral sites. This is confirmed by a decrease in intensity of the Si-O-Al^{IV} vibrations at 730

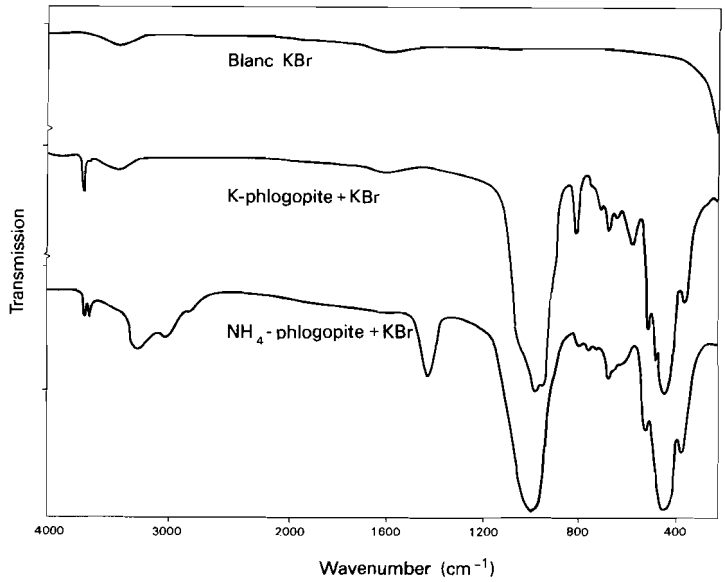

Fig. 5. Infrared (IR) spectograms of ammonium-phlogopite, synthetic (potassium-)phlogopite and of a pure KBr-tablet as reference for background corrections. For explanation see text.

and 660 cm^{-1}. The relatively strong Mg_2Al-OH vibration in the NH_4-phlogopite indicates a rather extended octahedral Al-substitution. The reason for this substitution, which is virtually absent in the K-phlogopite, may be the compensation of the charge deficiency, caused by the 80–90% NH_4 occupancy in the alkali-layer.

Discussion and conclusions

The hydrothermal synthesis of ammonium-phlogopite turns out to be relatively simple. The incorporation of the ammonium-ion in the phlogopite crystal structure is clearly demonstrated by IR-spectroscopy. The available studies on natural biotites (Honma & Itihara, 1981; Duit et al., 1986) prove that the ammonium-ion may be a common substitute for potassium.

The ammonium-phlogopite was made for use in hydrothermal experiments on $K^+-NH_4^+$ exchange at metamorphic conditions. The crystallographical and mineralogical characterization of the phlogopite used in the latter experiments is important. The crystallinity and the grain size may seriously effect the exchange kinetics during the exchange experiments. The data on potassium and ammonium exchange between the phlogopite and a vapour phase at elevated temperatures and pressures can be applied in thermodynamic calculations on natural element distribution data. Geothermometry and the calculation of equilibrium fluid compositions are options after evaluation of the phlogopite system (Bos et al., in prep.) and the muscovite system (Voncken et al., 1987).

A pure ammonium-phlogopite or biotite has not been reported from natural rocks. However, the presence of several ammonium-silicates in active volcanic areas suggests that these areas provide an appropriate environment to discover a pure natural ammonium-phlogopite, formed through the alteration of primary potassium-phlogopite by am-

monium-rich hydrothermal solutions. Stable high-ammonium biotites may also exist in medium grade metamorphic oil-shales or other medium-grade rocks rich in organic matter, where ammonium-rich fluids may be produced by degassing of organic material under reducing circumstances; this is evidenced by the high-ammonium biotite from the Belgian Ardennes.

Acknowledgments

Joyce Wevers is gratefully acknowledged for her critical comments on the interpretation of the IR-spectrograms and Gert Kastelein for his technical support in the HPT laboratory.

References

Barker, D.S. 1964. Ammonium in alkalifeldspar – Amer. Mineral. 49: 851–858

Barrer, R.M.1950. Ion-exchange and ion-sieve processes in crystalline processes – J. Chem. Soc. (1950): 2342–2350

Barrer, R.M., J.W. Baynham & N. McCallum. 1953. Hydrothermal chemistry of silicates. Part V. Compounds structurally related to analcime – J. Chem. Soc. (1950): 4035–4041

Barrer, R.M. & L.W.R. Dicks. 1966. Chemistry of soil minerals – III. Synthetic micas with substitutions of NH_4 for K, Ga for Al, and Ge for Si – J. Chem. Soc. Lond. (A): 1379–1385

Barrer, R.M. & L.W.R. Dicks. 1967. Chemistry of soil minerals – IV. Synthetic alkylammonium montmorillonites and hectoites – J. Chem. Soc. Lond. (A): 1523–1529

Duit, W., J.B.H. Jansen, A. van Breemen & A. Bos. 1986. Ammonium micas in pelitic rocks as exemplified by Dôme de l'Agout (France) – Amer. J. Sci. 286: 702–732

Erd, R.C., D.E. White, J.J. Fahey & D.E. Lee. 1964. Buddingtonite, an ammonium feldspar with zeolitic water – Amer. Mineral. 49: 831–849

Eugster, H.P. & J.L. Munoz. 1966. Ammonium micas: possible sources of atmospheric ammonia and nitrogen – Science 151: 683–686

Gruner, J.W. 1939. Ammonium mica synthesized from vermiculite. Amer. Mineral. 24: 428–433

Hallam, M. & H.P. Eugster. 1976. Ammonium silicate stability relations – Contrib. Mineral. Petrol. 57: 227–244

Hazen, R.M. & D.R. Wones. 1972. The effect of cation substitutions on the physical properties of trioctahedral micas – Amer. Mineral. 57: 103–129

Higashi, S. 1978. Dioctahedral mica minerals with ammonium ions – Mineral. J. 9: 16–27

Higashi, S. 1982. Tobelite, a new ammonium dioctahedral mica – Mineral. J. 11: 138–146

Honma, H. & Y. Itihara. 1981. Distribution of ammonium in minerals of metamorphic and granitic rocks – Geochim. Cosmochim. Acta 45: 983–988

Hori, H., K. Nagashima, M. Yamada, R. Miyawaki & T. Marubashi. 1986. Ammonioleucite, a new mineral from Tatarazawa, Fujioka, Japan – Amer. Mineral. 71: 1022–1027

Juster, T.C. 1984. Very low-grade metamorphism of pelites associated with coal, Northeastern Pennsylvania – M.S. thesis, University of Wisconsin-Madison, 101 pp

Loughnan, F.C., F.I. Roberts & A.W. Lindner. 1983. Buddingtonite (NH_4-feldspar) in the Condor oil-shale deposit, Queensland, Australia – Mineral. Mag. 47: 327–334

Norris, T.L. & O.A. Schaeffer. 1982. Total nitrogen contents of deep sea basalts – Geochim. Cosmochim. Acta 46: 371–379

Stevenson, F.J. 1962. Chemical state of nitrogen in rocks – Geochim. Cosmochim. Acta 26: 797–809

Tsunashima, A., F. Kanamaru, S. Ueda, M. Koizumi & T. Matsushita. 1975. Hydrothermal syntheses of amino acid-montmorillonites and ammonium-micas – Clays and Clay Minerals 23: 115–118

Tuttle, O.F. 1949. Two pressure vessels for silicate-water studies – Geol. Soc. Amer. Bull. 60: 1727–1729

Vedder W. 1965. Ammonium in muscovite – Geochim. Cosmochim. Acta 29: 221–228

Voncken, J.H.L., J.M.R. Wevers, A.M.J. van der Eerden, A. Bos & J.B.H. Jansen. 1987. Hydrothermal synthesis of Tobelite, $NH_4Al_2Si_3AlO_{10}(OH)_2$, from various starting materials and implications for its occurrence in nature – Geol. Mijnbouw 66: 259–269

Wlotzka, F. 1961. Untersuchungen zur Geochemie des Stickstoffs – Geochim. Cosmochim. Acta 24: 106–154

Yamamoto, T. & M. Nakahira. 1966. Ammonium ions in sericites – Am. Mineral. 51: 1775–1778

Chapter 3

Nitrogen storage in biotite: An experimental study of the ammonium and potassium partitioning between 1M-phlogopite and vapour at 2 kb

ARIEJAN BOS, WILLEM DUIT*, AD M. J. VAN DER EERDEN and J. BEN H. JANSEN
Department of Chemical Geology, Institute for Earth Sciences, University of Utrecht, P. O. Box 80.021, 3508 TA Utrecht, The Netherlands

(*Received June* 26, 1987; *accepted in revised form February* 24, 1988)

Abstract—The NH_4^+ and K^+ distribution between phlogopite and a chloride vapour phase was investigated at 550°C and 2000 bars. Some preliminary data are reported for 650°C and 2000 bars. The apparent distribution coefficient, $K_D^* = (NH_4^+/K^+)_{P,T}^{phlogopite}/(NH_4^+/K^+)_{1\ bar,\ 25°C}^{vapour}$, is 1.29 ± 0.30 at 550°C and 1.44 ± 0.20 for the preliminary data at 650°C. At 550°C a series of runs was performed to study the equilibration time of the exchange reaction. Bulk compositions requiring a large change in solid composition did not equilibrate within 28 days, indicating a rather sluggish reaction mechanism.

The extrapolation to low NH_4^+ concentrations in natural rock systems may provide estimates of NH_4^+ concentrations for metamorphic fluids in equilibrium with NH_4^+ bearing minerals. The assumption that Rb^+ behaves similarly to NH_4^+ allows a rough estimate of the distribution coefficients for NH_4^+ in other minerals. Semiquantitative modelling based on the derived distribution coefficients of NH_4^+ and Rb^+ may elucidate fluid/rock equilibria during closed system behaviour. The release of nitrogen by breakdown of NH_4-bearing biotite during prograde or retrograde processes in metamorphic rocks may explain the presence of N_2-gas in fluid inclusions.

INTRODUCTION

THE OCCURRENCE OF nitrogen in metamorphic areas, its behaviour during metamorphism and its origin have been studied during the last two decades. Nitrogen in the form of NH_4^+ commonly replaces K^+ in natural potassium silicates in minor amounts. The ammonium feldspar buddingtonite (ERD *et al.*, 1964), the ammonium muscovite tobelite (HIGASHI, 1982), ammonioleucite (HORI *et al.*, 1986) and ammonium illite (JUSTER, 1987) are the only natural ammonium endmembers of potassium silicates. The controversy on the origin of nitrogen has focussed on whether it is sedimentary or mantle-derived (EUGSTER and MUNOZ, 1966; HALLAM and EUGSTER, 1976; KREULEN and SCHUILING, 1982; GLASSLEY *et al.*, 1984). Recent studies on the NH_4^+ content of potassium silicates show substantial proof of a sedimentary origin of the nitrogen and have provided NH_4^+ distribution coefficients for the common potassium silicates (HONMA and ITIHARA, 1981; DUIT *et al.*, 1986). Experimental studies on ammonium silicates are restricted to mineral synthesis (*e.g.*, GRUNER, 1939; BARKER, 1964; EUGSTER and MUNOZ, 1966; BOS *et al.*, 1987; VONCKEN *et al.*, 1987, 1988) and to a study on the stability of tobelite and buddingtonite in an ammonia- and hydrogen-buffered, potassium-free system (HALLAM and EUGSTER, 1976). SHIGOROVA *et al.* (1982) synthesized a complete isomorphous series between muscovite and its ammonium analogue tobelite. No work is published on the NH_4^+-K^+ exchange reaction and its dependence on temperature and pressure. An MSc-study on the distribution of NH_4^+ between feldspars and coexisting vapour (LORCH, 1978) suggested a positive temperature dependence of the distribution coefficient in hydrogen-buffered experiments.

As a reference for the NH_4^+-K^+ exchange reaction the analogous reaction with Rb^+ may be considered. Rb^+ also substitutes for K^+ and is comparable to NH_4^+ in ionic size: 1.52 Å for Rb^+ (SHANNON and PREWITT, 1969) *versus* 1.48 Å for NH_4^+ (PAULING, 1960). The similarity in ionic size is reflected in the unit cell volumes of the endmember phlogopites: 510.0 $(Å)^3$ for rubidium phlogopite (HAZEN and WONES, 1972) and 504.19 $(Å)^3$ for ammonium phlogopite (EUGSTER and MUNOZ, 1966). Potassium phlogopite has a unit cell volume of 497.0 $(Å)^3$ (HAZEN and WONES, 1972), related to the smaller size of the K^+ ion of 1.38 Å (SHANNON and PREWITT, 1969). In natural rock systems the distributions of Rb^+ between various mineral pairs (DE ALBUQUERQUE, 1975) are quite similar to NH_4^+ distributions (DUIT *et al.*, 1986). The Rb^+-K^+ exchange reaction has been studied experimentally with several potassium silicates (LAGACHE, 1968; LAGACHE and CARRON, 1972; BESWICK, 1973; VOLFINGER, 1974, 1976; FUNG and SHAW, 1978; VONCKEN *et al.*, in prep.). From these studies it can be concluded that the distribution coefficient of Rb^+ between a mineral and chloride vapour increases with increasing temperature, and that Rb^+ is preferred by the potassium silicates in the rising order: alkali-feldspar, muscovite, phlogopite and annite. HONMA and ITIHARA (1981) demonstrated that this systematic effect is similar for the NH_4^+ ion in minerals of natural rocks. They attributed the effect to the length of the shortest potassium-oxygen (K-O) distance, which increases from alkali-feldspar to annite.

In order to provide an experimental background for the interpretation of field phenomena, a study of the distribution of NH_4^+ between phlogopite and a coexisting supercritical fluid was undertaken. This paper presents the data on the experiments at 550°C and 2000 bars total pressure, as well as preliminary results at 650°C and 2000 bars.

EXPERIMENTAL METHODS

The experiments were carried out in Tuttle-type pressure vessels, using argon as a pressure medium. Pressures were continuously monitored by ordinary Bourdon-type pressure gauges, that were checked regularly against a calibrated Heise pressure gauge. The accuracy was better than ±10 bars. Temperatures were measured to within ±5°C with chromel-alumel thermocouples, calibrated against melting standards at 327.5°C and 620°C. After the desired run-du-

* Died July 26, 1985.

ration the vessels were quenched by compressed air to room temperature within about 10 minutes. For a number of runs, intended to study the speed of the exchange reaction, a specially designed rapid-quench pressure vessel was used. A Tuttle-type vessel, which can be rotated, is extended with an extra watercooled pressure chamber. During the experiment the vessel is hanging in the furnace. The experiment is terminated by removing the furnace and rotating the vessel upside down. The capsule will fall freely towards the watercooled chamber. For these experiments the isobaric cooling rate was approximately 3 to 4 seconds from experimental to room temperature.

In the exchange runs synthetic pure endmember phlogopites were reacted with a NH_4Cl-KCl solution. The endmember phlogopites were synthesized in advance of the exchange experiments. The ammonium phlogopites were synthesized hydrothermally from oxide powder mixtures and a mixture of ammonium-carbonate (NH_4HCO_3) and ammonium-carbamate ($NH_4CO_2NH_2$) at 550°C and 2000 bars following the method of EUGSTER and MUNOZ (1966). The potassium phlogopites were synthesized hydrothermally from $K_2O \cdot SiO_2$ glass and oxide powder mixtures at 650°C and 2000 bars. Table 1 lists the starting materials. The synthetic mica products were studied optically, by X-ray diffraction (XRD), scanning electron microscopy (SEM) and infra-red analysis (IR). The NH_4- and K-phlogopites were typically well crystallized. The NH_4-phlogopites were up to 5 micrometers in size, being somewhat larger than the K-phlogopites, which did not exceed 2 micrometers. The XRD pattern of the NH_4-phlogopite is consistent with a 1M structure. The K-phlogopite XRD reflections match closely those obtained by HAZEN and WONES (1972) for the synthetic 1M polytype.

For the exchange experiments 30 to 40 milligrams of phlogopite together with 50 microliters of a NH_4Cl-KCl solution of variable NH_4^+/K^+ ratio were sealed in a noble metal capsule. The chloride solutions were mostly 2.1 molal; in a few cases a 4.2 molal solution was taken. The chloride solution was injected first into the capsule and subsequently a weighed quantity of phlogopite was added. As much air as possible was squeezed out to limit contamination by atmospheric N_2, O_2 and CO_2. Theoretically the nitrogen, introduced by atmospheric contamination, could increase the total amount of nitrogen in the experiments with the lowest total NH_4^+ concentrations by *ca.* 5 molepereent. In most experiments, however, the nitrogen contamination will not exceed 1 to 2 molepercent of the total nitrogen amount of the capsule system. The capsules were welded shut with an are-welder. Fluid loss during welding was prevented by welding in water or ice-water, if necessary. Capsules having weight differences before and after welding of more than 0.2 mgs were discarded. Some runs were buffered by the oxygen buffer nickel-bunsenite (NNO). In the buffered experiments the charge was sealed in a platinum capsule, which, in turn, was sealed with the oxygen buffer in a gold capsule (EUGSTER and SKIPPEN, 1967). In the unbuffered experiments the charge was placed directly in a gold capsule.

THE CHEMICAL SYSTEM

The reactions of interest at the experimental conditions are

$$\text{K-phlogopite} + NH_{4aq}^+ \leftrightarrow \text{NH}_4\text{-phlogopite} + K_{aq}^+ \quad (1)$$

$$NH_{4aq}^+ + Cl_{aq}^- \leftrightarrow NH_4Cl_{aq}^0 \quad (2)$$

$$K_{aq}^+ + Cl_{aq}^- \leftrightarrow KCl_{aq}^0 \quad (3)$$

Table 1. List of chemicals used

$K_2O.SiO_2$ glass	Prepared after SCHAIRER and BOWEN (1955) with $KHCO_3$ and cristobalite
$KHCO_3$	Merck suprapur
Cristobalite	Prepared from Merck pA purified quartz, heated to 1500°C
$NH_4NH_2CO_2.NH_4HCO_3$	(sal volatile)
$SiO_2.nH_2O$	Merck pA, heated to 1200°C for 24 hrs.
MgO	Merck pA, heated to 1200°C for 2 hrs.
γ-Al_2O_3	Merck pA
NH_4Cl	Merck pA
KCl	Merck pA
H_2O	Doubly distilled

$$H_{aq}^+ + Cl_{aq}^- \leftrightarrow HCl_{gas} \quad (4)$$

$$H_{aq}^+ + NH_{3\ gas} \leftrightarrow NH_{4aq}^+ \quad (5)$$

$$N_{2\ gas} + 3H_{2\ gas} \leftrightarrow 2NH_{3\ gas} \quad (6)$$

$$2H_2O_{gas} \leftrightarrow 2H_{2\ gas} + O_{2\ gas}. \quad (7)$$

The fluid composition is controlled by reactions (1) to (7). Available data on reaction (3) (RITZERT and FRANCK, 1968) and reaction (4) (HELGESON and KIRKHAM, 1976; FRANTZ and POPP, 1978) predict mainly undissociated KCl and HCl at run conditions. For reactions (2) and (5) data are available only below 300°C (HITCH and MESSMER, 1976). At low temperatures NH_3 is dominant over NH_4^+ only in moderately alkaline solutions, but above ca 220°C it becomes dominant even in acidic solutions. There is little tendency to form NH_4Cl. At run conditions it is not probable that all NH_4^+ is dissociated, because in the experiments using K-phlogopite and a NH_4Cl solution as starting materials sufficient NH_4-phlogopite has been formed to demand the presence of NH_4^+ in the fluid. Experiments at 750°C and 2 kbar on silicate melts in the presence of a NH_4Cl-bearing fluid, which are presently being performed in our laboratory, suggest the presence of mainly undissociated NH_4Cl. For the chloride-free system data are available on reaction (6) and (7) (STULL and PROPHET, 1971). An oxygen buffer fixes the $(f_{NH_3})^2/f_{N_2}$ ratio, which can be calculated using the methods of FRENCH (1966) and assuming ideal fluid mixing. Fugacity coefficients in the calculations were taken from several authors (H_2O: HELGESON and KIRKHAM, 1974; O_2 and N_2: RYZHENKO and VOLKOV, 1971; H_2: SHAW and WONES, 1964, and MEL'NIK, 1978; NH_3: MEL'NIK, 1978). Results of these calculations at a fixed $P(NH_3 + N_2)$ are presented in Fig. 1. At the experimental conditions of 550°C and 2000 bars, and with the NNO-buffer a partial ($NH_3 + N_2$) pressure above 10^{-3} bar fixes N_2 as the dominant species. For a given $P(NH_3 + N_2)$, f_{NH_3}/f_{N_2} appears to be relatively constant over a large temperature interval. If all nitrogen in the fluid phase were present as N_2 and NH_3, $P(NH_3 + N_2)$ would vary between 5 and 30 bars, depending on the initial amount of NH_4Cl and NH_4-phlogopite.

The departure from ideal mixing during the exchange reaction is assumed to be small for the concentration ranges involved. Experiments at other molalities and concentrations are being carried out for verification. Assuming ideal mixing, the distribution coefficient of NH_4^+ between phlogopite and vapour is equivalent to the equilibrium constant of reaction (1) and is defined as

$$K_D = (NH_4^+/K^+)^{\text{phlogopite}}/(NH_4^+/K^+)^{\text{vapour}}. \quad (8)$$

As the NH_4^+/K^+ ratio of the vapour is unknown at P and T because of insufficient data, an apparent K_D^* is formulated as

$$K_D^* = (NH_4^+/K^+)^{\text{phlogopite}}_{P,T}/(NH_4^+/K^+)^{\text{vapour}}_{1\text{ bar},\ 25°C}. \quad (9)$$

It is assumed that during quenching the composition of the solid does not change.

Two series of runs, AB39 and AB40, were performed for the determination of the rate of reaction (1). In these series the runs were not oxygen buffered. Each series consisted of reversals (K-phlogopite + NH_4Cl-solution, NH_4-phlogopite + KCl-solution) at 550°C and 2000 bars for run durations of 1 hour at 28 days. The capsules were quenched to room temperature within a few seconds. No quench products were observed.

ANALYTICAL PROCEDURES

After the experiments any leakage was detected by reweighing the capsules. The outer capsule and the nickel-bunsenite buffer were removed. The buffer was checked by XRD and never appeared to be exhausted. The exchange run capsule was cleaned thoroughly in a dilute solution of sulfuric acid. To prevent loss of NH_3 during the recovery of the solution, the capsules were punctured and opened in a dilute solution of sulfuric acid, in which practically all NH_3 and NH_4^+ will dissolve. NH_4^+ absorbed on the phlogopite surface is simultaneously removed by the acid solution. After puncturing, a tiny vapour bubble escaped from most of the capsules. It is not yet clear if the bubble consists of sealed-in atmosphere or N_2 formed from NH_3 during run conditions (see Discussion). The solid phase was

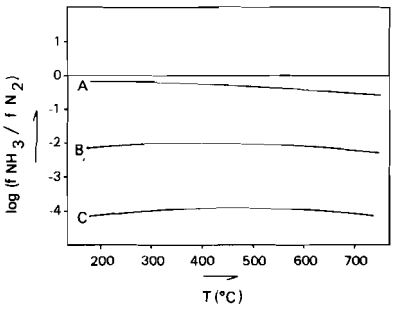

FIG. 1. Calculated log (f_{NH_3}/f_{N_2}) ratios at 2000 bars total pressure as a function of temperature at nickel-bunsenite buffered conditions and for different ($NH_3 + N_2$) partial pressures in a chloride-free chemical system. $P(NH_3 + N_2)$ for curve A: 0.001 bar, for curve B: 1 bar, and for curve C: 1000 bars.

separated from its solution in a high speed centrifuge and rinsed three times. Subsequent chemical analyses showed that the solution yielded normally around 80 to 90 percent of the initial amount of ammonium and potassium. The relatively high yield suggests a low N_2 gas content of the capsule after quenching. The run solution was analyzed separately for NH_4^+ and K^+. NH_4^+ was analyzed by a colorimetric method using the Berthelot colouring reaction (VERDOUW *et al.*, 1978). The degree of colouring, being an indicator of NH_4^+ concentration, was measured at λ = 660 nm with a Perkin-Elmer type 550S spectrophotometer. K^+ was analyzed by atomic absorption spectrometry (AAS) with a Perkin-Elmer type 460 spectrometer.

After drying, the phlogopite was examined under the optical microscope, by XRD and in most cases by SEM. All phlogopites exhibited clearly improved crystallization compared to the starting products. Sizes of 10 to 20 microns were normally observed. Other phases were not detected. XRD patterns for the phlogopite solid solutions display systematic changes with composition, especially for the (001)-reflections, providing evidence for structurally bound NH_4^+. The reflections are well defined and show no broadening due to intergrowths of NH_4-phlogopite and K-phlogopite. The crystals are thus considered to be real solid solutions. K^+ and NH_4^+ concentrations in the solid phase were analyzed separately. For the K^+ analysis a few milligrams of the phlogopite were dissolved in concentrated HF and evaporated to dryness at *ca.* 150–160°C. The residue was dissolved in 1:1 HCl, diluted and measured by AAS. For the NH_4^+ analysis the method of STEVENSON (1960) was followed. A few milligrams of phlogopite were sealed in glass tubes together with 2 ml of concentrated sulfuric acid. Heating of the tubes to 400°C caused destruction of the structure of the phlogopite, releasing the structurally bound NH_4^+. The liberated NH_4^+ was transferred to volumetric flasks by means of steam distillation. This NH_4^+ containing solution was analyzed applying the colorimetric method described above. The NH_4^+/K^+ ratio of the phlogopite was checked by a partially independent analytical procedure in which a few milligrams of the phlogopite were dissolved in a concentrated H_2SO_4/HF solution at 80°C. After dissolution a saturated solution of boric acid was added to neutralize excess HF. The solution was treated as described for the separate NH_4^+ and K^+ analysis of the phlogopite. The NH_4^+/K^+ ratios obtained are within 5 to 10% of the values obtained by the normal method of separate NH_4^+ and K^+ analysis.

The analytical errors for both phlogopite and vapour are estimated to be within 5% for potassium and within 10% for ammonium, based on duplicate analyses.

RESULTS

The analytical results are listed in the Tables 2, 3 and 4, and are used to construct the diagrams of Figs. 2, 3 and 4. In the diagrams $X_{NH_4^+}$ (defined as $NH_4^+/(NH_4^+ + K^+)$ in mole fractions) of the phlogopite is plotted along the lower horizontal axis, and $X_{NH_4^+}$ of the vapour along the upper horizontal axis. The final $(X_{NH_4^+})^{vapour}$ is the $X_{NH_4^+}$ after the experiment, measured at 1 bar and 25°C. The mole fraction of $(NH_4^+ + K^+)$ in the solution relative to the total amount of $(NH_4^+ + K^+)$ of the capsule system is plotted along the vertical axis. The bulk composition defines a point on the line connecting the initial vapour and phlogopite composition of each experiment, indicated by extrapolation of the short line. In closed system runs and in the case of comparable behaviour of both alkali-ions the line connecting the vapour and phlogopite composition will rotate around this point to the equilibrium position (BESWICK, 1973). Equilibrium is assumed if the tie-lines reach parallel positions, especially when coming from opposite directions. It is important to note that, if the amounts of starting materials are known, the analysis of only one component is sufficient to construct the tie-line of the final compositions. In these experiments, however, the NH_4^+ and K^+ concentrations of both phlogopite and vapour were analyzed, providing a check on the accuracy of the individual analyses and on the integral experimental method. Because a tie-line diagram becomes confusing when larger

Table 2. Results of the nickel-bunsenite buffered experiments at 550°C with 2.1 molal chloride solutions, except 17-2 and 21-1, which had 4.2 molal solutions.

	$X_{NH_4^+}$ i 1)		$X_{NH_4^+}$ f 2)		NH_4^+/K^+ f 3)		
Run no.*)	solid	vapour	solid	vapour	solid	vapour	K_D 4)
17-1	1.00	0.60	0.78	0.68	3.57	2.11	1.69
17-2	0.00	1.00	0.56	0.71	1.25	2.46	0.51
18-1	1.00	0.40	0.72	0.63	2.57	1.72	1.49
18-2	0.00	0.79	0.47	0.46	0.89	0.83	1.07
19-1	1.00	0.20	0.56	0.46	1.25	0.85	1.46
19-2	0.00	0.58	0.29	0.32	0.41	0.47	0.87
21-1	1.00	0.00	0.37	0.19	0.60	0.23	2.63
21-2	0.00	0.39	0.23	0.21	0.31	0.26	1.16
41-1	1.00	0.00	0.50	0.41	1.00	0.70	1.42
41-2	1.00	0.00	0.44	0.37	0.78	0.59	1.33
41-5	0.00	1.00	0.50	0.61	1.00	1.59	0.63
41-6	0.00	1.00	0.45	0.66	0.82	1.92	0.43
20-4**)	1.00	0.80	0.90	0.86	8.71	5.94	1.46

*) Run conditions: P_{tot}=2000 bars, T=550°C, t=504 hrs
**) Run no. 20-4 is an unbuffered 4 kb experiment and has not been used in the K_D calculations

1) $X_{NH_4^+}$ i = $NH_4^+/(NH_4^+ + K^+)$ initial molar ratio
2) $X_{NH_4^+}$ f = $NH_4^+/(NH_4^+ + K^+)$ final molar ratio
3) NH_4^+/K^+ f = NH_4^+/K^+ final molar ratio
4) K_D = $(NH_4^+/K^+)_{phlogopite}^{f}/(NH_4^+/K^+)_{vapour}^{f}$

Table 3. Results of the nickel-bunsenite buffered experiments at 650°C. All experiments contained 2.1 molal chloride solutions.

	$X_{NH_4^+}$ i 1)		$X_{NH_4^+}$ f 2)		NH_4^+/K^+ f 3)		
Run no.*)	solid	vapour	solid	vapour	solid	vapour	K_D 4)
42-3	1.00	0.00	0.54	0.40	1.17	0.68	1.74
42-4	1.00	0.00	0.52	0.42	1.09	0.72	1.52
42-7	0.00	1.00	0.60	0.54	1.50	1.21	1.23
42-8	0.00	1.00	0.58	0.51	1.37	1.04	1.32

*) Run conditions: P_{tot}=2000 bars, T=650°C, t=504 hrs
1) to 4) See Table 2 for the notes.

Table 4. Results of the unbuffered reaction rate experiments with 2 molal chloride solutions.

Run no.*)	$X_{NH_4^+}$ i 1) solid	vapour	$X_{NH_4^+}$ f 2) solid	vapour	NH_4^+/K^+ f 3) solid	vapour	K_D 4)	Run time (hrs)
39-4	0.00	1.00	0.17	0.91	0.20	9.86	0.02	1
39-6	1.00	0.00	0.87	0.12	7.01	0.14	51.47	1
39-3	0.00	1.00	0.24	0.85	0.32	5.70	0.06	4
39-5	1.00	0.00	0.84	0.18	5.36	0.23	23.61	4
39-14	0.00	1.00	0.30	0.80	0.43	4.13	0.10	24
39-10	1.00	0.00	0.69	0.26	2.19	0.36	6.09	24
40-16	0.00	1.00	0.37	0.73	0.58	2.68	0.22	48
40-12	1.00	0.00	0.63	0.28	1.68	0.38	4.40	48
40-17	0.00	1.00	0.44	0.68	0.78	2.17	0.36	168
40-13	1.00	0.00	0.58	0.31	1.38	0.44	3.15	168
40-15	0.00	1.00	0.50	0.63	1.02	1.66	0.61	672
40-11	1.00	0.00	0.56	0.36	1.25	0.55	2.28	672

*) Run conditions: P_{tot}=2000 bars, T=550°C.
1) to 4) See Table 2 for the notes

amounts of data are plotted, the results of the buffered runs at 550°C are plotted also in Fig. 5, in which the composition of the vapour is plotted against the composition of the phlogopite (ORVILLE, 1972) and in a logarithmic NH_4^+/K^+ ratio plot (Fig. 6). Bearing in mind the analytical errors of 5 to 10 percent, it is evident from Fig. 5, that it is not possible to evaluate deviations from ideal mixing behaviour in the phlogopite. In addition the reaction-rate runs are plotted in Fig. 6. The non-equilibrium distribution coefficients calculated from these runs are plotted *versus* run time in Fig. 7.

The distribution coefficient at 550°C and 2000 bars has been calculated as the mean of the log K_D^*-values of the oxygen-buffered runs and amounts 1.29 ± 0.30 (calculated without the obvious non-equilibrium runs 17-2, 21-1, 41-5 and 41-6). On the basis of the parallel tie-line positions of the runs at 650°C and 2000 bars equilibrium is assumed and allows the calculation of a preliminary K_D^* of 1.44 ± 0.20.

DISCUSSION

In Figs. 2, 3 and 4 the tie-lines of final vapour and solid composition seldom pass exactly through the rotation point. The deviations may be caused by:

1. *Analytical errors.* These are expected to be within 5% (for the K^+ analysis) to 10% (for the NH_4^+ analysis), considering the small quantities of materials used during the runs and considering the NH_4^+ analytical procedure, which is susceptible to contamination or loss of NH_3- (and N_2-) gas, especially during the opening procedures of the capsules. These errors in themselves could account for all deviations.

2. *Non-equivalent chemical behaviour of the alkali ions.* In contrast to K^+, which is a mono-atomic ion, NH_4^+ is a complex ion. Association with a chloride ion according to the reactions (2) and (3) may change the NH_4^+/K^+ ratio of the vapour. NH_3 and N_2 formation according to reactions (5) and (6) will lower the NH_4^+ concentration, thus lowering the NH_4^+/K^+ ratio of the vapour. However, this cannot be demonstrated in the diagrams of Figs. 2 and 4. The systematic displacement of the tielines towards the potassium side, which is evident in the diagram of Fig. 3, will be discussed under the next point. A reason for not detecting systematically lower $X_{NH_4^+}$ values in the vapour may be that NH_3-gas present at run conditions has been measured as NH_4^+ afterwards, indicating that the amount of N_2 gas was negligible. The change in K_D^* as a function of reaction time (Fig. 7) exhibits a generally symmetrical change in the K_D^* of the reversals, also rejecting the idea of substantial nitrogen formation. A slightly more convex form of the curve determined for the experiments using NH_4-phlogopite as a starting product is apparent. It may indicate the greater ease with which a K^+ ion replaces an NH_4^+ ion in the NH_4-phlogopite structure than the opposite reaction.

3. *Non-stoichiometric composition of the phlogopite.* In Fig. 3, exhibiting the runs with NH_4-phlogopite as the initial solid, a systematic displacement of the tie-lines towards the potassium side of the diagram is obvious. This systematic displacement is absent in Fig. 2, displaying the runs with K-phlogopite as the initial solid. An explanation would be that in the ammonium phlogopite the K-layer is not fully occupied by ammonium. Part of the ammonium and potassium in the vapour will therefore be consumed to occupy the K-layer, which causes a shift of the rotation points and a corresponding shift

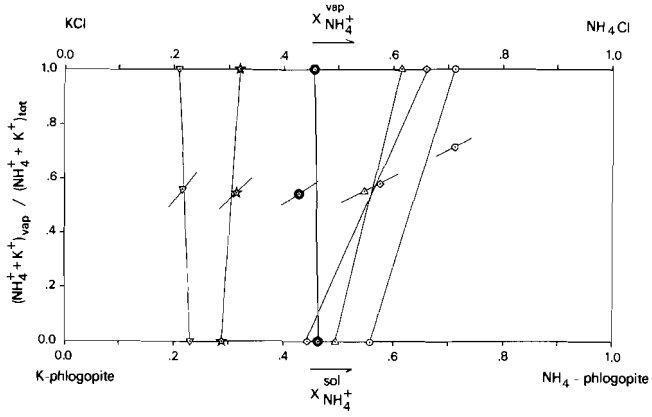

FIG. 2. Results of the runs with K-phlogopite and NH_4Cl/KCl-solutions at 550°C and 2000 bars. For explanation see text. The short lines indicate the initial compositions, the long lines the final compositions. For each run the initially fixed rotation point, the final solid and the final vapour compositions are indicated by identical symbols.

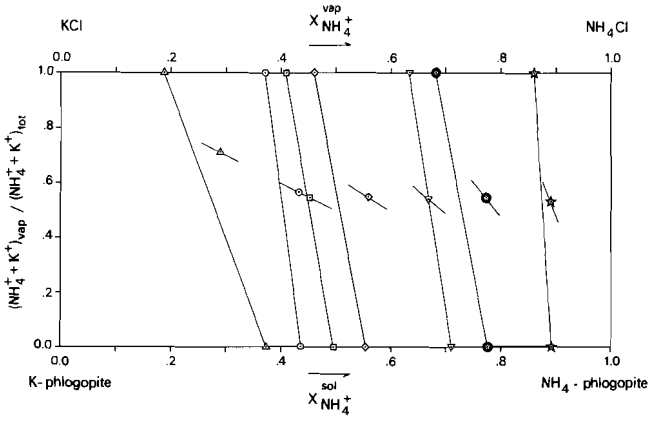

FIG. 3. Results of the runs with NH_4-phlogopite and NH_4Cl/KCl-solutions at 550°C and 2000 bars. For explanation see Fig. 2 and text.

of the tie-lines towards the potassium side of the diagram of Fig. 3. A chemical check with accurate analyses of the ammonium phlogopite endmember produced ammonium yields of 85 to 95 molepercent, confirming this hypothesis.

4. *Open system behavior.* Loss or gain of components in the system may cause systematic shifts of tie-line positions. A well-known cause for the loss of components from the system is the diffusion of hydrogen through the capsule wall. However, diffusion of H_2 through the gold capsule will be negligible at the experimental temperature of 550°C, though some diffusion may take place at 650°C. Evidence for diffusion is absent for both the 550°C and 650°C experiments.

At 550°C the exchange reaction (1) was expected to be at equilibrium within 21 days on the basis of diffusion calculations, using an estimated diffusion rate for an NH_4^+ ion in a K-phlogopite crystal following FREER (1981). The activation energy Q and the preexponential factor D_0 are not known, but Q is estimated to be 100 kJ mole^{-1} based on diffusion data for Rb^+ in biotite (HOFMANN and GILETTI, 1970). For D_0 we have chosen an average (hypothetical) value of 10^{-8} m^2 sec^{-1}. With these data the homogenization of a K-phlogopite crystal of 10 micrometer diameter is reached after *ca.* 6 hours. However the series of runs performed to determine the rate of reaction (1) proves that, at least for starting compositions which require a large shift in the composition of the solid phase, equilibrium was not attained even after 28 days (Fig. 7). The 3 week runs 17-2, 21-1, 41-5 and 41-6, which also demanded a large shift in their solid composition and which apparently have not reached their equilibrium positions, support the observation that the reaction is rather sluggish. Extrapolation of the experimental data allows the prediction of an equilibration time of *ca.* 130 days at 550°C. Runs requiring smaller compositional changes of the solid

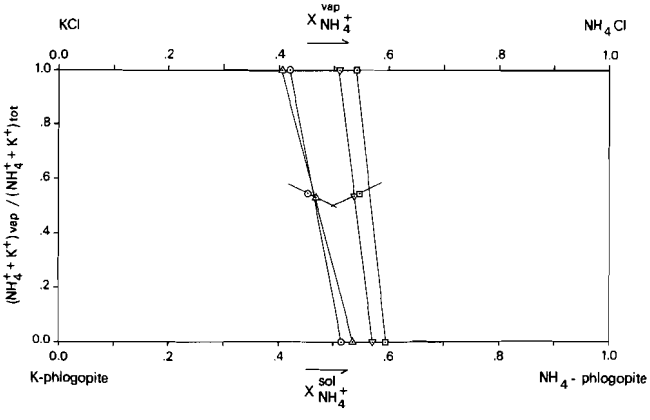

FIG. 4. Preliminary results of the exchange experiments at 650°C and 2000 bars. For explanation see Fig. 2 and text.

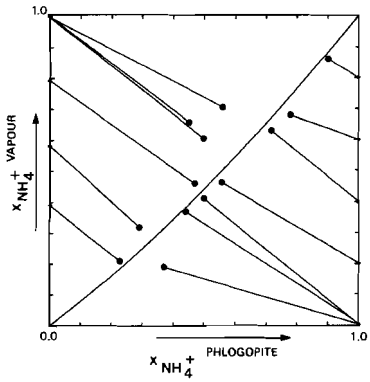

FIG. 5. Distribution plot for the buffered experiments at 550°C. The thin lines in the figure connect initial compositions (small dots) and final compositions (large dots). The curve is drawn for the calculated $K_D^{*phlogopite/vapour}$ of 1.29.

phase have attained the equilibrium of the NH_4^+-K^+ distributions more closely. This is reflected in the more or less parallel tie-line positions, and in the fact that some connection lines of the runs with K-phlogopite as a starting product in contrast to those of the NH_4-phlogopite runs pass thorugh the vertical position. At 650°C equilibrium is reached more rapidly than at 550°C, demonstrated by the parallel tie-line positions for the 3 week duration runs of both reversal pairs, which all required large changes in their solid compositions. The reaction rate is estimated to be roughly 10 times faster at this temperature.

The rather simple exchange reaction (1) was expected to be a first-order reaction, demanding a linear relationship between the logarithm of the concentration *versus* time. The

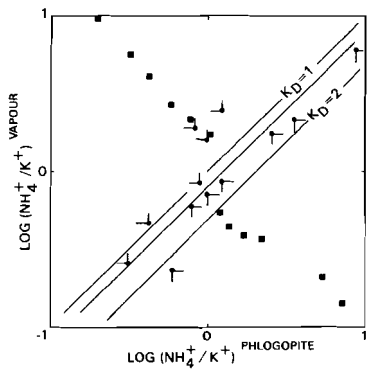

FIG. 6. Logarithmic NH_4^+/K^+ ratio plot for the buffered experiments (dots) and the unbuffered reaction rate experiments (squares) at 550°C. The small lines at the dots indicate for these runs the direction from which the composition of both the vapour (vertical line) and solid phase (horizontal line) is coming. The lines for $K_D^{*phlogopite/vapour}$ equal to 1 and 2 are indicated, with the line for K_D^* = 1.29 in between.

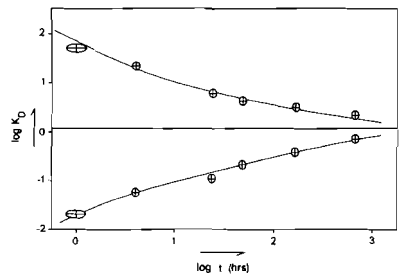

FIG. 7. Log K_D of the reaction rate experiments as a function of log t (run time in hours). The estimated errors are denoted by ellipsoids.

approach to equilibrium composition in the reaction rate experiments, however, is slower than predicted by first-order reaction behaviour and may be caused by kinetic constraints on the diffusion of NH_4^+ and K^+ through the crystal lattice. The relatively large increase in the crystal sizes during the experiments indicates not only pure exchange, but also recrystallization and crystal growth at equilibrium conditions. One of the time consuming factors could be the dissolving of the small initial phlogopite crystals during the growth of the equilibrium phlogopites. Moreover, if the newly formed crystal-material zones grow over the old crystals, diffusional distances increase and it becomes more difficult for the initial crystals to reequilibrate.

BESWICK (1973) presumed a miscibility gap in phlogopite for the analogous Rb^+ exchange reaction at 500°C and 2000 bars. At this moment there is no evidence for an unmixing region in the NH_4^+-K^+ system at the investigated temperature and pressure conditions. XRD patterns show no peak broadening due to the intergrowth of compositionally different phases, and sharp IR-spectrometric absorption bands support arguments for only one homogeneous phase.

Table 5 compares the distribution coefficients obtained in this study with the distribution coefficients of Rb^+ in phlogopite obtained by BESWICK (1973) and VOLFINGER (1976). Additionally in Table 5 the K_D-values for NH_4^+ and Rb^+ in annite/vapour-, muscovite/vapour- and sanidine/vapour-experiments by several authors are listed. The increase in $K_D^{*NH^+4/K^+}$ with temperature for our phlogopite/vapour experiments is consistent with the results of LORCH (1978) on NH_4^+ distributions in his feldspar/vapour experiments, and with the results of the Rb^+ distributions in the experiments of BESWICK (1973), whose experimental methods were comparable to the methods applied in this study. The temperature effect on the distribution coefficient $K_D^{Rb^+/K^+}$ is clearly present for the experiments on phlogopite by VOLFINGER (1976), but it is small or even absent for his experiments on muscovite and sanidine. The validity of the Rb^+ data for muscovite is questionable because of the presence of an unmixing region between potassium and rubidium muscovite up to 600°C (VONCKEN *et al.*, in prep.). A K_D for NH_4^+ comparable to that for Rb^+ should be expected on the basis of their almost equal ionic size, which is confirmed by the results of LORCH (1978), BESWICK (1973) and VOLFINGER (1974) for their feldspar/vapour experiments.

Table 5. A compilation of experimentally determined Rb/K and NH_4/K distribution coefficients

	K_D *)	mCl^- **)	P(kb)	T(°C)						Author
				400	500	550	600	650	700	800	
Phlogopite	NH_4/K	2	2			1.29		1.44			This work
id	Rb/K	***)	1		1.22		1.54			1.89	VOLFINGER (1976)
id	Rb/K	0.7	2		0.64				1.11	1.28	BESWICK (1973)
Annite	Rb/K	***)	1				2.27				VOLFINGER (1974)
Muscovite	Rb/K	***)	1	0.50	0.50		0.48				VOLFINGER (1976)
Sanidine	NH_4/K	4	2	0.15	0.25		0.48				LORCH (1978)
id	Rb/K	****)	0.8				0.42				LAGACHE (1968)
id	Rb/K	***)	1	0.26	0.40		0.42			0.42	VOLFINGER (1976)
id	Rb/K	0.7	2		0.17				0.33	0.45	BESWICK (1973)

*) $K_D = (X^+/K^+)_{phlogopite}/(X^+/K^+)_{vapour}$ (molar ratios); X^+ is NH_4^+ or Rb^+
**) mCl^-: molar chloride concentration
***) mCl^- varying from 3.10^{-2} to 1.5
****) mCl^- varying from 0.25 to 1

GEOLOGICAL APPLICATIONS

1. The experimental results of this study may find geological application in geothermometry. Most experimentally determined NH_4^+ and Rb^+ distribution coefficients for mineral/vapour equilibria correlate positively with temperature (Table 5). The results of LORCH (1978) combined with those of this study predict a temperature dependence of the $K_D^{NH_4^+/K^+}$ between alkalifeldspar and phlogopite expressed by

$$\ln K_D = -2.105 * 10^3/T(\mathrm{K}) + 1.308. \qquad (10)$$

The temperature dependence turns out to be not very strong and an application as geothermometer demands extremely accurate NH_4^+ analyses. With the best existing experimental data and the most precise analytical methods an accuracy of 50–100°C is the best that can be attained.

2. Extrapolation of the K_D to the low NH_4^+ concentrations as they occur in natural rocks allows the calculation of NH_4^+ concentrations in chloride-bearing metamorphic fluids. NH_4^+ concentrations in minerals reflect the composition of the equilibrium metamorphic fluid with respect to nitrogen species. Consider a biotite containing 1000 ppm NH_4^+, which is well above the average natural value and equals an $X_{NH_4^+}$ of *ca.* 0.025, in equilibrium with a chloride-bearing metamorphic fluid. At a P_{fluid} of 2000 bars and a temperature of 550°C the $X_{NH_4^+}$ in the fluid will be *ca.* 0.02. It is assumed that at these conditions NH_4^+ and NH_4Cl are the dominant nitrogen species. Probably the presence of the Cl^- ion in the fluid shifts the reactions (2), (5) and (6) towards the right-hand side, thus minimizing the N_2 concentration.

3. The distribution coefficients may be used in semiquantative modelling of NH_4^+ during metamorphism of individual rock samples. The following closed rock system may serve as an illustration. Consider a pelitic schist containing 38 wt% biotite with an Mg/(Mg + Fe) ratio of 0.30 and an NH_4^+ content of 1500 ppm, 15 wt% muscovite and 2 wt% of a metamorphic fluid as the main NH_4^+-bearing phases. The fluid is assumed to be a 2.1 molal KCl aqueous solution, with small amounts of NH_4Cl equivalents in equilibrium with the biotite at 450°C. The $K_D^{biotite/vapour}$ and its temperature dependence has been estimated from a combination of the experimentally determined NH_4^+ and Rb^+ distribution coefficients for phlogopite and annite (Table 5). The K_D is estimated to be 1 at 450°C and the temperature function is approximately expressed by the equation

$$\ln K_D^* = -1.7074 * 10^3/T(\mathrm{K}) + 2.3611. \qquad (11)$$

The natural $K_D^{muscovite/biotite}$ of 0.43 is derived by HONMA and ITIHARA (1981) and it is assumed to be practically independent of temperature. If the schist in question is heated from 450°C to 650°C, assuming that along the heating trajectory no mineral reactions occur and that the system remains closed and in chemical equilibrium, a redistribution of the NH_4^+ will take place between the fluid and the micas. For the assumed data and limitations the increase in temperature results in an increase of the NH_4^+ concentration in biotite from 1500 ppm to *ca.* 1525 ppm, and in muscovite from 645 ppm to *ca.* 656 ppm. Lower chloride salinites and lower fluid contents, which are more realistic, will produce even smaller increases. A more significant increase in NH_4^+ concentrations can be accomplished by mineral reactions. If an NH_4^+-bearing mineral is consumed by a reaction, the liberated NH_4^+ will be redistributed among the other NH_4^+-incorporating minerals present. Consider the above mentioned schist again; if all of the muscovite broke down to alkalifeldspar at 650°C, while the biotite remained unaffected, the NH_4^+ concentration in the biotite would increase from *ca.* 1500 ppm to 1660 ppm. If half of the biotite reacted to alkalifeldspar, the NH_4^+ concentration of the remaining biotite would increase to *ca.* 2500 ppm. From these arguments it may be concluded that temperature alone has a small effect on the absolute NH_4^+ concentrations in the metamorphic minerals in a closed system under equilibrium conditions and that effective changes in the concentrations can be attained only by reactions affecting NH_4^+-bearing minerals.

4. The progressive enrichment of ammonium in phlogopite is a possible mechanism to store nitrogen in the lower crust. The presence of nitrogen in fluid inclusions in high-grade migmatite and granulite terranes (SWANENBERG, 1980; KREULEN and SCHUILING, 1982; DUIT *et al.*, 1986; VAN DE KERKHOFF, in prep.) may be explained partly by the decomposition of NH_4-phlogopite outside its stability field. Preliminary investigations on the stability of the NH_4-phlogopite indicate decomposition temperatures around 750°C at 2000 bars, which is slightly above the incipient melting temperature of wet granitic compositions. On the other hand, retrogra-

dation of NH_4-bearing biotite in metamorphic rocks into chlorite and muscovite will easily liberate N_2-gas.

CONCLUSIONS

1. At 550 and 650°C and 2000 bars phlogopite favours NH_4^+ over K^+ indicated by a $K_D^{*NH_4^+/K^+}$ between phlogopite and vapour of 1.29 ± 0.30 at 550°C and 1.44 ± 0.20 at 650°C.

2. At 550 and 650°C the phlogopites form a homologous series between the NH_4- and the K-endmember.

3. A positive correlation of the $K_D^{*NH_4^+/K^+}$ between phlogopite and vapour with temperature can be demonstrated experimentally, but the temperature dependence does not appear to be very large.

4. NH_4-phlogopites are stable at the low f_{NH_3}/f_{N_2} ratios present at normal metamorphic conditions.

5. At the experimental conditions the presence of chloride ions favours the development of NH_4^+ ions and NH_4Cl molecules in the solution.

6. Time experiments on the rate of the exchange reaction at 550°C indicate a rather sluggish reaction mechanism. The experiments predict equilibration times of several months for certain compositions.

7. The $K_D^{NH_4^+/K^+}$ between muscovite and vapour and its temperature dependence will be needed before NH_4^+/K^+ distributions can be used as a geothermometer.

8. Reactions affecting NH_4^+-bearing minerals may have large influences on the NH_4^+ concentrations in the remaining NH_4^+-incorporating phases.

9. The increase of the $K_D^{phlogopite/vapour}$ with temperature provides a mechanism to store nitrogen in the lower crust.

Acknowledgements—This experimental petrologic study was performed mainly with financial support of the University of Utrecht. The noble metals were financed partially by the Dr. H. M. E. Schürmann Foundation. We thank Prof. E. Althaus of the University of Karlsruhe for providing the MSc. thesis of R. Lorch, and Jack Voncken for unpublished data on the NH_4-K and Rb-K exchange reaction on muscovite. Further we thank Ger Kastelein for technical assistance in the HPT laboratory, Frits Geelen for performing the SEM work and Charles Laman for providing the X-ray diffractograms. The IR equipment was supplied by WACOM-ZWO. For critical reading of the manuscript and many helpful suggestions leading to substantial improvements, we are gratefully acknowledged to John B. Brady, D. Jenkins, Sakiko Olsen, Olaf Schuiling, Toni Senior, John Valley, Bernard J. Wood, an anonymous reviewer and especially to Lukas Baumgartner and Maria Luisa Crawford for their extensive advice.

Editorial handling: B. J. Wood

REFERENCES

BARKER D. S. (1964) Ammonium in alkalifeldspar. *Amer. Mineral.* **49**, 851–885.

BESWICK A. E. (1973) An experimental study of alkali metal distributions in feldspars and micas. *Geochim. Cosmochim. Acta* **37**, 183–208.

BOS A., HAAS G. J. L. M. DE, VONCKEN J. H. L., EERDEN A. M. J. VAN DER and JANSEN J. B. H. (1987) Hydrothermal synthesis of ammonium-phlogopite. *Geologie en Mijnbouw* **66**, 251–258.

DE ALBUQUERQUE C. A. R. (1975) Partition of trace elements in coexisting biotite, muscovite and potassium feldspar of granitic rocks. Northern Portugal. *Chem. Geol.* **16**, 89–108.

DUIT W., JANSEN J. B. H., BREEMEN A. VAN and BOS A. (1986) Ammonium micas in pelitic rocks as exemplified by Dôme de l'Agout (France). *Amer. J. Sci.* **286**, 702–732.

ERD R. C., WHITE D. E., FAHEY J. J. and LEE D. E. (1964) Buddingtonite, an ammonium feldspar with zeolitic water. *Amer. Mineral.* **49**, 831–849.

EUGSTER H. P. and MUNOZ J. L. (1966) Ammonium micas: possible sources of atmospheric ammonia and nitrogen. *Science* **151**, 683–686.

EUGSTER H. P. and SKIPPEN G. B. (1967) Igneous and metamorphic reactions involving gas equilibria. In *Researches in Geochemistry* (ed. P. H. ABELSON), Vol 2, pp. 492–520. J. Wiley & Sons.

FRANTZ J. D. and POPP R. K. (1978) The ionization constant of HCl as a function of temperature and pressure. *Carnegie Inst. Wash. Yearb.* **77**, 823–826.

FREER R. (1981) Diffusion in silicate minerals and glasses: a data digest and a guide to the literature. *Contrib. Mineral. Petrol.* **76**, 440–454.

FRENCH B. M. (1966) Some geologic implications of equilibrium between graphite and a C-O-H gas phase at high temperatures and pressures. *Rev. Geophys.* **4**, 223–253.

FUNG P. C. and SHAW D. M. (1978) Na, Rb and Tl distributions between phlogopite and sanidine by direct synthesis in a common vapour phase. *Geochim. Cosmochim. Acta* **42**, 703–708.

GLASSLEY W. E., BRIDGEWATER D. and KONNERUP-MADSEN J. (1984) Nitrogen in fluids effecting retrogression of granulite facies gneisses: a debatable mantle connection. *Earth. Planet. Sci. Lett.* **70**, 417–425.

GRUNER J. W. (1939) Formation and stability of muscovite in acid solutions at elevated temperatures. *Amer. Mineral.* **24**, 624–628.

HALLAM M. and EUGSTER H. P. (1976) Ammonium silicate stability relations. *Contrib. Mineral. Petrol.* **57**, 227–244.

HAZEN R. M. and WONES D. R. (1972) The effect of cation substitutions on the physical properties of trioctahedral micas. *Amer. Mineral.* **57**, 103–129.

HELGESON H. C. and KIRKHAM D. H. (1974) Theoretical prediction of the thermodynamic properties of aqueous electrolytes at high pressures and temperatures: I. Summary of the thermodynamic/electrostatic properties of the solvent. *Amer. J. Sci.* **274**, 1089–1198.

HELGESON H. C. and KIRKHAM D. H. (1976) Theoretical prediction of the thermodynamic properties of aqueous electrolytes at high pressures and temperatures. III. Equation of state for aqueous species at infinite dilution. *Amer. J. Sci.* **276**, 97–240.

HIGASHI S. (1982) Tobelite, a new ammonium dioctahedral mica. *Mineral J.* **11**, 138–146.

HITCH B. F. and MESSMER R. E. (1976) The ionization of aqueous ammonia to 300°C in KCl media. *J. Sol. Chem.* **5**, 667–680.

HOFMANN W. A. and GILETTI B. J. (1970) Diffusion of geochronologically important nuclides in minerals under hydrothermal conditions. *Eclogae Geol. Helv.* **63/1**, 141–150.

HONMA H. and ITIHARA Y. (1981) Distribution of ammonia in minerals of metamorphic and granitic rocks. *Geochim. Cosmochim. Acta* **45**, 983–988.

HORI H., NAGASHIMA K., YAMADA M., MIYAWAKI R. and MARUBASHI T. (1986) Ammonioleucite, a new mineral from Tatarazawa, Fujioka, Japan. *Amer. Mineral.* **71**, 1022–1027.

JUSTER T. C., BROWN P. E. and BAILEY S. W. (1987) NH_4-bearing illite in very low grade metamorphic rocks associated with coal, northeastern Pennsylvania. *Amer. Mineral.* **72**, 555–565.

KREULEN R. and SCHUILING R. D. (1982) N_2-CH_4-CO_2 fluids during formation of Dôme de l'Agout, France. *Geochim. Cosmochim. Acta* **46**, 193–203.

LAGACHE M. (1968) Etudes expérimentales de la répartition des éléments-traces entre la leucite, l'orthose et des solutions hydrothermales. *Compt. Rend.* **267**, 141–144.

LAGACHE M. and CARRON M. J. P. (1972) La distribution des éléments alcalins entre les biotites et les muscovites des roches granitiques. *Compt. Rend. Acad. Sci. Paris* **275**, 157–159.

LORCH R. (1978) Verteilungsgleichgewicht von Ammonium- und Kalium-ionen zwischen Silicaten und fluiden Phasen, in Abhängigkeit von Druck und Temperatur. Diplomarbeit, Univ. Karlsruhe.

MEL'NIK YU. P. (1978) *Thermodynamic Properties of Gases and Conditions of Abyssal Petrogenesis.* Naukova dumka, Kiev, 152p.

ORVILLE P. M. (1972) Plagioclase cation exchange equilibria with aqueous chloride solutions: results at 700°C and 2000 bars in the presence of quartz. *Amer. J. Sci.* **272,** 234–272.

PAULING L. (1960) *The Nature of the Chemical Bond, and the Structure of Molecules and Crystals: An Introduction to Modern Structural Chemistry,* 3rd edn. Cornell Univ. Press, 644p.

RITZERT G. and FRANCK E. U. (1968) Electrische Leitfähigkeit wässriger Lösungen bei hohen Temperaturen und Drucken. *Ber. Busenges.* **64,** 798–808.

RYZHENKO B. N. and VOLKOV V. P. (1971) Fugacity coefficients of some gasses in a broad range of temperatures and pressures. *Geochem. Intl.* **8,** 468–481.

SCHAIRER J. F. and BOWEN N. L. (1955) The system K_2O-Al_2O_3-SiO_2. *Amer. J. Sci.* **253,** 681–746.

SHANNON R. D. and PREWITT C. T. (1969) Effective ionic radii in oxides and fluorides. *Acta Cryst.* **B25,** 925–946.

SHAW H. R. and WONES D. R. (1964) Fugacity coefficients for hydrogen gas between 0° and 1000°C, for pressures to 1000 atm. *Amer. J. Sci.* **262,** 918–929.

SHIGOROVA T. A., KOTOV N. V., KOTEL'NIKOVA YE. N., SHMAKIN B. M. and FRANK-KAMENITSKIY V. A. (1982) Synthesis, diffractometry and IR spectroscopy of micas in the series muscovite to the ammonium analog. *Geochem. Intl.* **18,** 76–82.

STEVENSON F. J. (1960) Microdetermination of nitrogen in rocks and silicate minerals by sealed tube digestion. *Anal. Chem.* **32,** 1704–1706.

STULL D. R. and PROPHET H. (1971) *JANAF Thermochemical Tables.* 2nd edn. Natl. Stand. Ref. Data Ser., U.S. Natl. Bur. Standards 37, 1141p.

SWANENBERG H. E. C. (1980) Fluid inclusions in high-grade metamorphic rocks from S.W. Norway. Ph.D. thesis, Univ. Utrecht, 147p.

VERDOUW H., ECHTELD C. J. A. VAN, and DEKKERS E. M. J. (1978) Ammonia determination based on the indophenol formation with sodium salicylate. *Water Research* **12,** 399–402.

VOLFINGER M. (1974) Effet de la composition des micas trioctaédriques sur les distributions de Rb et Cs à l'état de traces. *Earth. Planet. Sci. Lett.* **24,** 299–304.

VOLFINGER M. (1976) Effet de la température sur les distributions de Na, Rb et Cs entre la sanidine, la muscovite, la phlogopite et une solution hydrothermale sous une pression de 1 kbar. *Geochim. Cosmochim. Acta* **40,** 267–282.

VONCKEN J. H. L., WEVERS J. M. A. R., EERDEN A. M. J. VAN DER, BOS A. and JANSEN J. B. H. (1987) Hydrothermal synthesis of tobelite, $NH_4Al_2Si_3AlO_{10}(OH)_2$, from various starting materials and implications for its occurrence in nature. *Geologie en Mijnbouw* **66,** 259–269.

VONCKEN J. H. L., KONINGS R. J. M., JANSEN J. B. H. and WOENSDREGT C. F. (1988) Hydrothermally grown buddingtonite, an anhydrous ammonium feldspar ($NH_4AlSi_3O_8$). *Phys. Chem. Minerals* (in press).

Chapter 4

Supplementary results of ammonium-potassium partitioning experiments between phlogopite and hydrothermal solution and the stability of ammonium- and potassium-phlogopite in the presence of different solutions at 2000 bars.

Abstract

Supplementary results for the distribution of NH_4 between phlogopite and a chloride-containing hydrothermal solution at 650°C and 2000 bars, and at nickel-bunsenite buffered conditions are presented. Combined with the results of the previous Chapter the average distribution coefficient $K_D^{NH4/K}$ between phlogopite and a 2M chloride solution is calculated as 1.33 ± 0.35 (1σ). Unbuffered exchange experiments were also performed at 750 and 850°C, but it appears that the ammonium-endmember becomes unstable at these conditions. The average distribution coefficients for the stable runs are calculated as 1.65 ± 0.85 at 750°C and 1.81 (average of two runs) at 850°C. If these results are combined with the 550°C results of the previous Chapter, the temperature dependence of the distribution coefficient between 550 and 850°C is calculated as: $\log K_D^{NH4/K\ (phlogopite/vapour)} = -243/T + 0.533$.

The stability of ammonium- and potassium-phlogopite has been investigated at the exchange conditions. Potassium-phlogopite is stable in H_2O, HCl and KCl solutions at 650°C. Ammonium-phlogopite is relatively stable in H_2O and NH_4Cl solutions, but is severely attacked by HCl solutions at this temperature. At nickel-bunsenite buffered conditions ammonium-phlogopite becomes unstable above 700°C, and decomposes to the assemblage enstatite-cordierite-(spinel) or enstatite-forsterite-spinel, depending on the composition of the fluid present.

Introduction

Additional results are presented here of experiments on the partitioning of ammonium and potassium between phlogopite and a hydrothermal phase at 650°C and 2000 bars. A part of these experiments was described in Chapter 3. In addition the results of two sets of experiments at 750°C and 850°C are described, also performed at 2000 bars. At these temperatures the ammonium-phlogopite becomes unstable and

Table 4.1. *Results of the nickel-bunsenite buffered experiments at 650°C with 2.1 molal chloride solutions.*

Run no.*)	X_{NH4+}^{i} 1) solid	vapour	s/v-ratio 4)	X_{NH4+}^{f} 2) solid	vapour	NH_4^+/K^+ f 3) solid	vapour	K_D 5)
26-1	0.00	0.20	1.60	0.08	0.07	0.09	0.08	1.13
26-2	1.00	0.78	1.73	0.85	0.87	5.85	6.69	0.87
27-1	0.00	0.42	1.55	0.31	0.25	0.46	0.33	1.37
27-2	1.00	0.59	1.55	0.86	0.77	6.30	3.33	1.89
28-1	0.00	0.61	1.57	0.39	0.28	0.65	0.39	1.66
28-2	1.00	0.40	1.81	0.64	0.62	1.80	1.63	1.10
29-1	0.00	0.79	1.57	0.37	0.34	0.60	0.51	1.14
29-2	1.00	0.20	1.64	0.63	0.63	1.68	1.69	1.00
30-1	0.00	1.00	1.56	0.59	0.45	1.45	0.82	1.77
30-2‡)	1.00	0.00	1.65	0.34	0.40	0.52	0.67	0.77

*) Run conditions: P_{tot} = 2000 bars, T = 650°C, t = 504 hours.
1) $X_{NH4}^{+\ i}$ = $NH_4^+/(NH_4^+ + K^+)$ initial ratio in molar proportions.
2) $X_{NH4}^{+\ f}$ = $NH_4^+/(NH_4^+ + K^+)$ final ratio in molar proportions.
3) $NH_4^+/K^{+\ f}$ = NH_4^+/K^+ final ratio in molar proportions.
4) s/v-ratio = initial phlogopite (mgs.)/initial vapour (mgs.).
5) K_D = $(NH_4^+/K^+)_{phlogopite}^{f}/(NH_4^+/K^+)_{vapour}^{f}$.
‡) The fluid of this experiment was lost almost completely before analysis.

Table 4.2. *Results of the unbuffered experiments at 750° and 850°C. All experiments contained 2.1 molal chloride solutions.*

Run no.*)	X_{NH4+}^{i} 1) solid	vapour	s/v-ratio 4)	X_{NH4+}^{f} 2) solid	vapour	$NH_4^+/K^{+\ f}$ 3) solid	vapour	K_D 5)
750°C								
32-1	0.00	1.00	1.96	0.43	0.38	0.75	0.60	1.25
32-2	1.00	0.00	1.99	0.39	0.35	0.64	0.54	1.17
33-1	0.00	1.00	2.06	0.63	0.28	1.67	0.57	2.95
33-2	1.00	0.00	1.90	0.32	0.31	0.47	0.45	1.06
33-3	0.00	0.39	2.11	0.17	0.07	0.20	0.08	2.71
33-4†)	1.00	0.60	2.04	0.94	0.18	16.24	0.22	73.16
850°C								
31-1†)	0.00	1.00	2.09	n.a.	0.52	n.a.	1.10	n.d.
31-2	1.00	0.00	1.99	0.52	0.40	1.08	0.67	1.62
31-3	0.00	0.40	2.12	0.29	0.17	0.40	0.20	2.00
31-4‡)	1.00	0.61	1.88	0.01	0.59	0.01	1.46	0.01

*) Run conditions: P_{tot} = 2000 bars, t = 168 hours.
1) to 5) See Table 4.1 for the notes.
†) Partly decomposed to enstatite.
‡) Completely decomposed to enstatite, cordierite and spinel.

decomposes, at least in the high ammonium range of the phlogopite solid solution. Only little data is available on the thermal decomposition of ammonium-phlogopite, whereas the stability of potassium-phlogopite is fairly well-known in the presence of pure H_2O.

The stability of potassium-phlogopite in H_2O solutions as a function of temperature was studied by Yoder and Eugster (1954), Crowley and Roy (1964), Luth (1967), Wones (1967) and Yoder and Kushiro (1969). Wendlandt (1981) studied the stability of potassium-phlogopite in H_2O-CO_2 mixtures at high CO_2 ratios. The stability in other solutions has not been studied experimentally. The stability of ammonium-phlogopite has been studied previously by Eugster and Munoz (1966) in a preliminary way: at 600°C and 2000 bars in the presence of H_2O-rich vapour ammonium-phlogopite is decomposed to talc and chlorite.

In addition to the exchange experiments, three sets of experiments to study the stability of ammonium- and potassium-phlogopite are described, all of which were performed at 2000 bars:

1. K-phlogopite with a H_2O, a 2M HCl and a 2M KCl solution at 650°C.
2. NH_4-phlogopite with a H_2O, a 2M HCl, a 1M and a 2M NH_4Cl solution at 650°C.
3. NH_4-phlogopite with a H_2O solution at 700°, 750°, 775° and 800°C.

Experimental and analytical procedures

The experimental procedures for the 650°C exchange and stability experiments are equivalent to the procedures, described in Chapter 3. The experiments were performed in Tuttle-type pressure vessels. The exchange experiments at this temperature were buffered with respect to hydrogen with a Ni-NiO buffer using a double capsule technique. An inner platinum capsule was filled with ammonium- or potassium-phlogopite and solution. The welded capsule was placed in a gold capsule, to which Ni, NiO and deionized water was added. Each gold capsule contained two platinum capsules, one with ammonium-phlogopite and one with potassium-phlogopite as starting mica composition, thus constituting a reversal pair. The 750°C and 850°C exchange experiments were not hydrogen-buffered, and were performed in gold capsules. The stability experiments between 700°C and 800°C were hydrogen-buffered with a Ni-NiO buffer, using the double capsule technique described above. The 750° and 850°C exchange experiments and the stability experiments between 700°C and 800°C were performed in an internally heated pressure apparatus, as described in Chapter 7. In Table 4.1 the starting conditions and the experimental conditions of the exchange experiments at 650°C are listed, whereas the experimental conditions for the exchange experiments at 750°C and 850°C are listed in Table 4.2. The experimental conditions for the runs of set 1 and 2 are given in Table 4.3, and those of set 3 in Table 4.4.

The analytical procedures for the ammonium and potassium determinations are described in detail in Chapter 3. The products of the stability runs of set 1 and 2 were analyzed with ICP emission spectrometry for all elements except for ammonium. All run products were checked by optical microscopy, SEM and XRD.

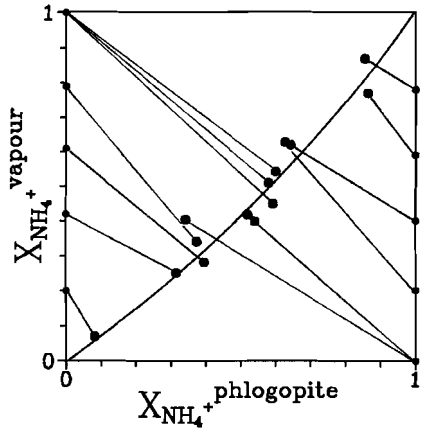

Figure 4.1. *Distribution plot for the experiments at 650°C, including the values obtained in Chapter 3. The final compositions (large dots) are connected with the initial compositions (small dots). The curve is drawn for the calculated average value of 1.33 for the* $K_D^{NH_4/K\ (phlogopite/vapour)}$.

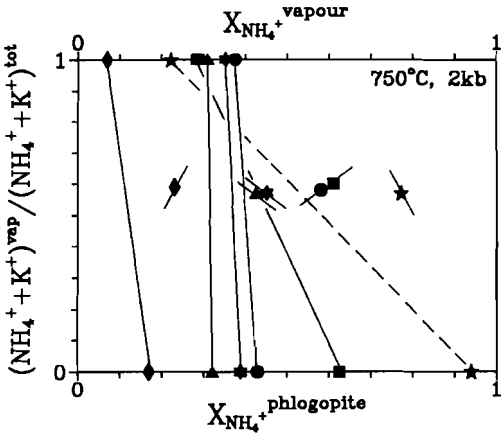

Figure 4.2. *Tie-line diagram for the experiments at 750°C. The short lines indicate the initial compositions of the phlogopite and vapour, the long lines connect the final compositions (see Chapter 3). The dashed line belongs to run 33-4, in which the phlogopite was partly decomposed.*

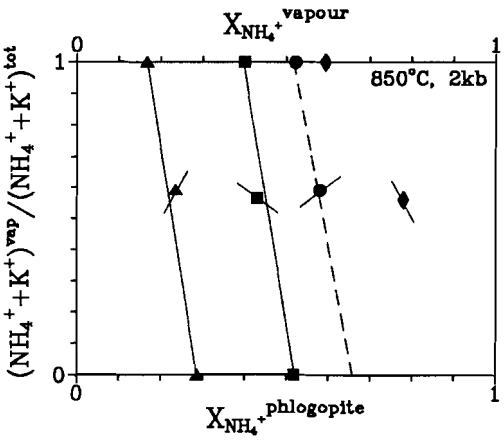

Figure 4.3. *Tie-line diagram for the experiments at 850°C. For an explanation see Figure 4.2 and Chapter 3. The dashed line belongs to run 31-1, of which the phlogopite compositions was not determined. The tie-line for run 31-4, in which the phlogopite was decomposed completely, is not drawn.*

Results

The analytical results of the ammonium and potassium analyses for the exchange experiments at 650°C are tabulated in Table 4.1. In Figure 4.1 the X_{NH4+}-values of the phlogopite are plotted versus the X_{NH4+}-values of the solution (compare Fig. 5 in Chapter 3). The distribution coefficients are calculated following the equations as defined in Chapter 3. The average of the exchange experiments including the 650°C experiments of Chapter 3 is 1.28 ± 0.35 (1σ), which is lower than calculated on the basis of the experiments of Chapter 3 alone. If the very low K_D of run 30-2 (of which run the fluid was lost afterwards almost completely) is omitted, an average value of 1.33 ± 0.32 (1σ) can be calculated. This value is indicated in Figure 4.1. Optical inspection of the phlogopite shows in all cases pure, fine-grained phlogopite. XRD indicates a few percent quartz, but this amount will have only a minor influence on the calculated distribution coefficients.

The results for the experiments at 750° and 850°C are given in Table 4.2. The results for these experiments are plotted in Figure 4.2 resp. 4.3. Optical and XRD inspection of the samples reveals partial or complete decomposition of the phlogopite in the high-ammonium range. The decomposition products are enstatite (A33-4 at 750°C; A31-1 and A31-4 at 850°C), cordierite and possibly spinel (A33-4 and A31-4). The phlogopite in A31-1 showed an enormous increase in crystal size: clear crystals with a diameter of more than 1 mm had formed. The X_{NH4+}-value of these mica crystals was not analyzed and the dashed tie-line in Fig. 4.2 for run A31-1 is based upon the composition of the vapour and of the rotation point. The runs at 750° and 850°C, in which the phlogopite remained stable, all show finegrained aggregates of phlogopite, while sometimes a small quartz crystal is observed. Quartz is present in quantities less than 1 to 2 volume-percent. The average K_D calculated for the 750°C experiments (excluding A33-4) is 1.65 ± 0.85. The average K_D of 1.81 at 850°C is based on the two experiments at the lower ammonium side.

The analytical results for the sets 1 and 2 of the stability experiments are tabulated in Table 4.3. The observed decomposition products are given in this table too. K-phlogopite remains stable in the different solutions, although a small part of the mica is dissolved. NH_4-phlogopite in the H_2O- and HCl-runs is severely attacked and the remaining solid phase has lost most of its ammonium. Optical inspection indicates that mica is still present, and has grown in some cases to 0.2 mm. The observed phases of the stability runs of set 3 are given in Table 4.4. In Figure 4.4 and 4.5 the results of the experiment sets 1, 2 and 3 are plotted in a MgO-SiO_2-Al_2O_3 triangle. In Figure 4.4 the compositions of the phlogopites with the coexisting solutions (sets 1 and 2) are plotted, whereas in Figure 4.5 the compositions of the observed phases of set 2 and 3 are plotted. Also plotted in this figure are the decomposition products talc and chlorite, observed by Eugster and Munoz (1966).

Discussion and conclusions

If the average K_D for the 650°C exchange experiments is compared with the K_D for the 550°C experiments, the difference in average K_D-value appears to be small, especially

Table 4.3. *Analytical results for the phlogopite stability runs with different hydrothermal solutions*[1)]. *For each series of experiments first the composition of the initial phlogopite is given. For the runs the composition of the final phlogopite is given in the first row in molar proportions, in the second row the composition of the reaction solution is given in ppm.*

	solution	K	NH_4	Mg	Al	Si
K-phlogopite		1.0	-	3.0	1.0	3.0
E111	H_2O	1.0	-	3.0	1.0	3.0
		759	-	21.5	25.3	255.9
E112[2)]	2M HCl	1.0	-	3.0	1.0	3.0
		7085	-	1809	26.1	149.0
E168	2M KCl	0.8	-	2.6	1.0	2.8
		58688	-	2567	366.7	1807
NH_4-phlogopite		-	1.0	3.0	1.0	3.0
E113[*)]	H_2O	-	0.04	3.1	1.0	3.9
		-	10400	49.1	96.0	472.4
E114[**)]	2M HCl	-	0.00	3.2	1.0	3.9
		-	26000	2160	51.1	845.3
NH_4-phlogopite		-	0.6	3.4	1.0	3.0
E192[†)]	1M NH_4Cl	-	0.4	3.3	1.0	3.2
		-	374.0	8005	497.5	1326
E193[†)]	2M NH_4Cl	-	0.6	3.4	1.0	3.2
		-	1609	16241	1186	1933

1) Experimental conditions: 650°C, 2000 bars, 336 hours.
2) Part of the solution was lost, so the absolute concentration values will be higher.
*) NH_4-phlogopite partly decomposed to quartz and mullite.
**) NH_4-phlogopite partly decomposed to quartz, mullite and an unidentified Al-silicate.
†) NH_4-phlogopite slightly altered to quartz and forsterite.

Table 4.4. *The stability runs of NH_4-phlogopite under Ni-NiO buffered conditions at temperatures between 700 and 800°C, at a pressure of 2000 bars. Each set consists of an experiment with NH_4-phlogopite as a starting product (first row) and of an oxide mix with NH_4OH as starting products (second row). The phase abbreviations are: NH_4-phlogopite: phl; enstatite: en; forsterite: fo; spinel: sp; talc: tc; quartz: qtz; unidentified Al-silicate: as.*

Run no.	T(°C)	t(hours)	Phases
IH12-1	700	72	phl
-2	700	72	phl
IH13-1	750	48	phl, fo, sp, tc
-2	750	48	phl, qtz, as
IH15-1	775	72	phl, en, fo, sp, tc
-2	775	72	phl, fo, tc, as
IH14-1	800	48	phl, en, fo, sp, tc
-2	800	48	phl, fo, sp, as

Figure 4.4. *Plot of the phlogopite and the hydrothermal solution compositions in the MgO-SiO_2-Al_2O_3 diagram. Coexisting phases are interconnected by tie-lines.*

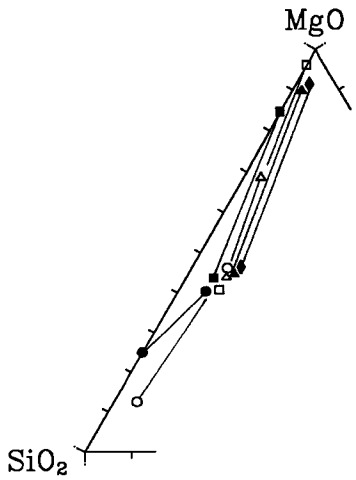

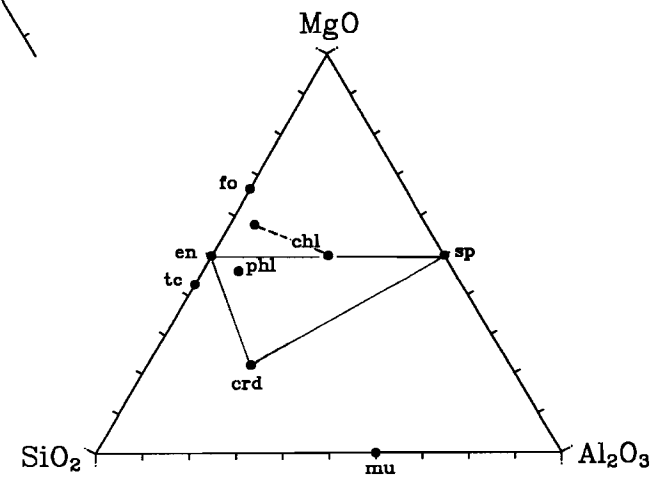

Figure 4.5. *Plot of the observed crystalline phases in the same composition triangle as Figure 4.4. Beside the phases, observed in our experiments, the decomposition products talc and chlorite, as observed by Eugster and Munoz (1966), are plotted. Abbreviations are explained in Table 4.2, except for mu = mullite, and chl = chlorite. For chlorite a composition range is indicated by a dashed line.*

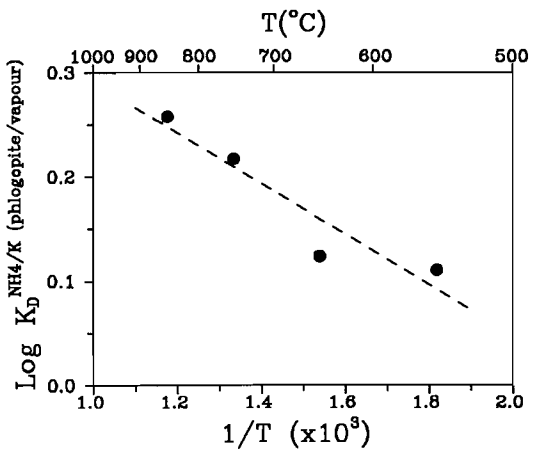

Figure 4.6. *A plot of the log of the distribution coefficients vs. the inverse temperature.*

in relation with the analytical error. If the tie-line diagram of Figure 4.2 is compared with Figure 4.3, and with Figs. 2 to 4 of Chapter 3, a remarkable shift of the tie-lines to more potassium-rich composition is observed at 750°C. If this shift is becoming more pronounced at higher temperatures, then it should be observed also at 850°C. This is not the case. As there were no experimental differences between the runs at 750° and 850°C, an explanation is not at hand at the moment.

The log values of the average K_D's at the different temperatures are plotted versus 1/T in Figure 4.6. The linear relation in this figure is expressed as

$$\log K_D^{NH4/K\ (phlogopite/vapour)} = -243/T + 0.533 \qquad (4.1).$$

The 650°C value for the distribution coefficient seems rather low. A reason other than analytical uncertainty cannot be given at the moment. The experimental and analytical treatment for these experiments was completely identical to the 550°C experiments.
The experiments at 750° and 850°C clearly indicate that under these experimental conditions the stability limit for ammonium-phlogopite is reached. The ammonium-phlogopite decomposes, most probably according to the reaction

$$10\ NH_4\text{-phlogopite} \dashrightarrow 25\ \text{clino-enstatite} + 1\ \text{cordierite} + 3\ \text{spinel} + 10\ NH_3 + 15\ H_2O \qquad (4.2).$$

This reaction is in agreement with the microscopical observation, that clino-enstatite is formed in large quantities, whereas cordierite and spinel are detected mainly with XRD. These observations are discussed hereafter in relation with the observations of the stability experiments on potassium- and ammonium-phlogopite.

The stability experiments indicate that potassium-phlogopite is stable in a H_2O solution, and is even relatively stable in a 2M HCl and KCl solution at 650°C and 2000 bars, although the fluid is clearly Mg-enriched. The ammonium-phlogopite is stable in the NH_4Cl solutions, but is decomposed to a great part in the H_2O and HCl solutions. The decomposition products are mainly quartz and mullite with K and Mg forming soluble Cl-complexes. A comparison with the results of Eugster and Munoz (1966), who observed talc and chlorite as decomposition products, and with the phase triangle in Figure 4.5 suggests that the phases observed in our study may represent metastable phases. Their experiments, which were also performed in H_2O vapour, confirm that NH_4-phlogopite becomes unstable under these conditions. Above 700°C ammonium-phlogopite breaks down in H_2O and a number of decomposition products is observed. The chemical analyses indicate, that the composition of ammonium-phlogopite approaches the theoretical composition, plotted in Figure 4.5. Above the stability field of the hydrous phases talc and chlorite, the decomposition of ammonium-phlogopite would logically produce the assemblage enstatite + cordierite + spinel. This assemblage is indeed observed, as described in the exchange experiments at 750°C and 850°C. The experiments of set 3 however produce no cordierite, but they do produce forsterite and talc. This can be explained, if it is assumed that the true composition of the phlogopite during experimentation shifts to higher Mg and lower Si and Al contents, thus passing the enstatite-spinel tie-line. The SiO_2-rich composition of the H_2O fluid of set 2 suggests, that the composition of the ammonium-phlogopite may indeed shift in this direction. In this way the phlogopite will decompose to enstatite, forsterite and spinel. Talc, which is only observed by XRD, may form during quenching by reaction of forsterite and/or

enstatite with the silica-rich aqueous solution. The unstable exchange experiments contained an NH_4Cl-rich solution, and the analytical results for the solutions of the stability experiments of set 2, containing NH_4Cl, indicate that the composition of the phlogopite will shift in the opposite direction. In this way the formation of cordierite can be explained. The experiments of set 3 indicate a NH_4-phlogopite decomposition temperature between 700° and 750°C at 2000 bars, in an aqueous vapour under Ni-NiO oxygen-buffered conditions.

References

Crowley M. S. and Roy R. (1964) Crystalline solubility in the muscovite and phlogopite groups. Am. Mineral. **49,** 348-362.

Eugster H. P. and Munoz J. L. (1966) Ammonium micas: possible sources of atmospheric ammonia and nitrogen. Science **151,** 683- 686.

Luth W. C. (1967) Studies in the system $KAlSiO_4$-Mg_2SiO_4-SiO_2-H_2O: I, Inferred phase relations and petrologic applications. J. Petrology **8,** 372-416.

Wendlandt R. F. (1981) Influence of CO_2 on melting of model granulite facies assemblages: a model for the genesis of charnockites. Amer. Mineral. **66,** 1164-1175.

Wones D. R. (1967) A low pressure investigation of the stability of phlogopite. Gechim. Cosmochim. Acta **31,** 2248-2253.

Yoder H. S. and Eugster H. P. (1954) Phlogopite synthesis and stability range. Geoch. Cosmoch. Acta, **6,** 157-185.

Yoder H. S. and Kushiro I. (1969) Melting of a hydrous phase: phlogopite. Am. Mineral. **267-A,** 558-582.

Chapter 5

The exchange of K and Mg, and of traces of Li, Rb and Zn between phlogopite and a chloride-solution.

Abstract

Exchange experiments with major and trace elements have been performed between phlogopite and a chloride-bearing hydrothermal solution at 650°C and 2000 bars. The trace elements studied were Li, Rb, Zn, Pb and Cu in concentrations to ca 1000 ppm. The relation of the distribution coefficient K_D for K between solution and phlogopite with the chloride molality was determined as: $K_D^K = 0.23 \times mCl^- + 0.11$. The K_D^{Mg} is low, if compared with the K_D^K. For the K_D^{Mg} the relation with mCl^- was determined as: $K_D^{Mg} = 0.014 \times (mCl^-)_2 + 0.009$. The linear relation of the K_D^{Rb} with mCl^- is poor, but normalized Rb/K-values of the solution and the phlogopite show a good linear relationship: $(Rb/K)^{solution} = 5.07 \times (Rb/K)^{phlogopite}$. The K_D^{Li} between solution and phlogopite is: $K_D^{Li} = 5.38 \times mCl^- + 5.01$. The K_D^{Li} is relatively high and seems to be governed by kinetic and crystallographical constraints. Zn exhibits no clear relation with mCl^-, whereas a relation of the normalized Zn/Mg-values also is not obvious. Zn shows on average a slight preference for the solution. The behaviour of Pb and Cu, which suffer from experimental problems, point to an identical exchange behaviour as Zn. The absence of a clear relation of the K_D^{Rb} and the K_D^{Zn} with mCl^- seems to indicate, that the distribution of these elements is mainly governed by their concentration.

Geological application of the results is restricted at this moment and will need more experimental work.

Introduction

Biotite, $K(Fe,Mg)_3AlSi_3O_{10}(OH)_2$, is a common and often a major mafic constituent of igneous and metamorphic rocks. Biotite is very important in the phase relations of crystalline rocks, of melting country-rock and of crystallizing magma. It is an important host for many ore-forming elements such as Zn, Pb and Cu and ore-related elements such as the alkalis NH_4, Rb and Li. During migmatization and melting of country-rock, the mineral and its stability, therefore, strongly influences the partitioning of the ore-forming and ore-related elements. The stability of the mineral phase is dependent on a number of parameters, of which the most important are the temperature T, the total pressure P, the oxygen fugacity f_{O_2}, the water fugacity f_{H_2O} and the Mg/Fe-ratio X_{Mg}. The stability of the Mg-endmember phlogopite was determined by Yoder and Eugster (1954), while the stability of the Fe-endmember annite was studied by Eugster and Wones (1962). Wones (1963) studied the phase relations of ferri-annite, in which

tetrahedral Al^{3+} is substituted by Fe^{3+}. Wones and Eugster (1965) determined the stability of biotite as a function of X_{Mg}. Depending on oxygen fugacity pure annite may be stable up to 800°C and pure phlogopite almost up to 1100°C. Exchange experiments in chloride-bearing systems by Beswick (1973) and Volfinger (1974, 1976) suggest that phlogopite is a rather stable phase also under these conditions. They do not report phases other than phlogopite after their experiments. After the exchange of Fe and Mg between phlogopite and chloride-bearing solution Schulien (1980) observed the formation of chlorite, probably due to lack of K in the solution. Some additional experiments on the stability of phlogopite in the presence of chloride-bearing hydrothermal solutions are described in Chapter 4.

Substitutions in biotite are common. The positions in the mica may be divided in four groups: 1) the interlayer sites, 2) the octahedral sites, 3) the tetrahedral sites and 4) the sites of the hydroxyl anions. The interlayer sites are predominantly occupied by K, but may also contain Na, Rb, Cs, NH_4, Ca and Ba. The common cations on the octahedral sites are Fe^{2+} and Mg, but substitutions are possible by the monovalent cation Li, the divalent cation Mn and the divalent ore-forming ions like Zn, Co, Ni or Cu. Other substitutions on the octahedral sites include Al, Fe^{3+}, Cr^{3+} and Ti^{4+}. The tetrahedral sites are occupied by Al and Si, but may be substituted by Fe^{3+} (Wones, 1963). Tetrahedral Ti^{4+} is controversial (Hartman, 1969). Studies by Farmer and Boettcher (1981) on phlogopites in South African kimberlites, and by Wendlandt (1977) and by Mansker et al. (1979) on high-Ba phlogopites seem to support the existence of tetrahedral Ti^{4+}. In the high-Ba phlogopites crystallochemical considerations, however, do not favour a tetrahedral position (Bol et al., 1989). The hydroxyl anion is commonly replaced by F and less extensively by Cl. The above mentioned substitutions can be divided in simple exchange reactions and coupled substitutions. One of the most important coupled exchange reactions is the Tschermak exchange:

$$(Mg, Fe^{2+})^{VI} + (Si^{4+})^{IV} \text{ ---> } (Al^{3+})^{VI} + (Al^{3+})^{IV} \qquad (5.1)$$

producing siderophyllite (the Fe^{2+}-rich phase) and Al-rich phlogopite (eastonite in older nomenclature). Ba normally involves a coupled substitution, while the Ti may be incorporated following other reaction schemes, one of which introduces vacancies on the octahedral sites (Dymek, 1983). If Al^{IV} is absent in the phlogopite structure, Li subsitutes for the divalent octahedral cations usually according to the scheme:

$$2(Mg, Fe^{2+})^{VI} \text{ ---> } Li + (Al^{3+})^{VI} \qquad (5.2)$$

Synthetic biotite endmembers with the above mentioned elements are numerous and are summarized by Hewitt and Wones (1984). The most important endmember phlogopite syntheses in the first group are for Na (Carman, 1969), NH_4^+ (Eugster and Munoz, 1966), Rb and Cs (Hazen and Wones, 1972). Ba-phlogopites were synthesized by Frondel and Ito (1967). In the second group biotite endmembers have been synthesized with Mg (Yoder and Eugster, 1954), Fe (Eugster and Wones, 1962; Wones, 1963), Co, Ni and Cu (Hazen and Wones, 1972). In the third group Al^{3+} in phlogopite has been replaced by Fe^{3+} (Wones, 1963) and by Ga^{3+} (Hazen and Wones (1972), while Si^{4+} was replaced by Ge^{4+} (Hazen and Wones, 1972). High-Ti phlogopites, which contain no tetrahedral Ti, were synthesized by Robert (1976). Kovalenko et al. (1968) synthesized high-Ti F-phlogopites and reported tetrahedral Ti. Endmembers in the fourth group have been

made only for F in phlogopite (Takeda and Morosin, 1975) and in annite (Munoz and Ludington, 1974). Synthesizing Cl endmembers appears to be impossible, due to the significantly larger ionic radius of Cl (1.81Å) relative to the ionic radii of OH (1.38Å) and F (1.31Å) (Munoz, 1984). The highest value for a natural chlorine-rich biotite (X_{Mg}=0.44) has been reported by Kamineni et al. (1982), in which slightly more than 13 mole% OH has been substituted by Cl.

Partial substitutions with all above mentioned elements are common in nature, but the experimental determination of partition coefficients between phlogopite and another phase concerns mainly the exchange of the interlayer cation K with Na (Volfinger, 1976), NH_4 (Bos et al., 1988), Rb and Cs (Hofmann and Giletti, 1970; Beswick, 1973; Volfinger, 1974, 1976; Fung and Shaw, 1978), and with the divalent Ba (Krausz, 1974). The exchange behaviour of Li in phlogopite was studied by Iiyama and Volfinger (1976) and Robert et al. (1983). Although Li substitutes for K on the basis of its valency, its size causes Li to occupy pseudo-octahedral sites in the phlogopite structure. Partitioning studies with divalent ions on the octahedral sites are restricted to the Fe-Mg partitioning (Ferry and Spear, 1978; Schulien, 1980). Exchange experiments between the halogens ions F^- and Cl^-, and the hydroxyl ion OH^- were performed by Munoz and Ludington (1974) and Munoz and Swenson (1981).

In this chapter a study on the partitioning of K, Rb, Mg, Li, Zn, Cu and Pb between a synthetic phlogopite and a hydrothermal chlorine-bearing solution is reported. The temperature and pressure conditions were 650°C and 2000 bars respectively. The chloride molality was varied 0.75 and 2. The results for Zn, Cu and Pb are only briefly discussed because of experimental analytical problems with these elements. A short evaluation of the more reliable results for geological implications will be given.

Experimental procedures

Phlogopite was synthesized from $K_2O.2SiO_2$ glass (following Schairer and Bowen, 1955), MgO, γ-alumina, cristobalite and deionized water. All used chemicals were analytical-grade. MgO was heated to 1200°C during 2 hours to remove CO_2 and H_2O, cristobalite was produced by heating amorphous SiO_2 at 1200°C during 24 hours. The oxide constituents were ground and thoroughly mixed under acetone in an achate mortar during 10 to 15 minutes. The powder with excess water was added to a one side welded gold capsule, followed by welding the other end with simultaneous cooling to prevent water loss.

The synthesis was performed at 600°C and 2000 bars during 2 to 3 weeks, using Tuttle-type pressure vessels. Temperatures were recorded with chromalumel thermocouples, calibrated against melting standards. Temperatures are believed to be accurate within ±3°C. Pressures were read with Bourdon-type pressure gauges, regularly calibrated against a Heise precision gauge, and they are accurate within ±50 bars. After the experiments the vessels were quenched to room temperature with compressed air. Quenching time from experimental temperature to 100°C was less than 10 minutes.

The synthetic phlogopite products were checked on purity by optical microscopy and X-ray diffraction. The composition was checked by wet chemical analysis not only for the major elements K, Mg and Al, but also for the trace elements Rb, Li, Cu, Zn and Pb.

Table 5.1. *Wet-chemical analyses of the synthetic phlogopites before (A66, A67) and after (A69 to A72) use in the exchange experiments. The analyses are in moles per formula unit.*

	Analytical technique	K	Mg	Al
A66	AAS	0.97 (average of 2 analyses)		
A67	ICP	0.99	3.0*)	0.96
A69	ICP	0.83	3.0*)	0.96
A70	ICP	0.83	3.0*)	0.92
A71	ICP	0.78	3.0*)	0.91
A71	ICP	0.82	3.0*)	0.93
A72	ICP	0.84	3.0*)	0.93

*) The analyses are normalized to 3 moles of Mg per formula unit.

Table 5.2. *The composition of the reaction solutions, which were used in the exchange experiments. Values for the elements are in ppm. The chloride molality of the different solutions is also indicated.*

	A69	A70	A71	A72	A72
K	46139	35654	18531	18531	17827
Mg	9564	7391	3841	3841	3695
Rb	1020	508	1020	508	254
Li	404	202	404	202	101
Zn	1008	503	1008	503	251
Pb	744	372	744	372	186
Cu	1008	403	1008	403	201

Table 5.3. *The quantities of phlogopite and reaction solution as weighed in the gold capsules. Also indicated are the chloride molality of the reaction solution (mCl^-) and the run duration in hours (hrs). The experimental conditions were 650°C and 2000 bars.*

	phlogopite	solution	phlog./sol.	mCl^-	t(hrs)
A69	81.6	270.0	0.30	1.97	168
A70	81.1	214.1	0.38	1.52	187
A71	82.7	209.1	0.40	0.79	169
A72	80.6	206.5	0.39	0.79	171
A73	84.5	208.0	0.41	0.76	171

Only pure synthetic products were used for the subsequent exchange experiments. The trace elements were in all analyses below the detection limit. Two series of exchange experiments were performed. The reaction solution was prepared by adding in trace concentrations the elements Li, Rb, Zn, Cu and Pb as chlorides to a KCl-$MgCl_2$ solution of varying chloride concentration. The molar K/Mg-ratio in the initial solution was taken at 5, as found in the phlogopite stability experiment in HCl (Chapter 4). Li- and Zn-chloride were produced by chlorination of their carbonates. About 200 to 300 mgs of solution were added to a one-side welded gold capsule first, followed by the addition of ca 80 to 85 mgs of synthetic phlogopite. Next the capsule was welded shut under continuous cooling in a water or ice-water bath. Capsules having weight differences over 0.2 mgs before and after welding were discarded. Welding was done with a carbon-arc. In Tables 5.1 and 5.2 the composition of the initial phlogopite and of the reaction solution is given, while the experimental conditions are tabulated in Table 5.3.

Analytical procedures

The synthetic phlogopite was checked on purity and crystallinity by optical microscopy and by XRD before and after the exchange experiment. After the experiment the gold capsule was thoroughly cleaned with acetone and deionized water. Next the capsule was cut open and the contents were removed. The solids were separated from the solutions with a centrifuge. The solid contents were thoroughly rinsed with deionized water several times. The solute was collected in volumetric flasks and analyzed by ICP (Li, K, Mg, Zn, Pb, Cu), AAS (Li, Rb, Zn) or AES (Rb). AAS/AES analyses were performed with a Perkin Elmer type 460 spectrometer. ICP analyses were performed on a multichannel ICP Optical Emission Spectrograph ARL 34000. The solids were dried at 120°C. For chemical analysis part of the solids were dissolved in a HF/H_2SO_4 mixture at 80°C. After dissolution the clear solution was evaporated to dryness at 160°C and dissolved in 1:1 HCl. This solution was washed in volumetric flasks, diluted and analyzed for the different elements using the techniques as described above. In all cases enough standards were added to detect systematic analytical errors and to correct for matrix effects.

Results

Wet-chemical analyses of the synthetic phlogopite with respect to the major elements, before and after the exchange experiments, are presented in Table 5.1. Optical microscopy of the phlogopite before the exchange experiment shows fine grained mica aggregates of 5 to 10 μm diameter, with some crystals up to 40 μm. About 2 vol% of impurities appear to be present, as observed with optical microscopy. XRD reveals the pattern of a 1M phlogopite, with no others phases detectable. The crystallinity of the phlogopite after the exchange experiments is only slightly improved, which can be concluded by observation with an optical microscope. A few percent of quartz can be detected with XRD after the experiments.

The results of the exchange experiments are given in Table 5.4 for the analyzed

Table 5.4. *Wet-chemical analyses of the major elements K, Mg and Al and of the trace elements in the phlogopite and in the reaction solutions, as analyzed with ICP emission spectroscopy. The values are in ppm. Contrations below the detection limit are designated d.l.*

	Phase	K	Mg	Al	Rb	Li	Zn	Pb	Cu
A69	solution	46792	11523	d.l.	751	395	874	339	118
	phlogopite	80892	181723	64162	241	26.7	281	246	150
A70	solution	36607	7634	d.l.	370	152	271	d.l.	0.3
phlogopite		84183	188824	63833	115	10.5	333	155	53
A71	solution	22003	3133	d.l.	584	343	800	d.l.	5.8
	phlogopite	81443	194103	65398	366	41	412	982	110
A72	solution	24847	3775	d.l.	331	169	360	61	132
	phlogopite	80737	184118	63124	165	17.2	287	131	52
A73	solution	25532	3734	d.l.	179	91	170	d.l.	59
	phlogopite	83251	185542	64217	64	10	259	d.l.	27.6

Table 5.5. *The distribution coefficients for the experiments A69-A73, defined as* $[X]^{solution}/[X]^{phlogopite}$. *The concentrations are expressed in ppm.*

	K	Mg	Rb	Li	Zn	Pb	Cu
A69	0.58	0.063	3.12	14.8	3.12	1.38	0.79
A70	0.43	0.040	3.23	14.5	0.81	-	0.01
A71	0.27	0.012	1.60	8.3	1.94	-	0.05
A72	0.31	0.021	2.00	9.8	1.26	0.46	2.54
A73	0.31	0.020	2.79	9.0	0.65	-	2.79

Table 5.6. *The normalized concentrations in the hydrothermal solution and the phlogopite, and the normalized distribution coefficients, defined as* $[X/Y]^{solution}/[X/Y]^{phlogopite}$. *The element ratios are calculated from the element weight concentrations and are multiplied by a factor of* 10^3. *The concentrations in the solution are placed in the first row, those of the phlogopite in the second row for each sample.*

	Li/K	$K_D^{Li/K}$	Li/Mg	$K_D^{Li/Mg}$	Rb/K	$K_D^{Rb/K}$	Zn/Mg	$K_D^{Zn/Mg}$
A69	8.44	25.57	34.3	233.3	16.05	5.39	75.8	49.1
	0.33		0.15		2.98		1.55	
A70	4.15	33.29	19.9	358.1	10.11	7.40	35.5	20.1
	0.12		0.06		1.37		1.76	
A71	15.59	30.96	109.5	518.3	26.54	5.91	255.3	120.3
	0.50		0.21		4.49		2.12	
A72	6.80	31.93	44.8	479.2	13.32	6.52	95.4	61.2
	0.21		0.09		2.04		1.56	
A73	3.56	29.67	24.4	452.2	7.01	9.12	45.5	32.6
	0.12		0.05		0.77		1.40	

element concentrations. For A69 and A70 the final composition of the reaction solution for K and Mg agrees fairly well with the initial composition. For A71 to A73 the K-concentration of solution has increased significantly, suggesting phlogopite dissolution. For A71 the Mg-concentration of the reaction solution has decreased. Phases other than phlogopite, except for a few percentage of impurities, are not observed. The distribution coefficient K_D for element X is defined as

$$K_D^X = [X]^{solution}/[X]^{phlogopite} \quad (5.3),$$

with X in ppm. The K_D does not imply chemical equilibrium, but is calculated from the observed element concentrations. The calculated distribution coefficients are listed in Table 5.5. For the major elements K and Mg the K_D is plotted against the chloride molality in Figure 5.1 and 5.2 respectively. The K_D^K as a function of chloride molality is calculated as

$$K_D^K = 0.23 \times mCl^- + 0.11 \quad (5.4).$$

For the K_D^{Mg} a power relation with chloride molality is expected on the basis of the following relations. A substitution equation for Mg can be written as

$$Mg^{phlogopite} + 2Cl^{-\,solution} = MgCl_2^{solution} \quad (5.5),$$

giving a reaction constant

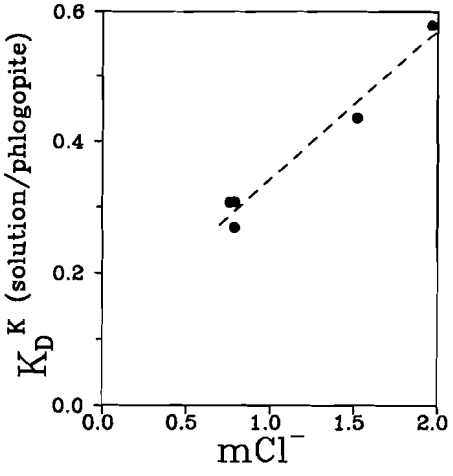

Figure 5.1. *K_D^K versus chloride molality. The K_D is defined as $[X]^{solution}/[X]^{phlogopite}$*

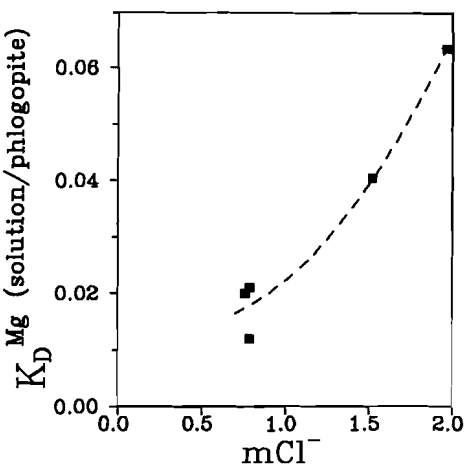

Figure 5.2. *K_D^{Mg} versus chloride molality. For K_D definition see Figure 1.*

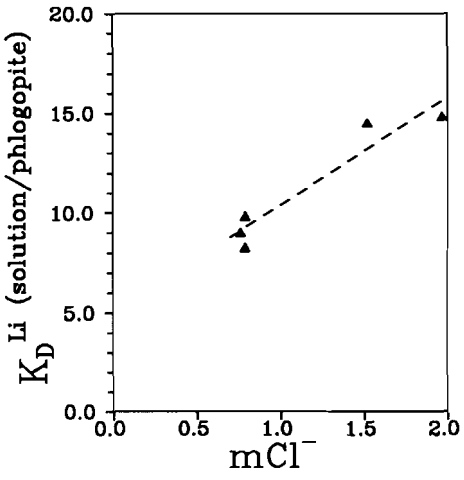

Figure 5.3. *K_D^{Li} versus chloride molality. For K_D definition see Figure 1.*

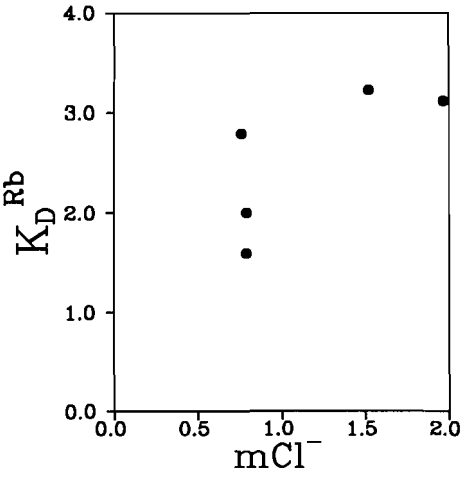

Figure 5.4. *K_D^{Rb} versus chloride molality. For K_D definition see Figure 1.*

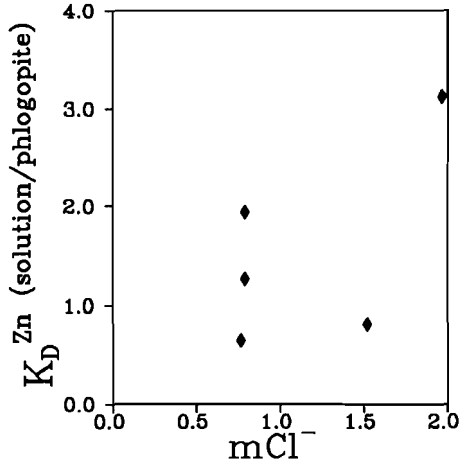

Figure 5.5. *K_D^{Zn} versus chloride molality. For K_D definition see Figure 1.*

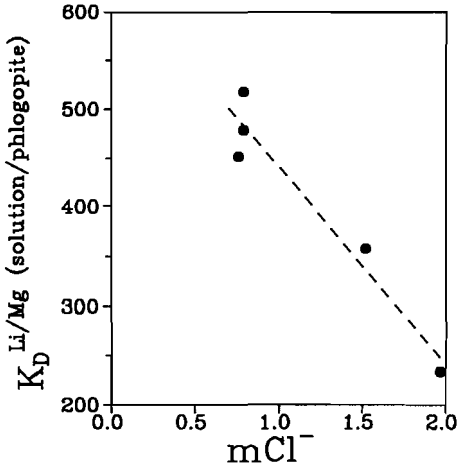

Figure 5.6. *$K_D^{Li/Mg}$ versus chloride molality. The K_D is defined as: $(Li/Mg)^{solution}/(Li/Mg)^{phlogopite}$*

$$K_r = \frac{[MgCl_2]^{solution}}{[Mg]^{phlogopite} \times [Cl^-]^{2\ solution}} \quad (5.6).$$

This relation can be rearranged to obtain the distribution coefficient

$$K_D^{Mg} = \frac{[MgCl_2]^{solution}}{[Mg]^{phlogopite}} = K_r \times (mCl^-)^{2\ solution} \quad (5.7).$$

If applied to the Mg data, this gives the relation

$$K_D^{Mg} = 0.014 \times (mCl^-)^2 + 0.009 \quad (5.8).$$

In Figure 5.3 the K_D for Li is plotted. The calculated linear relation with chloride molality is

$$K_D^{Li} = 5.38 \times mCl^- + 5.01 \quad (5.9).$$

The K_D-values for Rb (Fig. 5.4) and for Zn (Fig. 5.5) show a very poor correlation with the mCl^-. Loss of Cu and Pb during experimentation resulted in only 3 respectively 2 K_D-values.

A normalized distribution coefficient can be defined as

$$K_D^{X/Y} = [X/Y]^{solution}/[X/Y]^{phlogopite} \quad (5.10),$$

where Y is K or Mg. For Li, Rb and Zn the normalized concentrations in the solution and in the phlogopite, and the normalized distributions coefficients are tabulated in Table 5.6. For Li/K, Rb/K and Zn/Mg the distribution coefficient does not provide a better correlation with chloride molality, however for Li/Mg a good, negative linear correlation results (Fig. 5.6). The normalized Li/K and Li/Mg values of the phlogopite are plotted versus those of the solution in Figures 5.7 and 5.8. The linear relations are expressed as

$$(Li/K)^{solution} = 29.5 \times (Li/K)^{phlogopite} \quad (5.11)$$

and

$$(Li/Mg)^{solution} = 480.7 \times (Li/Mg)^{phlogopite} \quad (5.12).$$

Rb/K of the phlogopite versus Rb/K in the solution shows a good linear correlation (Fig. 5.9), according to the least squares fitted equation

$$(Rb/K)^{solution} = 5.07 \times (Rb/K)^{phlogopite} \quad (5.13).$$

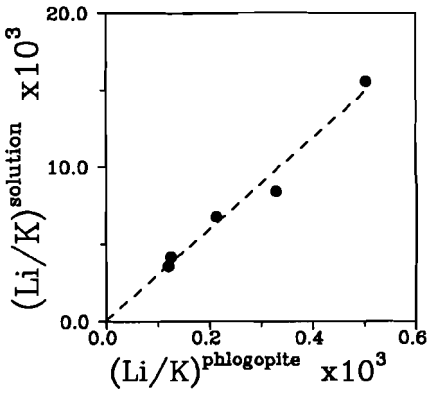

Figure 5.7. *$(Li/K)^{solution}$ versus $(Li/K)^{phlogopite}$. For the Figures 5.7 to 5.10 the element ratios are calculated from the element weight concentrations.*

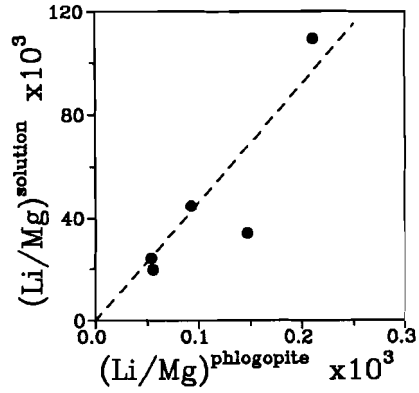

Figure 5.8. *$(Li/Mg)^{solution}$ versus $(Li/Mg)^{phlogopite}$. See caption of Figure 5.7.*

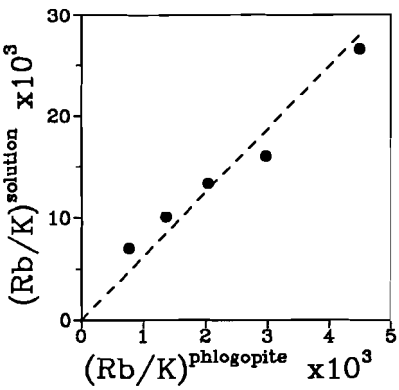

Figure 5.9. *$(Rb/K)^{solution}$ versus $(Rb/K)^{phlogopite}$. See caption of Figure 5.7.*

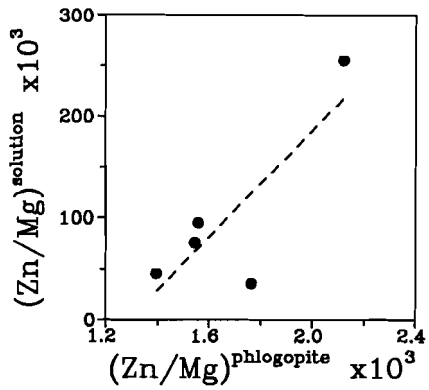

Figure 5.10. *$(Zn/Mg)^{solution}$ versus $(Zn/Mg)^{phlogopite}$. See caption of Figure 5.7.*

The Zn/Mg values of the phlogopite and the solution are plotted in Figure 5.10. Despite the scatter a linear relation is calculated as

$$(Zn/Mg)^{solution} = 265 \times (Zn/Mg)^{phlogopite} - 0.3 \qquad (5.14).$$

Discussion

The major elements K and Mg. The linear relationship of the distribution of major alkali K between phlogopite and hydrothermal solution as a function of chloride molality is clearly demonstrated in Figure 5.1. For the divalent Mg a non-linear relationship is assumed (Fig. 5.2), but the results are certaimly not conclusive enough to support this assumption. The reaction solution is enriched in K relative to the initial solution for all experiments, especially for the low chloride molalities. Mg is enriched in the reaction solution at the chloride molalities of 1.52 and 1.98, but depleted in the low chloride solutions. The low Mg solubility was observed also by Volfinger and Robert (1979). In their experiments a relationship with chloride concentration was absent. The large difference between the K_D^K and the K_D^{Mg} results in a strongly incongruent dissolution of the phlogopite. This may be due to the small grainsize of the reacting phlogopites, which consequently have a large crystal/solution interface area. K especially in the interface area may be preferentially removed relative to the tighter-bound Mg.

The trace elements Li and Rb. The relations for the distribution of the trace alkalis Rb and Li with mCl^- are more like the behaviour of K than of Mg. If this relation is compared with the equilibrium results of Beswick (1973), who obtained for the K_D (defined as: (Rb/K) in the solution/(Rb/K) in the phlogopite) a value of 1.56 at 500°C and of 0.90 at 700°C at a pressure of 2 kb, the K_D value of 5.07 obtained for the experiments of this study is too high. The experiments of Beswick are performed with a high Rb concentration. Volfinger (1976), whose experiments contained Rb in the same concentration range (1-2000ppm) as this study, established a low K_D values of 0.65 at 600°C and of 0.53 at 800°C. The starting solids in his study were gels of phlogopite composition and the phlogopites were synthesized during the 'exchange'. Hofmann and Giletti (1970) obtained distribution coefficients of Rb/K between an alkali chloride solution and a natural biotite at temperatures of 550, 650 and 700°C and 2 kb. Their reversal values of 0.81 to 0.83 were relatively constant, and significantly lower than the experimental results with synthetic phlogopites. Certainly, the annite component of the biotite will have a strong preference for Rb, as predicted by the distribution value of 0.44 between chloride solution and annite, determined by Volfinger (1974) at 600°C and 1 kb. Our experiments are dependent on solid state diffusion and they probably do not represent chemical equilibrium. In Chapter 3 a comparison is made between the distribution behaviour of NH_4 and Rb in phlogopite. The NH_4 partitioning results appeared to be comparable with similar experiments for Rb by e.g. Beswick (1973). The kinetics of NH_4 partitioning was studied at a temperature of at 550°C. It was demonstrated that equilibrium could be approached after ca 28 days. If the comparison remains valid at higher temperatures, the run time of 7 days would be sufficient for the Rb exchange to approach equilibrium. The fact that this seems not to be the case if compared with other studies, seems to indicate a kinetic exchange barrier, leaving Rb in

excess in the fluid.

Theoretically Li behaves differently from the other alkalis, because of its very small size. Although it may substitute for K, its size forces Li to occupy a (pseudo-)octahedral site (Robert et al., 1983). The plots of Li/K and Li/Mg (Figs. 5.7 and 5.8) give evidence for a preference of Li for K- instead for Mg-substitution. An explanation for the rather low Li concentrations of the phlogopite may be, that Li substitutes for Mg according to reaction (5.2). Some dissolution of the phlogopite during the experiment may provide Al, which can be incorporated on octahedral positions. However, the Al concentrations of the solution are for all experiments below the detection limit of the analytical procedure, and therefore only a very limited substitution seems possible. A $K_D^{Li/K}$ of 0.4 is found after crystallization of a synthetic phlogopite in the presence of a hydrothermal solution, containing Li concentrations below 100ppm (Iiyama and Volfinger, 1976; Volfinger and Robert, 1979). They obtained values for the $K_D^{Li/K}$ of 30 to 40 for the high Li runs. In their experiments the kinetic exchange barrier was circumvented by the direct crystallization from a stoichiometric gel, resulting in distribution values, which are not comparable directly with true exchange experiments.

The divalent trace elements Zn, Pb and Cu. The K_D^{Zn} versus mCl^- (Fig. 5.5) does not display an obvious relation. For the Zn/Mg in the solution versus the phlogopite (Fig. 5.10) a linear relation is more pronounced. Cu and Pb are suspected to suffer from absorption by the gold capsule, which is observed also in the melt-solution distribution experiments of the next chapters. The assumption, that the oxygen fugacity is high enough during the experiments to have all elements in the ionic state, may not be correct. Apparently a reaction occurs, producing metallic Cu and Pb. The K_D results for these elements indicate a distribution behaviour more or less comparable with Zn. However, the valid experiments are too few to draw conclusions.

Metallogenic and geological implications. The absence of a clear linear relationship for the trace elements Zn and also Rb with chloride molality and the presence of a linear relationship of the normalized concentrations of most trace elements in the solution versus the phlogopite, seems to indicate, that the chloride molality is not the primary factor, which influences the distribution. The distribution of Rb and Zn is primarily determined by the concentration of these trace elements. Geological applications of the results of the experiments are limited at the moment. Probably all trace elements represent more or less non-equilibrium conditions, due to kinetic exchange constraints and reversal experiments will be needed. From the present experiments the strong preference of Mg for the phlogopite is notable. The preference of Li for the solution instead of the phlogopite is remarkable, but this may be caused by the absence of sufficient Al, to perform the coupled substitution (2). Rb shows a slight preference for the solution at all chloride molalities. Li and Rb behave more like K in their exchange behaviour than Mg. The elements Zn and Pb seem to prefer the phlogopite phase at low chloride molalities, but more experiments are needed for reliable conclusions.

Conclusions

Exchange experiments between phlogopite and a hydrothermal solution were performed in the stability field of the phlogopite.

For K and Mg a linear relationship of the distribution coefficient with chloride molality is observed. The K_D for these elements approaches equilibrium and is calculated as $K_D^K = 0.23 \times mCl^- + 0.11$ and $K_D^{Mg} = 0.014 \times (mCl^-)^2 + 0.009$.

The values for the K_D^{Rb} seem to be non-equilibrium values if compared with other studies. Comparison with NH_4 indicate slower reaction kinetics than expected.

Li concentrations after the exchange experiments are low in the phlogopite. The exchange seems to be influenced by a slow exchange process and by a low availability of Al for coupled Li-Al substitution for Mg.

Zn distributions indicate a preference of the phlogopite for Zn at very low chloride molality.

The Pb and especially Cu suffer from absorption by the capsule wall.

References

Beswick A. E. (1973) An experimental study of alkali metal distributions in feldspars and micas. Geochim. Cosmochim. Acta **37,** 183-208.

Bol L. C. G. M., Bos A., Sauter P. C. C. and Jansen J. B. H. (1989) Barium-titanium-rich phlogopites in marbles from Rogaland, southwest Norway. Amer. Mineral. **74,** 439-447.

Bos A., Duit W., van der Eerden, A. M. J. and Jansen J. B. H. (1988) Nitrogen storage in biotite: An experimental study of the ammonium and potassium partitioning between 1M-phlogopite and vapour at 2kb. Geochim. Cosmochim. Acta **52,** 1275-1283.

Carman J. H. (1969) The study of the system $NaAlSiO_4$-Mg_2SiO_4-SiO_2-H_2O from 200 to 5000 bars and 800°C to 1100°C and its petrologic application. Ph.D.Thesis, Penn. State Univ., 290pp.

Dymek R. F. (1983) Titanium, aluminium and interlayer cation substitutions in biotite from high-grade gneisses, West Greenland. Amer. Mineral. **68,** 880-899.

Eugster H. P. and Munoz J. L. (1966) Ammonium micas: possible sources of atmospheric ammonia and nitrogen. Science **151,** 683- 686.

Eugster H. P. and Wones D. R. (1962) Stability relations of ferruginous biotite, annite. J. Petrol. **3,** 82-125.

Farmer G. L. and Boettcher A. L. (1981) Petrologic and crystal-chemical significance of some deep-seated phlogopites. Amer. Mineral. **66,** 1154-1163.

Ferry J. M. and Spear F. S. (1978) Experimental calibration of the partitioning of Fe and Mg between biotite and garnet. Contrib. Mineral. Petrol. **66,** 113-117.

Frondel C. and Ito J. (1967) Barium-rich phlogopite from Långban, Sweden. Ark. Mineral. Geol.

4, 445-447.
Fung P. C. and Shaw D. M. (1978) Na, Rb and Tl distributions between phlogopite and sanidine by direct synthesis in a common vapour phase. Geochim. Cosmochim. Acta **42,** 703-708.
Hartman P. (1969) Can Ti^{4+} replace Si^{4+} in silicates? Mineral. Mag. **37,** 103-129.
Hazen R. M. and Wones D. R. (1972) The effect of cation substitutions on the physical properties of trioctahedral micas. Amer. Mineral. **57,** 103-129.
Hewitt D. A. and Wones D. R. (1984) Experimental phase relations of the micas. In: Bailey S. W. (ed.) Reviews in mineralogy Vol.13: Micas, 584pp.
Hofmann A. W. and Giletti B. J. (1970) Diffusion of geochronologically important nuclides in minerals under hydrothermal conditions. Eclogae geol. Helv. **63,** 141-150.
Iiyama J. T. and Volfinger M. (1976) A model for trace-element distribution in silicate structures. Mineral. Mag. **40,** 555-564.
Kamineni D. C., Bonardi M. and Rao A. T. (1982) Halogen-bearing minerals from Airport Hill, Visakhapatnam, India. Amer. Mineral. **67,** 1001-1004.
Kovalenko N. I., Kashayev A. A., Znamenskiy Ye. B. and Zhuravleva R. M. (1968) Entry of titanium into micas (experimental studies). Geochem. Int. **5,** 1099-1107.
Krausz K. (1974) Potassium-barium exchange in phlogopite. Can. Mineral. **12,** 394-398.
Mansker W. L., Ewing R. C. and Keil K. (1979) Barium-titanian biotites in nephelinites from Oahu, Hawaii. Amer. Mineral. **64,** 156-159.
Munoz J. L. (1984) F-OH and Cl-OH exchange in micas with applications to hydrothermal ore deposits. in: Bailey S. W. (ed.) Reviews in Mineralogy Vol.13: Micas, 584pp.
Munoz J. L. and Ludington S. (1974) Fluorine-hydroxyl exchange in biotite. Amer. J. Sci. **274,** 396-413.
Munoz J. L. and Swenson A. (1981) Chloride-hydroxyl exchange in biotite and estimation of relative HCl/HF activities in hydrothermal fluids. Econ. Geol. **76,** 2212-2221.
Robert J. L. (1976) Titanium solubility in synthetic phlogopite solid solutions. Chem. Geology **17,** 213-227.
Robert J. L., Volfinger M., Barrandon J. N. and Basutçu M. (1983) Lithium in the interlayer space of synthetic trioctahedral micas. Chem. Geology **40,** 337-351.
Schairer J. F. and Bowen N. L. (1955) The system K_2O-Al_2O_3-SiO_2. Amer. J. Sci. **253,** 681-746.
Schulien S. (1980) Mg-Fe partitioning between biotite and a supercritical chloride solution. Contrib. Mineral. Petrol. **74,** 85-93.
Takeda H. and Morosin B. (1975) Comparison of observed and predicted structural parameters of mica at high temperatures. Acta Crystall. **B31,** 2444-2452.
Volfinger M. (1974) Effet de la composition des micas trioctaédriques sur les distributions de Rb et Cs à l'état de traces. Earth. Planet. Sci. Lett. **24,** 299-304.
Volfinger M. (1976) Effet de la température sur les distributions de Na, Rb et Cs entre la sanidine, la muscovite, la phlogopite et une solution hydrothermale sous une pression de 1 kbar. Geochim. Cosmochim. Acta **40,** 267-282.
Volfinger M. and Robert J. L. (1979) Le lithium dans une phlogopite de synthèse. Bull. Minéral. **102,** 26-32.
Wendlandt R. F. (1977) Barium-phlogopite from Haystack Butte, Highwood Mountains, Montana. Carnegie Institution of Washington Year Book **76,** 534-539.
Wones D. R. (1963) Phase equilibria of "ferriannite", $KFe_3^{2+}Fe^{3+}Si_3O_{10}(OH)_2$. Amer. J. Sci. **261,** 581-596.
Wones D. R. and Eugster H. P. (1965) Stability of biotite: experiment, theory and application. Amer. Mineral. **50,** 1228- 1272.
Yoder H. S. and Eugster H. P. (1954) Phlogopite synthesis and stability range. Geochim. Cosmochim. Acta, **6,** 157-185.

Chapter 6

The partitioning of Na, K, Li, Zn and Pb between a haplogranitic melt and chloride-bearing solution at 850°C and 5kb.

Abstract

The partitioning of the trace elements Li, Zn and Pb and of the major elements Na and K between a haplogranitic liquid and a chloride solution has been studied experimentally as a function of chloride concentration to a maximum of 4 mCl^-, at 850°C and 5 kb. The distribution coefficients for K, Na and Li between hydrothermal solution and melt exhibit a linear relationship with chloride molality with K_D slope of 0.26, 0.40 and 0.33 respectively. Li distribution coefficients are intermediate between the data for Na and K, but were expected to be smaller than for Na on the basis of its smaller radius. It is therefore concluded, that Li follows an exchange mechanism different from the major alkalis. The distribution coefficients for Zn and Pb between solution and melt are related linearly to the squared chloride molality, with K_D slopes of 0.68 and 1.09 respectively. Zn partitioning coefficients agree fairly well with published results of Holland (1972), while both Zn and Pb partitioning coefficients are intermediate between the results from Holland (1972) and Urabe (1985). This study has applications in geology regarding magma-vapour interaction and ore deposition. In the simple haplogranitic system all alkalis partition preferentially in the melt up to chloride molalities of ca 3 for Na and even 4 for K, with Li in between. The divalent Zn and Pb are enriched strongly in the vapour phase at already very low chloride molalities, which indicates only few accommodating sites for these ions. Interaction of the granite with a chloride solution will cause K enrichment of the granite with respect to Na and Li, and a strong depletion with respect to Zn and Pb.

Introduction

Experimental studies on the distributions of major and trace elements between granitic liquids and solutions are of vital importance for explaining the ore-forming processes related to granite bodies. Elaborate work was performed by Holland (1972), who studied the partitioning of Na, K, Ca, Mg, Mn and Zn between a high-silica melt and a chloride solution. A notable investigation was reported recently by Urabe (1985), who demonstrated a relation between element partitioning and alkalinity of the granitic melt. Many experimental studies on element partitioning are difficult to interpret and

provide ambiguous results, which are mutually contradictory. Probably the experimental results are strongly influenced by small, easily overlooked differences in the starting compositions of the melt and the hydrothermal solution. Compositional factors which are of importance in this respect may be the OH- and H_2O-content (Oxtoby and Hamilton, 1978), the Cl-content (Kilinc and Burnham, 1972; Burnham, 1979), the alkalinity (Urabe, 1985), the silica content (Brückner, 1983), the hydrogen fugacity f_{H2} (Luth and Boettcher, 1986) and the presence of major divalent ions in the experimental melt composition (Naney and Swanson, 1980). Physical factors are the experimental temperature and pressure, especially the PT-conditions in relation to the distance above the liquidus surface. All factors influence directly or indirectly the degree of polymerization of the melt structure, which in its turn has effects on the available sites for trace elements and thus on their equilibrium concentration. Certainly the time necessary for reaching equilibrium will be influenced by changes in melt structure and the approach of chemical equilibrium has to be demonstrated in all experimental studies. To prevent a shift of the melt composition with respect to the major elements by reaction with the hydrothermal solution during the experiment, the solution must contain these elements already in equilibrium concentrations.

The purpose of this study is to determine the partitioning coefficients of Li, Zn, Cu, Sn and Pb in trace concentrations, and of Na and K in main concentration between a haplogranitic melt and a hydrothermal solution as a function of chloride concentration (up to 4 mCl^-) for a constant melt composition at 850°C and 5 kb. Na, K and Zn distributions are reported by Holland (1972) for a melt of granitic composition for chloride molalities in the solution up to 6, at ca 850°C and 2 kb. Urabe (1985) determined the distribution of Na, Pb and Zn between an alkaline and a peraluminous granitic melt containing Na and Ca, but no K, and a hydrothermal chloride containing solution at 800°C and 3.5 kb. Experimental Li distributions are not reported in the available literature. Cu, Zn and Pb distribution coefficients are reported by Khitarov et al. (1982) between a melt of granitic composition and a NaCl containing hydrothermal solution at 700-900°C and 2-3 kb. The starting melt compositions were prepared from natural porphyritic biotite granites of unknown composition. Rhyabchikov et al. (1981) determined the concentration of Cu in a haplogranitic melt and a chloride containing solution at 750°C and 1.5 kb under nickel-bunsenite buffered conditions. Candela and Holland (1984) studied the partitioning behaviour of Cu between a granitic melt of similar composition as used by Holland (1972) and a chloride containing solution at 750°C and 1.4 kb. The distribution of Sn was studied by Nekrasov et al. (1980) between a quartz-albite melt and chloride containing solution at 850°C and 1 kb, under oxygen-buffered conditions. Manning (1981) studied the distribution of Sn between a haplogranitic melt and a F-containing solution at 800°C and 1 kb.

The experimental conditions (850°C and 5kb) of this study resemble those in migmatitic and charnockitic areas where during migmatisation granitic liquids were formed, causing a redistribution of both major and trace elements between the different phases. Chlorine as complexing agent in the fluid has been chosen because fluid inclusion and theoretical studies point at the very important role of chloride complexes during magmatic processes (Roedder, 1984; Eugster, 1985). Moreover chlorine has a very low solubility in magmatic liquids and it does not form stable minerals (Burnham, 1979).

Distribution coefficients

Holland (1972) published the equilibrium distribution of the monovalent Na^+-and K^+-ion between silicate melt and a hydrothermal chloride solution. The Na-distribution is linearly dependent on the chloride concentration of the solution. Following Holland (1972) the distribution coefficient of Na between melt and vapour is defined as:

$$K_D^{Na}(vap/melt) = \frac{m_{NaCl}^{vap}}{m_{NaO_{0.5}}^{melt}} = k(1) \times mCl^- \qquad (6.1)$$

K_D is the distribution coefficient, m is the molarity, vap is vapour, k(1) is a constant and mCl^- is the chloride molality of the solution. The linear relationship is valid even for rather high concentrations (Holland, 1972; Urabe, 1985; this work). The equation can be written in a similar way for all monovalent alkali ions like K or Li. It is established that the solubility of chlorine in the silicate melt is very low (Kilinc and Burnham, 1972) and it is therefore assumed that all chlorine is present in the solution.

Following Urabe (1985) the exchange reaction for divalent ions between silicate melt and chloride solution at equilibrium can be written as

$$MeCl_2^{vap} + 2NaO_{0.5}^{melt} = MeO^{melt} + 2NaCl^{vap} \qquad (6.2)$$

Na in equation (6.2) stands for any monovalent alkali element in the system. The reaction constant K_{eq} for this equation can be expressed as

$$K_{eq} = \frac{m_{MeO}^{melt} \times (m_{NaCl}^{vap})^2}{m_{MeCl_2}^{vap} \times (m_{NaO_{0.5}}^{melt})^2}$$

$$= \frac{X_{MeO}^{melt} \times (X_{NaCl}^{vap})^2}{X_{MeCl_2}^{vap} \times (X_{NaO_{0.5}}^{melt})^2} \times \frac{a_{MeO}^{melt} \times (a_{NaCl}^{vap})^2}{a_{MeCl_2}^{vap} \times (a_{NaO_{0.5}}^{melt})^2} \qquad (6.3)$$

where X is the concentration of the complex and a is the activity coefficient.

The divalent metaloxide is assumed to be diluted in the melt. Then the activity coefficient a^{MeO}_{melt} will approach 1, and equation (6.3) combined with (6.1) reduces to

Table 6.1. *Initial composition of the 5kb glass. The oxide concentrations are given in weight percentage.*

	1)	2)	3)
SiO_2	78.0	70.9	77.6
Al_2O_3	13.3	12.1	12.6
K_2O	3.99	3.63	4.63
Na_2O	4.71	4.29	5.14

1) waterfree composition, measured with ICP
2) composition, recalculated to a 9 wt% H_2O content
3) theoretical waterfree composition (Luth, Jahns and Tuttle, 1964)

Table 6.2. *Initial (first row) and final (second row) compositions (in ppm) of the reaction solutions. The pH of the unreacted and reacted solution is mentioned similarly. The chloride molality is given for the unreacted solution only. Element concentrations below the detection limit are designated d.l.*

	A11	A17	A18	A14	A15*)	A16	A12	A13	A19	A20
Al	---	---	---	---	---	---	---	---	---	---
	d.l.	d.l.	d.l.	d.l.	---	d.l.	d.l.	10.7	35.1	192.9
K	7310	14619	21925	29260	36557	7310	14619	21925	29260	36557
	7998	12369	15922	25340	---	5732	14689	19547	25844	33216
Na	13454	26879	40309	53761	67193	13454	26879	40309	53761	67193
	14897	27637	38971	48787	---	16223	25946	35530	50374	66379
Li	199.7		(all solutions)							
	34.5	47.0	52.1	56.7	---	30.2	46.9	59.0	52.6	80.2
Pb	1018		(all solutions)							
	39.6	226	d.l.	402	---	d.l.	289	316	513	568
Zn	502.1		(all solutions)							
	200	196	10.6	331	---	27.6	171	366	237	411
Cu	500.3		(all solutions)							
	28.1	32.3	24.2	37.2	---	24.7	32.1	29.2	35.7	44.1
Sn	5584			(only for the solutions with mCl^- of 3.09 and 3.86)						
	---	---	---	d.l.	---	---	---	---	d.l.	12.1
mCl	0.77	1.55	2.32	3.09	3.86	0.77	1.55	2.32	3.09	3.86
pH	1.78	2.02	1.89	1.14	1.05	1.78	2.02	1.89	1.14	1.05
	6.71	6.63	---	6.62	---	7.11	6.55	6.5	7.01	7.10

*) The reaction solution of this experiment was lost afterwards.

$$K_D^{Me}(vap/melt) = \frac{X_{MeCl_2}^{vap}}{X_{MeO}^{melt}} = \frac{k(1)^2}{K_{eq}} \times (mCl^-)^2$$

$$= k(2) \times (mCl^-)^2 \qquad (6.4)$$

where k(2) is a constant.

For traces of divalent metal ions the distribution coefficient should produce a linear relationship with the squared chloride molality (Holland, 1972; Urabe, 1985). The deviation from the linear relation reported by Khitarov et al. (1982) is explained by Urabe (1985) as the result of an unintended shift in alkali concentration of the melt composition during prolonged experimentation.

For traces of trivalent ions a similar systematic linear relationship of the distribution coefficient with the cubed chloride molality is proposed by Flynn and Burnham (1978).

Experimental procedures

The starting glass compositions were prepared according to the gel preparation method described by Hamilton and Henderson (1968). The gels were fired at 1200°C during 30 minutes under atmospheric conditions causing complete vitrification. The glasses were carefully ground in an achate mortar and stored in a desiccator until the preparation of the run capsules. SiO_2 contamination by grinding was not detected. An ICP emission spectrography analysis of the starting glass is given in Table 6.1 and is compared with the eutectic composition in this system at 5kb (Luth, Jahns and Tuttle, 1964).

The experimental solution containing Na, K, Li, Zn, Cu, Sn and Pb was prepared from analytical grade chlorides except for Li and Zn. These two elements were added as chlorides, prepared by chlorination of carbonates. Sn was added only to the two solutions with the highest chloride molality, because it hydrolyzed rapidly in the low chloride solutions. A relatively high concentration of this element was added, as a loss during experimentation was expected. The initial Na and K concentrations were calculated from the distribution coefficients provided by Holland (1972) to approach their equilibrium concentrations at the involved P and T. Initial element concentrations in the experimental solution are listed in Table 6.2.

The capsules were prepared from platinum tubing of 4.1 or 5.4 mm inner diameter with 0.2 mm wall-thickness. The capsules were welded with a carbon-arc. Weighed quantities of experimental solution and starting glass (Table 6.3) were added to a one-side welded capsule, followed by welding the other end of the capsule under continuous cooling in a water-bath. Capsules having weight differences of more than 0.2 mgs. before and after welding were discarded.

All experiments were performed at 5000 bars and 850°C in a Tempress internally heated pressure vessel. Pressures were monitored by a manganin cell, calibrated against a Heise precision gauge. Pressure accuracy was ±20 bars at 5000 bars. The pressure

Table 6.3. *Experimental conditions of the runs. All runs were performed at 850°C and 5000 bars.*

Run no.	Starting glass wt (mgs)	Starting solution wt (mgs)	Run time (hrs)
A11	87.0	72.0	16
A17	88.3	75.0	16
A18	92.3	77.1	16
A14	115.9	78.5	16
A15	100.0	78.0	16
A16	86.9	72.1	49
A12	90.2	72.1	49
A13	92.8	74.0	49
A19	128.9	75.3	49
A20	106.3	80.2	49

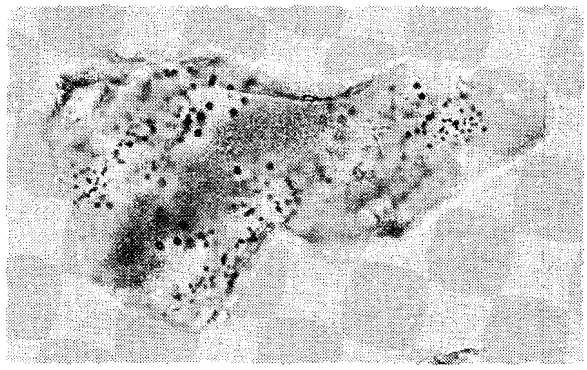

Figure 6.1. *A microphoto of a glass fragment (run A20). Bar = 70μm.*

Figure 6.2. *A SEM micrograph of salt cubes in a cracked fluid inclusion, crystallized after evaporation of the fluid. Bar = 1μm.*

medium was argon gas. Temperatures were recorded with three Pt90Rh10 thermocouples, placed at 20 mm intervals in a molybenum sampleholder. The temperature gradient over the sample capsules was normally within 5°C, with a temperature accuracy of ±3°C.

Experiment duration was 16 hours for A11, A17, A18, A14 and A15, and 49 hours for A16, A12, A13, A19 and A20. Diffusion calculations and previous experimental results predicted that equilibrium has been attained within the selected run durations.

Rapid quenching of the reaction is important to prevent back-reaction between melt (glass) and solution. The quenching time was ca 5 minutes for the cooling from 850°C to 250°C, and another 5 minutes was necessary for cooling below 100°C. Taking into consideration the slow diffusion rates of ions in the viscous silicate melt, and the rapidly decreasing rates during quenching, back-reactions were almost completely prevented. Association or dissociation of compounds during quenching is assumed to be not essential for the determination of the distribution coefficients, as they are defined for the total element combination in both glass and solution.

After the experiment any leakage was checked by reweighing the capsules. Subsequently the capsules were thoroughly rinsed in dilute acid and deionized water, followed by drying. The capsule was pierced with a needle, and the pH of the extruding droplet of the hydrothermal solution was measured with a micro-electrode. After the measurement the electrode needle tip was rinsed with deionized water, and the capsule was opened completely. The glassy contents were rinsed several times and the solute contents of the capsule were collected in volumetric flasks. The diluted hydrothermal solution was analyzed directly, or stored in polyethylene containers. The glass was dried in a stove at 120°C.

Analytical procedures

For chemical analysis the hydrothermal solutions were normally measured directly with a multichannel ICP Optical Emission Spectrograph ARL 34000. The glasses were dissolved in hydrofluoric acid (HF) at 80°C in PTFE containers. The clear solution was cooled to ambient temperature. In order to obtain a Si analysis the solution was not evaporated, but enough saturated borate solution was added to bind excess F^-. The solution was washed in volumetric flasks and analyzed by ICP. All analyses were performed using ample blanks and standards to correct for matrix effects and systematic deviations. The analyses were partly checked by Atomic Absorption Spectrometry (AAS) using a Perkin Elmer 460 spectrometer. The accuracy of the ICP analyses is estimated to be within 5 to 10% , depending on the elements measured. Electron microprobe analyses using a JEOL-8600 Superprobe were performed on some of the glasses to check the homogeneity with respect to the major elements and to compare with the results of the ICP-analyses.

The glasses were checked on absence of crystalline phases always by optical microscopy, and occasionally by X-ray diffraction (XRD) and scanning electron microscopy (SEM).

Table 6.4. *Final compositions of the glasses: major oxides (wt%) and minor elements (ppm).*

	A11	A17	A18	A14	A15	A16	A12	A13	A19	A20
SiO_2	67.4	68.8	68.5	72.9	69.2	68.0	70.8	65.3	69.7	70.9
Al_2O_3	13.0	13.1	13.1	13.5	13.5	13.2	13.6	13.7	12.7	12.8
K_2O	3.76	3.84	4.12	4.13	3.90	3.90	3.90	3.58	3.65	3.69
Na_2O	4.84	5.25	5.49	6.67	5.36	5.36	5.67	5.13	5.41	5.49
total	89.0	91.0	91.2	97.2	92.0	90.5	94.0	87.7	91.5	92.9
Li	105.6	93.2	80.2	57.9	60.0	109.1	90.2	69.0	56.0	58.9
Pb	621	391	259	201	122	553	429	158	54.5	d.l.
Zn	201	146	145	53	21	296	141	54.5	52.5	37.5
Cu	22.6	19.1	20.8	7.2	4.8	20.3	8.0	4.2	4.4	2.9
Sn	-	-	-	139	173	-	-	-	134	191

Table 6.5. *A comparison between ICP and Microprobe analyses. F indicates Microprobe analyses of larger fragments, S of smaller spherical glass beads. All values are given in weightpercentage. The numbers between the brackets give the number of analyses.*

		F (4)	S (1)	ICP
A11	SiO_2	69.4 ± 0.6	68.6	67.4
	Al_2O_3	13.3 ± 0.1	14.6	13.0
	K_2O	2.1 ± 0.1	2.2	4.8
	Na_2O	1.8 ± 0.1	1.9	3.8
	Cl	0.17 ± 0.12	0.01	
		F (3)	S (3)	ICP
A12	SiO_2	68.5 ± 2.5	68.1 ± 1.0	70.8
	Al_2O_3	13.5 ± 0.4	13.8 ± 0.2	13.6
	K_2O	2.3 ± 0.2	2.2 ± 0.1	5.1
	Na_2O	2.0 ± 0.3	2.0 ± 0.1	3.6
	Cl	0.11 ± 0.04	0.11 ± 0.04	
		F (5)	S (15)	ICP
A14	SiO_2	68.5 ± 0.8	69.2 ± 0.9	72.9
	Al_2O_3	13.3 ± 0.3	14.0 ± 0.4	13.5
	K_2O	2.1 ± 0.2	2.1 ± 0.1	6.7
	Na_2O	1.8 ± 0.1	1.6 ± 0.2	4.1
	Cl	0.03 ±0.02	0.10 ± 0.06	

Results

The solid contents of a capsule normally consisted of a few larger glass beads and of varying (occasionally numerous) amounts of small glass spheres of different size. Macroscopically most glasses had a milky appearance due to the presence of tiny aqueous inclusions (Fig. 6.1). The small spheres however were in most cases completely transparant. Microscopically all products showed a clear, inclusion-free rim, with a thickness independent of the size of the glass body. Optical inspection of both the reaction solution and the glassy products from runs A11 to A20 revealed no crystalline phases except for sample A16: SEM inspection of the cracked surface of a glass sphere revealed some salt crystals in a fluid inclusion (Fig. 6.2). Cracking of the inclusion during preparation of the sample had caused evaporation of the water contents leaving the crystalline chloride salt residu. Microscopical inspection of the inner wall of the platinum capsule showed a glass coating, consisting of numerous small glass spheres. Also here no crystalline products were observed.

The composition of the hydrothermal solution. The initial and final compositions of the hydrothermal solutions, analyzed with ICP, are reported for Na, K, Al and for the trace elements Li, Zn, Pb, Cu and Sn in Table 6.2. In addition the (initial) chloride molality of the solution, and the initial and the quench pH of the hydrothermal solution are listed.

The composition of the glass. The composition of the glass products with respect to major oxides and minor elements as analyzed by ICP are listed in Table 6.4. The major elements are not recalculated to 100% : the remaining quantity is assumed to be water or HCl dissolved in the melt. If this assumption is correct, then the amount of water present in the melt is 9.04 ± 2.12 wt% (exclusive the deviating amount of A14). The ICP-analyses of the glasses are compared with microprobe analyses of the glass products and listed in Table 6.5. Both larger glass fragments and smaller glass spheres were analyzed with the microprobe, and the average analyses are presented separately. The analyses yield too low Na and K conecentrations, due to evaporation during the analyses. If these values are corrected to the concentrations measured by ICP, also here the analyses point at a H_2O-content of ca 9% .

For the major elements Na, K, Al and Si the total yields of recovery for glass and solution vary between 90 and 96 weightpercent. The yields for Li, Zn and Pb are ca 80 wt%, 68 wt% and 63 wt% respectively (Table 6.6). The yields for Sn and Cu are 44 wt% and 10 wt% respectively.

The distribution coefficients. For all elements except for Si, Sn, H and O the distribution coefficients are calculated with the relations (6.1) and (6.4) and the values are tabulated in Table 6.7. In the Figures 6.3 to 6.6 the experimentally determined distribution coefficients for the alkali's Na, K and Li, and for the divalent ions Zn and Pb are plotted as a function of the chloride content of the hydrothermal solution. As discussed by Holland (1972) and Urabe (1985) a linear relation for the monovalent elements with chloride molality is expected on a linear/linear-plot. For the monovalent elements, the alkalis K, Na and Li, the linear trend is evidently illustrated. If it is assumed that the trends can be extrapolated through (0,0) the least squares fitted equations are

$K_D^{Na} = 0.40 \times mCl^-$ (6.5) ; $K_D^{K} = 0.26 \times mCl^-$ (6.6) and $K_D^{Li} = 0.33 \times mCl^-$ (6.7).

Table 6.6. *Mass-balance for the elements of the capsule system. Initial (first row) and final (second row) quantities are in mgs. for the major elements Si, Al, K and Na, and mgs. multiplied by a factor 10^3 for the trace elements. For Si and Al the probably very small amount in the solution relative to the glass is not taken into account. For each element and for each sample the average yield after the experiment is given in the last column and the last row respectively.*

	A11	A17	A18	A14	A15	A16	A12	A13	A19	A20	%
Si	31.02	31.48	32.91	41.33	35.66	30.99	32.16	33.09	45.96	37.90	
	27.41	28.38	28.53	40.55	32.36	27.64	29.87	28.34	42.03	35.25	91±4
Al	6.42	6.51	6.81	8.55	7.37	6.41	6.65	6.84	9.51	7.84	
	6.00	6.11	6.39	8.29	7.14	6.06	6.26	6.27	8.76	7.18	94±2
K	3.32	3.90	4.55	5.83	5.76	3.32	3.92	4.50	6.16	6.04	
	3.27	3.70	4.29	5.79	-	3.22	3.93	4.10	5.79	5.62	96±3
Na	4.76	5.80	6.94	8.92	9.04	4.76	5.82	6.84	9.33	9.45	
	4.17	5.42	6.55	9.06	-	4.59	5.59	5.98	8.54	9.06	94±4
Li	13.98	14.28	14.26	14.19	13.78	14.00	13.73	13.68	13.61	14.17	
	11.61	11.60	11.13	10.76	-	11.61	11.37	10.46	10.81	11.97	80±3
Zn	39.26	40.12	40.05	39.86	38.72	39.32	38.56	38.44	38.23	39.81	
	31.51	26.88	14.35	29.69	-	27.64	24.51	30.23	23.00	33.24	68±14
Pb	72.49	74.07	73.94	73.58	71.49	72.59	71.20	70.97	70.58	73.50	
	56.80	50.64	23.87	51.97	-	48.06	58.63	36.44	42.10	40.45	63±15
Cu	32.45	33.18	33.10	32.94	32.00	32.50	31.87	31.77	31.60	32.90	
	3.94	4.01	3.65	3.48	-	3.50	2.94	2.40	2.44	3.14	10±2
Sn	-	-	-	41.78	40.59	-	-	-	40.08	41.73	
	-	-	-	16.12	19.13	-	-	-	17.25	20.34	44±5
%	92±5	93±2	92±4	99±2	-	94±4	96±3	89±3	92±1	93±2	

Table 6.7. *The distribution coefficients K_D, calculated from the values of Table 6.2 and 6.4. The K_D is defined $[X]^{solution}/[X]^{glass}$.*

	Na	K	Li	Zn	Pb	Cu	Al*)
A11	0.41	0.26	0.33	1.00	0.06	1.25	0.00
A17	0.71	0.39	0.50	1.34	0.58	1.67	0.00
A18	0.96	0.47	0.65	0.00	0.00	1.16	0.00
A14	1.01	0.74	0.98	6.28	2.00	5.15	0.00
A15	distribution coefficients not determined						
A16	0.41	0.18	0.28	0.09	0.00	1.22	0.00
A12	0.62	0.45	0.52	1.21	0.67	4.01	0.00
A13	0.93	0.66	0.85	6.72	2.00	6.91	0.16
A19	1.27	0.85	0.94	4.52	9.41	8.12	0.52
A20	1.63	1.08	1.36	10.95	>20.65	15.31	2.86

*) K_D-values x 10^3

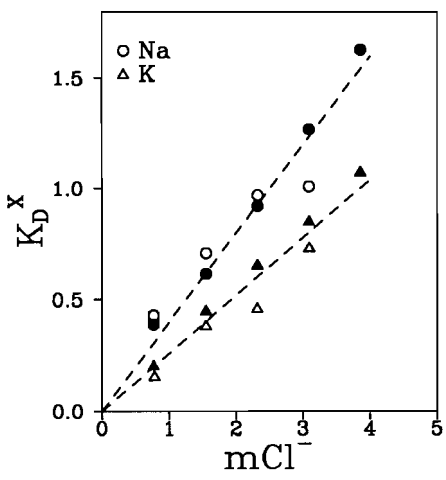

Figure 6.3. *The partition coefficients of Na and K vs. the chloride molality of the hydrothermal solution. The 16-hour runs are indicated with open symbols, the 49-hour runs with closed symbols.*

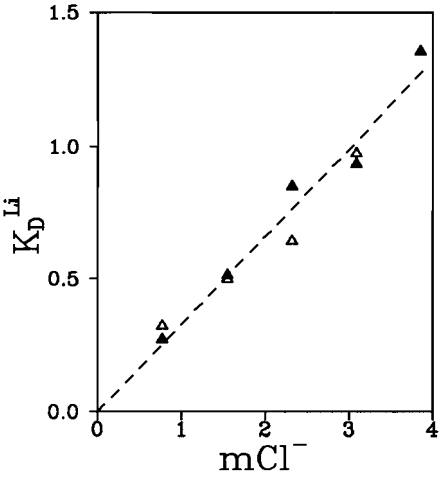

Figure 6.4. *The partition coefficients of Li vs. the chloride molality of the hydrothermal solution. For the symbols see Figure 6.3.*

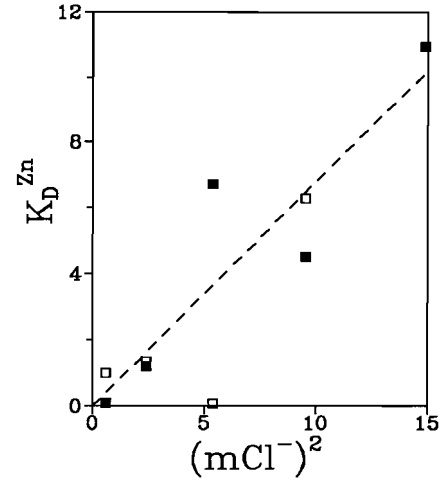

Figure 6.5. *The partition coefficient of Zn versus the squared chloride molality of the hydrothermal solution. For the symbols see Figure 6.3.*

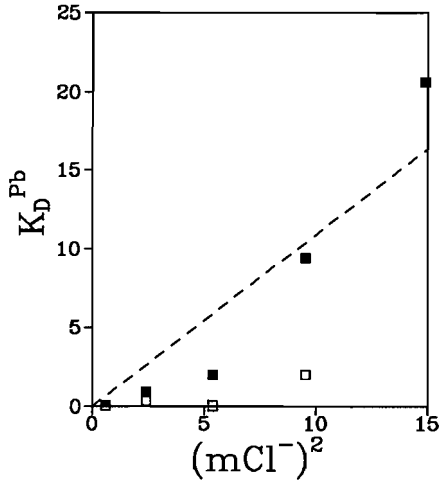

Figure 6.6. *The partition coefficient of Pb versus the squared chloride molality. For the symbols see Figure 6.3.*

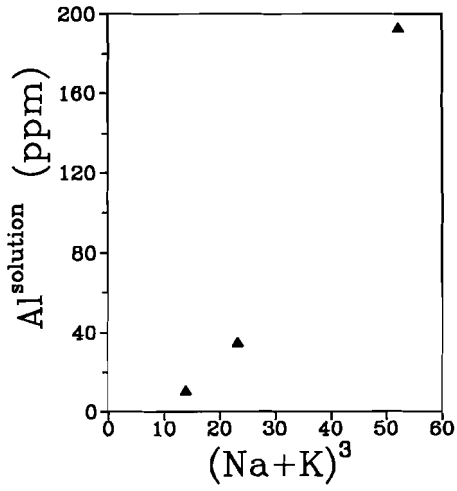

Figure 6.7. *A plot of Al vs. $(Na+K)^3$ in the hydrothermal solution.*

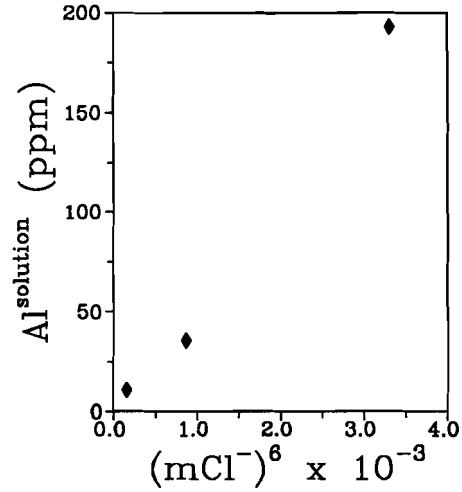

Figure 6.8. *A plot of Al vs. $(mCl)^6$ in the hydrothermal solution.*

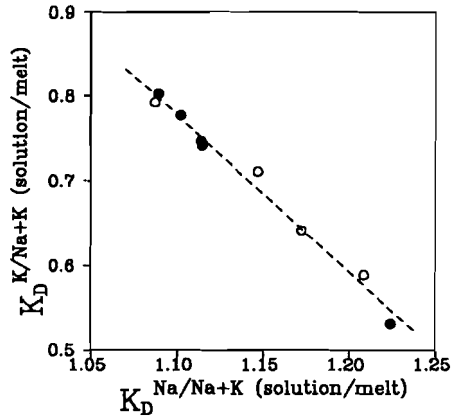

Figure 6.9. *A plot of the normalized distribution coefficients of Na vs. K.*

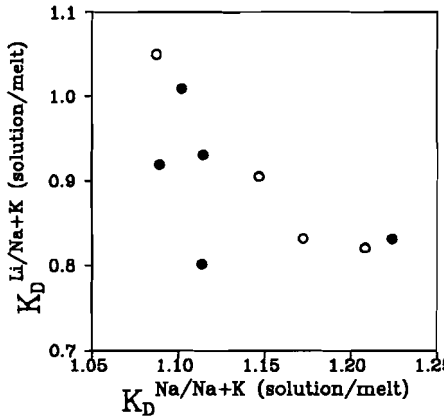

Figure 6.10. *A plot of the normalized distribution coefficients of Li vs. Na.*

These relations indicate that the value for the distribution coefficient of Na, K and Li between vapour and melt is 1 for a chloride molality of 2.5, 4 and 3 respectively. At lower chloride concentrations these elements will be incorporated preferentially in the melt.

The partition coefficients for the divalent ions Zn and Pb are plotted against the squared chloride molality. The scatter in the results especially for Pb is rather large, pointing at analytical errors and/or non-equilibrium conditions, due to the assumed diffusion into the capsule. The least squares fitted equations for Zn and Pb are calculated as

$$K_D^{Zn}(vap/melt) = 0.68 \times (mCl^-)^2 \quad (6.8) \quad \text{and} \quad K_D^{Pb}(vap/melt) = 1.09 \times (mCl^-)^2 \quad (6.9).$$

The relations indicate that Zn and Pb will enter preferentially the melt below chloride molalities of 1.2 and 1 respectively, which is considerably lower than for the monovalent alkali ions.

The distributions for Cu and Sn are not intensively considered. The low yield for these elements points at large losses during experimentation and their distributions may suffer from non-equilibrium conditions between melt and hydrothermal solution. The distribution coefficients for Sn are not tabulated in Table 6.7, as in all but one run the concentration in the solution was below the detection limit of the ICP. It can be noticed however, that Sn seems to have a strong preference for the melt relative to the hydrothermal solution. The most probable explanation for the losses of Cu and Sn, and also partly of Zn and Pb during experimentation is the loss of these elements into or even through the platinum capsule wall.

Although Al is not detected in most of the hydrothermal solutions, significant concentrations are measured in the higher chlorine, 49-hours runs. The K_D is not linearly related to the cubed chloride molality, but there appears to be a linear relation of Al in the solution with $(Na+K)^3$ (Fig. 6.7) and with $(mCl^-)^6$ (Fig. 6.8), which suggests the existence of a complex of the form $(Na,K)_3AlCl_6$.

Discussion

The comparison of the Microprobe and the ICP analyses of the glass products (Table 6.5) points mainly at analytical difficulties for the alkalis Na and K. The Microprobe analyses of the H_2O-rich glasses exhibit substantial alkali losses due to vaporization in vacuum during the analysis time. The differences between the SiO_2- and Al_2O_3-analyses of the larger glass fragments and the smaller spheres are not significant. The SiO_2-analyses are comparable to the values measured by ICP. The analyses by Microprobe all yield totals between 86 and 87%. After correction for the alkali loss, based on the concentrations measured for Na and K by ICP, the totals are in the same order as the ICP analyses. It may imply, that both analytical methods yield a 9 wt% H_2O-content.

The alkali elements Na, K and Li. In the Figures 6.3 and 6.4 the distribution coefficients for the alkalis Na, K and Li all show a linear relationship with chloride concentration. The distribution coefficient for Na is noticeably larger than for K,

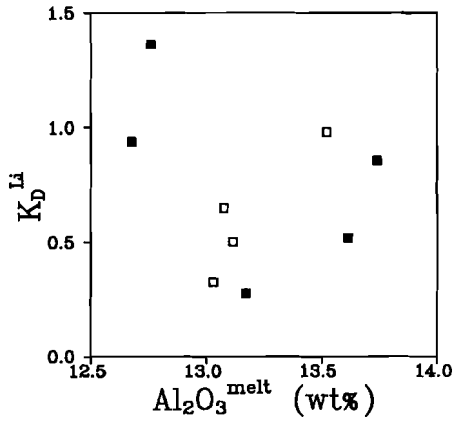

Figure 6.11. *K_D^{Li} plotted as a function of the Al_2O_3 content of the melt.*

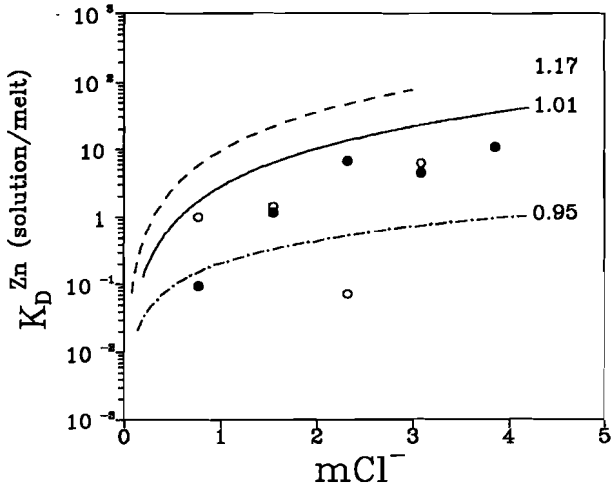

Figure 6.12. *A comparison of the Zn partition data from this study (circles) with the data of Holland (1972, solid line), and those of Urabe for his alkaline (dashed-dotted line) and aluminous (dashed line) experiments. For the different experimental series within these studies the molar (Al/Na+K) ratio of the melt is indicated.*

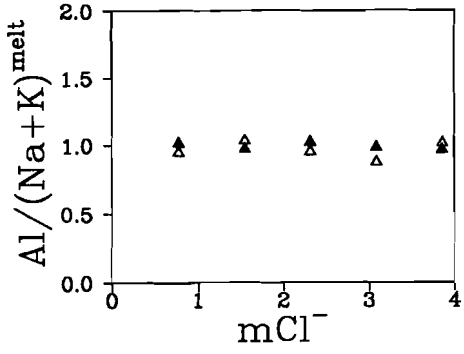

Figure 6.13. *The molar ratio (Al/Na+K) in the melt versus the chloride molality in the reaction solution. Open triangles are for the 16-hour runs, while the closed triangles are for the 49-hour runs.*

indicating a preference of Na for the vapour phase relative to K at 850°C and 5 kb. The distribution coefficient ratio K_D^K/K_D^{Na} for the experiments A11 to A20 is determined to be 0.65. Holland (1972) established for this coefficient a value of 0.74 at 850°C and 2 kb. A series of experiments at 2kb and 750°C performed at our lab produced a ratio of 0.58 (Chapter 7), which is considerably lower than the value of Holland (1972). If all values are correct and comparable, it may indicate that the distribution coefficient ratio is a function of P and T.

Surprisingly, the Li behaviour is intermediate between Na and K, despite its small ionic radius. Na and K have ionic radii of 1.02Å and 1.38Å respectively, while Li has a ionic radius of only 0.59Å (all radii taken for sixfold coordination; Shannon and Prewitt, 1969). Lithium, however, is present in trace concentrations, and it may display an exchange behaviour according Henry's law, whereas the other alkalis, which are available as major components in relatively high concentrations, may partition following a non-ideal behaviour. Secondly, the difference may originate in the melt structure. Jambon and Semet (1978), who studied the diffusion of Li in obsidian, observed a deviation from the diffusion behaviour compared with the other alkalis, which were found to have decreasing diffusivities with increasing ionic radius (Hofmann, 1980). Jambon and Semet (1978) found an identical diffusivity for both Li and Na. They suggested that below a critical ionic radius the mobility of an ion is not affected by size. If this deviation in behaviour is caused by the structure of the melt, it may indicate an exchange reaction with different ionic sites in the melt structure, like e.g. the Al-sites. A normalized distribution coefficient is defined as

$$K_D^{X/(Na+K)} = (X/(Na+K)^{solution})/(X/(Na+K)^{melt}) \qquad (6.10)$$

where X may be Li, Na or K. If the normalized K_D for Na is plotted versus the normalized K_D for K (Fig. 6.9), a good negative linear relation is obtained. If the normalized K_D for Li is plotted versus the normalized K_D for Na (Fig. 6.10), a diffuse negative linear relationship is obvious. From these figures it may be concluded, that Na and K show mutual exchange, but that Li substitutes only partly for the alkalis Na (and K), and partly by another exchange mechanism. If the K_D^{Li} is plotted versus the alumina content of the melt (Fig. 6.11), a similar diffuse negative linear relationship is observed as in Figure 6.10, which may indicate in this case a substitution relation with Al. With the available data it is not possible, however, to draw far-reaching conclusions on the nature of this mechanism.

The trace elements Zn, Pb, Cu and Sn. In Figures 6.5 and 6.6 the distributions for Zn and Pb are depicted. The concentration values for the elements in solution and melt are listed in Table 6.2 and 6.4 respectively. The results show a rather diffuse linear relationship with the squared chloride molality. The scatter can be explained by analytical problems, slow diffusion rates (and long equilibration time) and uptake of the elements by the capsule-wall. The results are slightly lower than the results of Holland (1972) and intermediate between the results of Urabe (1985) for the silicate melts of alkaline and aluminous composition. A comparison of the Zn results with the results of Holland (1972) and those of Urabe (1985) is drawn in Figure 6.12, where the Al/alkali-ratios for the different melt compositions are labelled. Cu and Sn suffered from substantial losses during the experiment (Table 6.2, 6.4 and 6.6). It is a well-known fact that a number of metals prefer a solid solution with the platinum of the capsule. The elements Sn and Cu may disappear almost completely from the capsule contents within

a few days (Urabe, 1985; Nekrasov et al., 1980), while the elements elements Zn and Pb may suffer substantial losses. The low yields after the experiment for the elements Zn, Pb, and Sn (Table 6.6) can be understood therefore in this way. The yield of Cu (ca 10%) is very low, especially if compared with the much higher yield for Sn (ca 44%). This may be satisfactorily explained by the fact, that Cu is reduced at a higher f_{O_2} than Sn. The distribution coefficients, determined for these elements, therefore do not represent pure melt/vapour interaction, but are influenced also by the vapour/platinum interaction. If it is assumed, that these elements react continuously with the platinum capsule, the rate at which the element is absorbed by the capsule wall and the diffusion rate of the element in the melt determine, whether the K_D reaches a melt/vapour equilibrium.

The composition of the melt and its effect on the element distributions. The alkalinity of the silicate melt has a critical influence on the distribution coefficients. Hunold and Brückner (1980) reported a large effect of the alkalinity of a silicate melt on the viscosity. Increasing the Al/Na-ratio of the melt from 0.95 to 1.17 (as is the case for Urabe's melt compositions) causes the viscosity to increase by a factor of 10^3, reaching a maximum in the viscosity at a ratio of 1.17. The viscosity increase is explained by the network constructing activity of Al, that produces a more stable polymer structure in the melt. Undoubtedly the structural change will influence the distribution of ions between the melt and a solution, and not in the last place the diffusion rate of the ions in the melt. Therefore, it was important for our investigations to keep the molar alumina/alkali-ratio close to one and as constant as possible. For the series A11 to A20 the average Al/(Na+K)-ratio of the melt is 0.99 ± 0.04 (Fig. 6.13). This value indicates, that the initial fluid was close to equilibrium with the melt, and that the melt composition did not change significantly during the experimental run. From Table 6.1, 2, and 4 it can be seen, that in most runs the concentrations of Na and K in the solution decreased slightly in favour of the melt. Aluminium-oxide solubilities in the coexisting fluid are low, and alumina becomes detectable only in the 49-hour runs at higher chlorinities. Therefore the exchange behaviour of the trace components is mainly a function of the salt- and chloride-concentration, and of run duration, where P, T and melt composition were held as constant as possible. It is not clear at present if the discrepancy in Zn distribution coefficients of this work and the work of Holland (1972) and Urabe (1985) are equilibrium differences caused by the composition and the polymer structure of the melt, or that it indicates a non-equilibrium situation, caused by a large difference in diffusivities of Zn in the melt compositions with highly different viscosities.

The uniform, neutral final pH of 6-7 of the quenched hydrothermal solution is interesting, despite the uniform acid initial pH in all cases (Table 6.2). The initial and final pH-values agree closely with the values of Urabe for his alkaline series with an Al/(Na+K)-ratio of 0.95, and may indicate H^+- or HCl-solubility in the melt. As stated by Burnham (1979), HCl is the only chloride complex, which is appreciably soluble in the melt phase at moderate pressures. Our experiments may confirm this statement, and the quench rate of the experiments apparently was sufficiently rapid to prevent the release of the HCl from the melt or glass during cooling. The amount of HCl relative to the total chlorine concentration is low, and although the Microprobe analyses reveal the presence of some Cl (Table 6.5), there is no information about the state, in which it was present in the melt.

Geological implications. The contents of HCl in the magma at high temperatures and pressures leads to the supposition that during cooling and depressurizing of a pluton a

reaction will occur, which liberates the HCl, followed by reactions of the liberated fluid with the crystallizing pluton. These reactions can be written as

$$HCl_{melt} \quad ---> \quad HCl_{vapour} \tag{6.11}$$

$$KO_{0.5\ melt} + HCl_{vapour} \quad ---> \quad KCl_{vapour} + 0.5H_2O \tag{6.12}$$

$$LiO_{0.5\ melt} + HCl_{vapour} \quad ---> \quad LiCl_{vapour} + 0.5H_2O \tag{6.13}$$

$$NaO_{0.5\ melt} + HCl_{vapour} \quad ---> \quad NaCl_{vapour} + 0.5H_2O \tag{6.14}$$

The differences in distribution coefficients for the alkalis (relations (6.5) to (6.7), and Figs. 6.3 and 6.4) support the common observation, that Li and Na are removed preferentially from a cooling pluton causing a relative enrichment of K in the crystallizing magma. In this way the melt itself provides the fluid by which it is attacked upon vesiculation during cooling and crystallization. An interesting feature of this process is, of course, the decrease of the alkalinity of the remaining melt, affecting rigorously the distribution of the divalent cations Zn and Pb. The Zn and Pb distributions may show an increase in vapour/melt distribution by a factor of 100 if the Al/alkali ratio increases only from 0.95 to 1.17 (Urabe, 1985) and thus these metals will effectively be removed into the solution during peraluminisation of the granite, caused by the alkali removal into the vapour phase.

Conclusions

The distribution of the alkali ions between chloride solution and haplogranitic melt increases linearly with increasing chloride content at the concentrations used.

The K_D^{Na} ($= 0.40 \times mCl^-$) and the K_D^{K} ($= 0.26 \times mCl^-$) result in an average distribution coefficient ratio K_D^{K}/K_D^{Na} of 0.65.

The K_D^{Li}, which is $0.33 \times mCl^-$, points at another solution mechanism in the melt than for Na and K, probably as a result of its small ionic size.

The distribution of the divalent ions Zn and Pb between chloride solution and haplogranitic melt increases linearly with increasing squared chloride concentrations, at 850°C and 5 kb. The distribution coefficients for these elements are determined as: $K_D^{Zn}(vap/melt) = 0.68 \times (mCl^-)^2$ and $K_D^{Pb}(vap/melt) = 1.09 \times (mCl^-)^2$.

The divalent ions Zn and Pb enter preferentially the melt below much lower chloride concentrations than the monovalent alkali ions.

The distribution of Cu and Sn is strongly influenced by reaction of these metals with the platinum capsule wall.

The uniform, neutral quench pH around 7 of the reaction solution indicates a relatively high capacity of buffering HCl in the melt at the conditions involved, practically independent of the actual chlorinity.

References

Brückner R. (1983) Structure and properties of silicate melts. Bull. Minéral. **106,** 9-22.

Burnham C. W. (1979) Magmas and hydrothermal fluids. In: H. L. Barnes (ed.) Geochemistry of hydrothermal ore deposits. J. Wiley and Sons, New York, 798pp.

Candela P. A. and Holland H. D. (1984) The partitioning of copper and molybdenum between silicate melts and aqueous fluids. Geochim. Cosmochim. Acta **48,** 373-380.

Eugster H. P. (1985) Granites and hydrothermal ore deposits: a geochemical framework. Mineral. Mag. **49,** 7-23.

Flynn T. R. and Burnham C. W. (1978) An experimental determination of rare earth partition coefficients between a chloride containing vapour phase and silicate melts. Geochim. Cosmochim. Acta **42,** 685-701.

Hamilton D. L. and Henderson C. M. B. (1968) The preparation of silicate compositions by a gelling method. Mineral. Mag. **36,** 832-838.

Hofmann W. A. (1980) Diffusion in natural silicate melts: a critical review. In: Hargraves R. B. (ed.) Physics of magmatic processes, Princeton Univ. Press, Princeton, New Jersey, 585pp.

Holland H. D. (1972) Granites, solutions and base-metal deposits. Econ. Geol. **67,** 281-301.

Hunold K. and Brückner R. (1980) Physikalische Eigenschaften und struktureller Feinbau von Natrium-Alumosilicatgläsern und -schmelzen. Glastechn. Ber. **53,** 149-161.

Jambon A. and Semet M. P. (1978) Lithium diffusion in silicate glasses of albite, orthoclase, and obsidian composition: an ion microprobe determination. Earth Planet. Sci. Lett. **37,** 445-450.

Khitarov N. I., Malinin S. P., Lebedev Ye. B. and Shibayeva N. P. (1982) The distribution of Zn, Cu, Pb, and Mo between a fluid phase and a silicate melt of granitic composition at high temperatures and pressures. Geochem. Intern. **19/4,** 123-136.

Kilinc I. A. and Burnham C. W. (1972) Partitioning of chloride between a silicate melt and coexisting aqueous phase from 2 to 8 kilobars. Econ. Geol. **67,** 231-235.

Luth W. C. and Boettcher A. L. (1986) Hydrogen and the melting of silicates. Amer. Mineral. **71,** 264-276.

Luth W. C., Jahns R. H. and Tuttle O. F. (1964) The granite system at pressures of 4 to 10 kilobars. J. Geophys. Res. **69,** 759-773.

Manning (1981) The use of radioactive tracers in determining the behaviour of tin in silicate-vapour systems. NERC rept. Progress in Experimental Petrology **5,** 15-16.

Naney M. T. and Swanson S. E. (1980) The effect of Fe and Mg on crystallization in granitic systems. Amer. Mineral. **65,** 639- 653.

Nekrasov I. Ya., Epel'baum M. B. and Sobolev V. P. (1980) Partition of tin between melt and chloride fluid in the granite-SnO-SnO_2-fluid system. Geochem. Intern. **19/4,** 165-168.

Oxtoby S. and Hamilton D. L. (1978) The discrete association of water with Na_2O and SiO_2 in NaAl-silicate melts. Contrib. Mineral. Petrol. **66,** 185-188.

Rhyabchikov I. D., Orlova G. P., Yefimov A. S. and Kalenchuk G. Ye. (1981) Copper in a granite-fluid system. Geoch. Int. **18,** 29-34.

Roedder E. (1984) Fluid inclusions. Reviews in Mineralogy, Vol. 12, 644pp.

Shannon R. D. and Prewitt C. T. (1969) Effective ionic radii in oxides and fluorides. Acta Cryst. **B25,** 925-946.

Urabe T. (1985) Aluminous granite as a source magma of hydrothermal ore deposits: an experimental study. Econ. Geol. **80,** 148-157.

Chapter 7

The exchange behaviour of the major elements Na and K, and of the trace elements Li, Rb, and Zn between a haplogranitic melt and coexisting vapour at 2 kb.

Abstract

The distribution of the alkali ions Na, K, Li and Rb, and of the divalent ions Zn, Pb and Cu between a haplogranitic melt and a chloride solution has been studied at 750°C and 800°C at 2kb. The melt has a eutectic composition in the system Na_2O-K_2O-Al_2O_3-SiO_2. The chloride concentration of the solution was varied between 0 and 4M. Experiments with the ions Na, K, Li, Zn, Pb and Cu were reversed, whereas Rb was added to the starting hydrothermal solution. Equilibrium was approached most closely for those ions, which were added to both the melt and the hydrothermal solution in expected equilibrium concentrations (Na, K), followed by the monovalent alkalis Li and Rb. The divalent ions Zn, Pb and Cu were far away from equilibrium within the maximum experimental run time of 4 days. Cu suffered from absorption by the platinum of the reaction capsule.

The linear relationships for Na, K, Li and Rb were calculated as $K_D^{Na} = 0.51 \times mCl^-$; $K_D^{K} = 0.32 \times mCl^-$; $K_D^{Li} = 0.47 \times mCl^-$ and $K_D^{Rb} = 0.28 \times mCl^-$. The $K_D^{Na/K}$ value at 750°C and 2kb is 0.62 and is almost identical to the value at 850°C and 5kb (=0.65, see Chapter 6). Li distributions are discussed in relation to the Al/(Na+K)-ratio of the melt and seem to be related to the polymeric structure in the melt. The K_D slope of Li versus mCl^- is not related to ionic size if compared with the other alkalis Na, K and Rb, as was already observed in Chapter 6.

The pressure, temperature and melt composition conditions caused very low rates of diffusion for the divalent ions, and results in terms of relations with chloride molality can be reported only for the runs, where at the starting conditions the initial trace element content was carried by the solution. If the trace elements were initially contained by the glass, the exchange kinetics were too slow to detect appreciable element concentrations in the reacted hydrothermal solution.

Introduction

In this chapter a series of exchange experiments of major and trace elements between haplogranitic melt and coexisting vapour are reported, which were performed at a pressure of 2kb and a temperature of 750 and 800°C. The cotectic composition of the melt in the chemical system K_2O-Na_2O-Al_2O_3-SiO_2-H_2O at this pressure in terms of

Table 7.1. *Analyses of the starting glasses. The concentrations of the major elements as oxides are in weight percent. The concentrations of the major elements are also tabulated in ppm x 10^{-4} (first row) and in ppm x 10^{-4}, assuming 6 wt% H_2O in the glass (second row). The trace elements are tabulated in ppm.*

	Glasses				
	Calc[1)]	Pure[2)]	LiZn[2)]	Li[3)]	Zn[3)]
SiO_2	78.7	78.0	77.6	78.5	78.3
Si	36.8	36.5	36.3	36.7	36.6
	34.6	34.3	34.1	34.5	34.4
Al_2O_3	12.4	13.3	12.6	12.5	12.3
Al	6.56	7.04	6.67	6.62	6.51
	6.17	6.62	6.27	6.22	6.12
K_2O	4.2	4.0	4.6	4.2	4.4
K	3.49	3.32	3.82	3.49	3.65
	3.28	3.12	3.59	3.28	3.43
Na_2O	4.7	4.7	5.1	4.6	4.9
Na	3.49	3.49	3.78	3.41	3.64
	3.28	3.28	3.55	3.21	3.42
Li	-	-	93.2	850	-
Zn	-	-	677	-	796
Pb	-	-	1086	-	-
Cu	-	-	468	-	-

1) Calculated composition, based on the cotectic melt composition in the system Na_2O-K_2O-Al_2O_3-SiO_2 (von Platen, 1965).
2) Measured composition, all elements with ICP emission spectrometry.
3) Measured composition, major elements with Microprobe analyses, trace elements with ICP emission spectrometry.

Table 7.2. *Composition of the starting reaction solutions for the A-runs. The concentration values are in ppm. The chloride molality (mCl) of the solution is mentioned.*

	LiZn1	Pure1	LiZn2	Pure2	LiZn3	Pure3
Na	15400	15400	30800	30800	61600	61600
K	7685	7685	15369	15369	30738	30738
Rb	1020	1020	1020	1020	1020	1020
Li	504	-	504	-	504	-
Zn	1008	-	1008	-	1008	-
Pb	1489	-	1489	-	1489	-
Cu	1008	-	1008	-	1008	-
mCl	0.87	0.87	1.73	1.73	3.47	3.47

quartz (qtz), albite (ab) and alkali-feldspar (kf) is: qtz : ab : kf = 34 : 40 : 26 (von Platen, 1965). The minimum melt temperature of this composition at 2kb and water-saturated conditions is 670°C. The melt was exchanged with an aqueous solution containing the chlorides of Na and K in amounts up to ca 3.5 moles/kg solution, to which the chlorides of Li, Rb, Zn, Pb and Cu were added in trace amounts. The molar Na/K-ratio in the solution before the exchange was constant for all experiments and the ratio was selected based on the comparable experiments by Holland (1972). The total amount of Na and K at each chloride molality was determined from his experiments and added to our experiments to prevent a compositional change of the melt by depletion of Na and K at the experimental PT-conditions. A change of the alkali content of the melt seriously influences the partitioning coefficient of elements like Zn and Pb (Urabe, 1985).

Previous studies on the distribution of elements between granitic liquids and chloride containing solutions, which are relevant to this study, are not very numerous. Holland (1972) reported Na, K and Zn distributions, while Urabe (1985) reported distributions for Na, Zn and Pb. Li distributions are not reported in the available literature. A few studies exist on the partitioning of Rb between a silicate melt, alkali-feldspar and a hydrothermal solution (Pierozynski and Henderson, 1978; Long, 1978). In these studies, however, only the solid phases were analyzed, and the composition of the experimental solution is not known. Cu distributions are reported by Ryabchikov et al. (1981) and Candela and Holland (1984), and Cu, Zn and Pb distributions by Khitarov et al. (1982).

The aim of this study is to obtain distribution coefficients for the above mentioned elements at 750 and 800°C at 2000 bars. The results will be compared with those of other studies and with the results of Chapter 6, and the geological implications will be discussed.

Experimental methods and techniques

All experiments were performed in an internally heated 4 kb pressure vessel. Pressure was applied using argon gas as a pressure medium. Pressures were monitored with a Bourdon-tube pressure gauge with an accuracy of ±50 bars. The furnace was designed with a single Kanthal winding. The temperature was recorded with a single chromel-alumel thermocouple in a molybdenum sampleholder. The temperature accuracy was ±3°C. The experimental temperature was reached ca 15 minutes after the start of an experiment. During cooling after the experiment the temperature of the sample capsules dropped below 100°C within 5 minutes. Crystalline quench phases were never observed in these experiments: all glasses appeared to be optically clear and homogeneous after the experiments.

Synthetic glass compositions were prepared using the procedure described by Hamilton and Henderson (1968) for making gels. After preparation the gel was fired at 1200°C for 30 minutes in air. The resulting glass was crushed in an achate mortar and kept in a desiccator before use.

The experiments were run at 750°C (the A-series) and at 800°C (the B-series), all at 2000 bars. For the reversal A-runs a pure glass, containing no trace elements, and a LiZn-glass, containing traces of Li, Zn, Pb and Cu were prepared. Rb was added to the

Table 7.3. *Experimental conditions of the A-runs. All runs were performed at 750°C and 2000 bars.*

Run no.	Glass	Wt (mgs)	Solution	Wt (mgs)	Run time (hrs)
A42	Pure	156.2	LiZn1	103.0	49
A43	LiZn	132.0	Pure1	111.2	49
A44	Pure	183.4	LiZn2	125.2	48.5
A45	LiZn	151.9	Pure2	105.1	48.5
A46	Pure	124.7	LiZn3	113.0	48
A47	LiZn	129.0	Pure3	113.4	48
A48	Pure	247.6	LiZn1	155.5	98
A49	LiZn	249.0	Pure1	138.6	98
A50	Pure	152.1	LiZn2	106.3	95
A51	LiZn	159.9	Pure2	189.8	95
A52	Pure	142.9	LiZn3	114.0	96.5
A53	LiZn	114.4	Pure3	111.5	96.5

Table 7.4. *Experimental conditions of the B-runs. All runs were performed at 800°C and 2000 bars.*

Run	Glass[1)]	Solution[1)]	mCl^-	Run time (days)
B1	Li	H_2O	0	8
B3	Zn	H_2O	0	8
B7	Zn	250 ppm Zn	0.01	6
B8	Li	250 ppm Li	0.04	6
B5	Zn	500 ppm Li	0.07	6
B6	Li	500 ppm Zn	0.02	6
B2	Li	1000 ppm Li	0.14	8
B4	Zn	1000 ppm Zn	0.03	8
B9	Zn	1000 ppm Li	0.14	2
B12	Li	1000 ppm Zn	0.03	2
B13	Li	Na,K[2)] + 1000 ppm Zn	2.0	2
B14	Li	Na,K[2)] + 500 ppm Li + 500 ppm Zn	2.0	2
B17	Li	Na,K[2)] + 216 ppm Li + 784 ppm Zn	2.0	2
B19	Li+Zn (1:1)	Na,K[2)] + 246 ppm Li + 754 ppm Zn	2.0	2
B15	Zn	Na,K[2)] + 500 ppm Li + 500 ppm Zn	2.0	2
B16	Zn	Na,K[2)] + 1000 ppm Li	2.0	2

[1)] For each run 40 mgs. of glass and of solution were used.

[2)] The concentration for these solutions was for Na: 16020 ppm, and for K: 11860 ppm. The concentration-ratio was calculated on the basis of the distribution coefficients determined by Holland (1972).

hydrothermal solution, and not to the initial glass. For this element the runs represent no reversals. The glasses were analyzed by ICP to check the composition (see Analytical Procedures). The results of the analyses are summarized in Table 7.1. The reaction solutions were prepared from analytical-grade reagents. The elements Na, K, Pb and Cu were added directly as chlorides to deionized water. Na and K were added to prevent a shift of the melt composition during run conditions by exchange of these elements with the hydrothermal solution. The amount of Na and K, necessary to prevent this compositional shift, was calculated with the results of Holland (1972) for Na and K distributions. Li- and Zn-chlorides were prepared from carbonates by adding hydrochloric acid. The chloride molality was calculated from the added amount of chlorides. Three solutions with different chloride molalities were prepared, and at each molality a second solution was made with the trace elements Li, Zn, Pb and Cu. Rb was added in trace amounts to all six solutions. The composition of the different solutions is mentioned in Table 7.2. The experimental conditions for the A-runs are given in Table 7.3. Two series of B-experiments were performed: a series at low mCl^- (to a maximum of 0.14) and a series at a mCl^- of 2. In these series only Zn and Li were present as trace elements. The starting composition of the glasses and of the hydrothermal solutions is given in Table 7.1 and 7.4. The experimental conditions are given in Table 7.4 too.

The capsules were made from platinum tubing which were welded with a carbon arc under atmospheric conditions. The capsules were welded on one side first. Next they were filled by adding the solution, followed by the addition of the required amount of glass. Subsequently the capsules were welded on the other side under continuous cooling in a water bath. Capsules, which had suffered a weight loss of more than 0.2 mgs during welding were discarded. Normally the capsules showed weight differences within 0.2 mgs before and after the experiment.

After the experiment the capsules were reweighed to detect any weight loss, due to leakage. The capsules were washed thoroughly and they were cut open with a sharp knife. The solute contents of the capsule were washed in volumetric flasks. The remaining glass was rinsed several times, and dried in a stove at 120°C.

Analytical procedures

All run products were checked for the presence of crystalline phases after the runs by optical microscopy. The inner capsule wall was inspected by microscopy for quench products. The dilute hydrothermal solutions were analyzed directly for all involved elements (except for Rb and Si) with a multichannel ICP Optical Emission Spectograph ARL 34000. For analyses of the glasses ca 40 to 110 mgs of glass fragments were dissolved in excess hydrofluoric acid (HF) at 80°C in PTFE (Teflon) containers overnight, followed by cooling to room temperature. The solution was evaporated to dryness at 160°C to remove all SiF_6^{2-} and excess HF. The residue was redissolved in HCl and diluted in volumetric flasks to the desired concentration. Two blanks, several glass standards and international rock standards were added to the series. The solutions were measured for all elements except for Rb with ICP emission spectrography. All Rb was analyzed by atomic emission spectrometry (AES) with a Perkin Elmer 460 spectrometer.

Table 7.5. *Analyses of the reacted glasses of the A-runs. All concentration values are in ppm. Concentrations, which are below the detection limit are designated d.l. From the experiments A44 and A48 two different glass beads were analyzed.*

	Na	K	Al	Li	Rb	Zn	Pb	Cu
A42	31730	34066	63774	220	239	70	252	2
A43	36934	35079	60884	78	36	501	927	2
A44	33326	33552	63589	169	290	11	22	d.l.
A44-2	34937	34340	65156	175	322	29	34	2
A45	38924	35046	60863	72	327	512	912	<1
A46	30134	30531	65463	148	470	23	51	3
A47	32264	34813	61964	50	447	432	866	6
A48	32175	31328	64441	206	436	54	157	2
A48-2	27075	31776	44558	198	478	28	101	1
A49	28812	30571	70810	77	321	402	828	7
A50	30720	31286	65511	193	407	36	65	2
A51	31366	31842	57898	63	524	412	788	3
A52	31537	29842	65574	141	384	22	35	4
A53	31856	34639	62324	46	453	413	720	8

Table 7.6. *Analyses of the reacted solutions of the A-runs. Concentration values are in ppm. Concentrations, which are below the detection limit are designated d.l.*

	Na	K	Li	Rb	Zn	Pb	Cu
A42	13717	9524	110	152	1016	968	264
A43	12775	8971	22	21	3	30	11
A44	29350	22830	192	266	122	905	248
A45	27158	18484	43	313	2	43	d.l.
A46	52419	30125	262	430	935	1376	253
A47	54629	35757	60	446	5	d.l.	33
A48	15379	9837	119	156	963	931	226
A49	14798	9378	27	138	2	d.l.	5
A50	36601	24446	230	380	1331	1283	349
A51	27211	16611	37	307	d.l.	d.l.	17
A52	55265	31748	261	571	963	1440	410
A53	60132	39321	59	523	1	d.l.	222

Results

After the experiments no crystalline phases were detected in the run products. The glasses were macroscopically milky due to numerous tiny fluid inclusions, but appeared to be optically clear and homogeneous.

The analyses of the experiments A42 to A53 are presented in Table 7.5 for the glasses and in Table 7.6 for the hydrothermal solutions. The analyses of the B-experiments are presented in Table 7.8 for the low mCl^- series and in Table 7.9 for the other series.

The distribution coefficients are calculated according to the equations, given in the paragraph 'Distribution coefficients' of Chapter 6. The calculated distribution coefficients for the A-experiments are tabulated in Table 7.7, and for the low- and high-chlorine B-experiments in Table 7.10. The distribution coefficients for the monovalent Na, K, Li and Rb are plotted versus the chloride molality in the Figures 7.1 to 7.4, while the coefficients for the divalent Zn, Pb and Cu are plotted versus the squared chloride molality in the Figures 7.5 to 7.7 respectively. For the B-experiments (circles) only the maximum and minimum values are plotted. The results of the B-experiments were not used for determining the linear correlation of the data, as the run temperature of these experiments was 50°C higher than of the A-experiments. A linear relationship of the monovalent cations with chloride molality is obvious for all distribution coefficients. The least square fitted equations for the elements Na, K and Li are calculated, assuming extrapolation through (0,0). The calculations produce the following relationships:

$K_D^{Na} = 0.51 \times mCl^-$ (7.1); $K_D^{K} = 0.32 \times mCl^-$ (7.2) and $K_D^{Li} = 0.47 \times mCl^-$ (7.3).

Rb cannot be calculated according to a least squares fitted equation, as Rb was only added to the hydrothermal solution. Thus the calculated distribution coefficient determines a maximum K_D slope. This maximum slope is calculated with the values of the experiments A48-2, A51 and A46, producing the relation:

$K_D^{Rb} = 0.28 \times mCl^-$ (7.4).

The divalent ions Zn, Pb and Cu suffer from non-equilibrium conditions, indicated by the reversal runs. A least squares fitted equation was not calculated for these elements, but the results will be discussed below.

Discussion

The alkali elements. For the alkali ions the linear relationship of the distribution coefficient with chloride molality is obvious. However it is also obvious, that equilibrium has not been reached completely for most runs. Concerning the results for the alkali ions, for which reversed exchange experiments were performed, the Li values of the A-series are farthest away from equilibrium. The Li values of the B-series are closer to equilibrium, probably because of the higher experimental temperature (800°C instead of 750°C). For Rb, which was only added to the vapour, the results are contradictory. For

Table 7.7. *The distribution coefficients K_D for the A-experiments, calculated from the values of Table 5 and 6. The K_D is defined $[X]^{solution}/[X]^{glass}$.*

	Na	K	Li	Rb	Zn	Pb	Cu
A42	0.43	0.28	0.50	0.64	14.4	3.84	111
A43	0.35	0.26	0.28	0.57	0.01	0.03	4.2
A44	0.88	0.68	1.16	0.92	110	42	∞
A44-2	0.84	0.66	1.10	0.83	42.7	27	∞
A45	0.70	0.53	0.59	0.96	0.00	0.05	0.00
A46	1.74	0.99	1.77	0.92	40.6	27	84
A47	1.69	1.03	1.20	1.00	0.01	0.00	5.3
A48	0.48	0.31	0.58	0.36	17.7	5.9	131
A49	0.51	0.45	0.35	0.43	0.01	0.00	0.8
A50	1.19	0.78	1.19	0.93	37.3	19.8	166
A51	0.87	0.52	0.59	0.59	0.00	0.00	5.1
A52	1.75	1.06	1.85	1.49	42.8	41.4	98
A53	1.89	1.14	1.29	1.16	0.00	0.00	29.2

Table 7.8. *ICP analyses of the reacted glasses and solutions for the experiments B1 to B12. The concentration values of the glasses are normalized on a K_2O content of 3.91 wt% for the reacted Li-glass and 4.14 wt% for the reacted Zn-glass (based on the initial concentration values of 4.2 resp. 4.4 wt% with a final H_2O content of 7 wt%).*

	Na	K	Al	Li	Zn
B1	386	98	91	9	0
	30600	32430	[1]	869	0
B2	2006	785	221	49	0
	31290	32430	[1]	1334	0
B3	1220	395	276	0	87
	31950	33970	[1]	0	495
B4	1052	492	120	0	55
	30840	33970	[1]	0	1052
B5	763	318	33	6	9
	35690	33970	[1]	358	676
B6	450	184	82	9	9
	34392	32430	[1]	843	459
B7	1942	425	237	0	22
	36370	33970	[1]	0	737
B8	693	147	53	12	0
	31850	32430	[1]	935	0
B9[2]	-	-	-	-	172
	34910	33970	[1]	872	550
B12	652	345	41	18	20
	33980	32430	[1]	817	713

[1] Al analyses of the glass too low

[2] Only the Zn content of the reacted solution of B9 was analyzed.

Table 7.9. *ICP analyses of the experiments B13 to B19. Normalization of the reacted glass concentration values as in Table 8. Concentrations, which are below the detection limit are designated d.l.*

	Na	K	Al	Li	Zn
B13	33150	20780	d.l.	443	925
	33140	32430	59460	433	133
B14	27250	17840	d.l.	568	429
	34160	32430	57540	736	97
B15	31510	21330	d.l.	230	1038
	35270	33970	59330	251	289
B16	28890	19430	d.l.	452	331
	35090	33970	54460	544	439
B17	29040	19640	d.l.	483	564
	34020	32430	53400	562	222
B19	28720	20420	d.l.	202	667
	33630	33200	45450	234	272

Table 7.10. *The distribution coefficients K_D for the B-experiments, calculated from the values of Tables 8 and 9. The K_D is defined as $[X]^{solution}/[X]^{glass}$.*

	Na	K	Li	Zn
B1	0.01	0.00	0.01	-
B3	0.04	0.01	-	0.02
B7	0.05	0.01	-	0.03
B8	0.02	0.00	0.01	-
B5	0.02	0.01	0.02	0.01
B6	0.01	0.01	0.01	0.02
B2	0.06	0.02	0.04	-
B4	0.03	0.01	-	0.05
B12	0.02	0.00	0.01	-
B13	1.00	0.64	1.02	6.96
B14	0.80	0.55	0.77	4.42
B17	0.85	0.61	0.86	2.54
B19	0.85	0.61	0.86	2.45
B15	0.89	0.63	0.92	3.59
B16	0.82	0.57	0.83	0.75

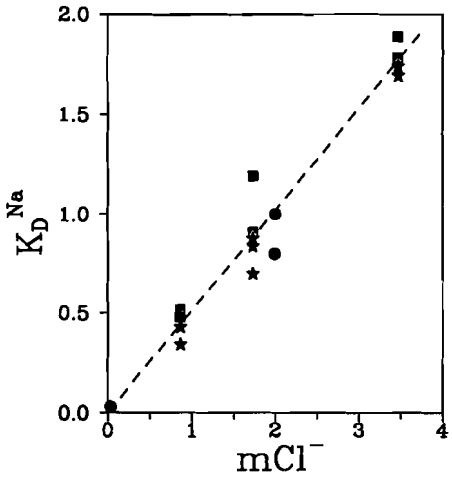

Figure 7.1. *K_D^{Na} versus chloride molality. The K_D is defined as $[X]^{solution}/[X]^{melt}$. The 48 hrs A-series experiments are denoted with stars, the 96 hrs A-series with squares and the B-series with circles. For the B-runs at 2 mCl only the lowest and highest K_D-value is plotted.*

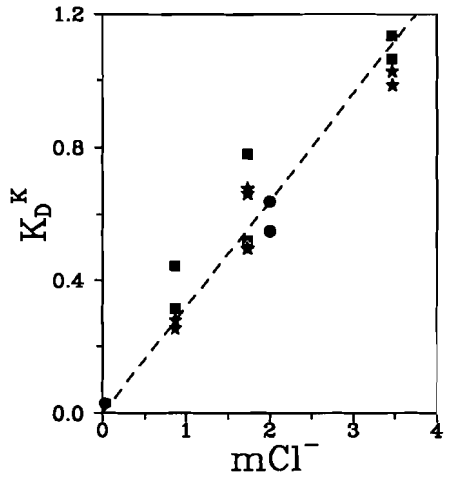

Figure 7.2. *K_D^K versus chloride molality. K_D definition and symbols are in Figure 7.1.*

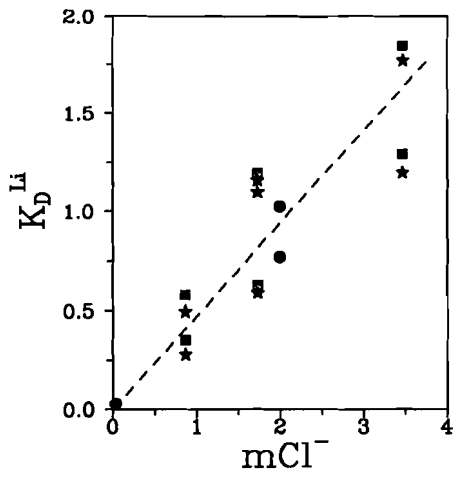

Figure 7.3. *K_D^{Li} versus chloride molality. K_D definition and symbols are in Figure 7.1.*

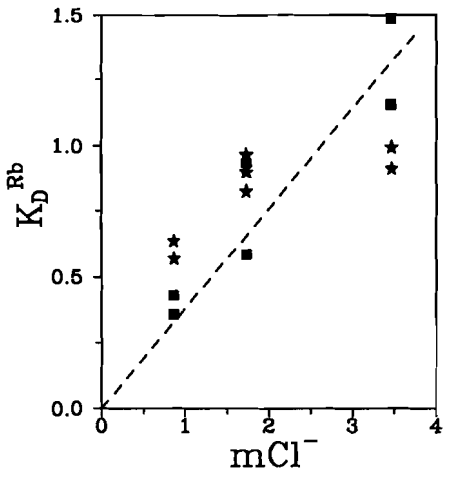

Figure 7.4. *K_D^{Rb} versus chloride molality. K_D definition and symbols are in Figure 7.1.*

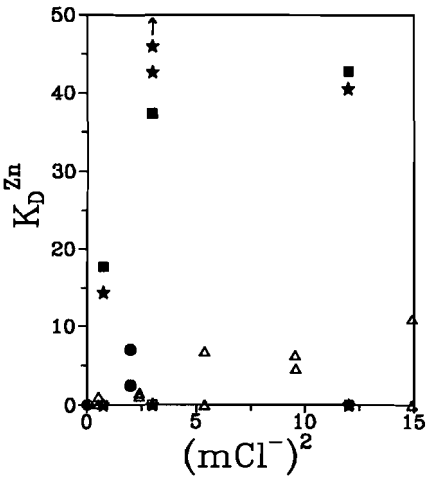

Figure 7.5. *K_D^{Zn} versus the squared chloride molality. K_D definition and symbols are in Figure 7.1. The results for the 5 kb runs of Chapter 6 are plotted for comparison with triangles.*

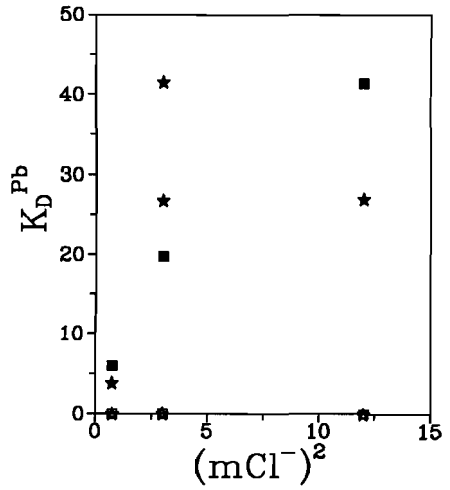

Figure 7.6. *K_D^{Pb} versus the squared chloride molality. K_D definition and symbols are in Figure 7.1.*

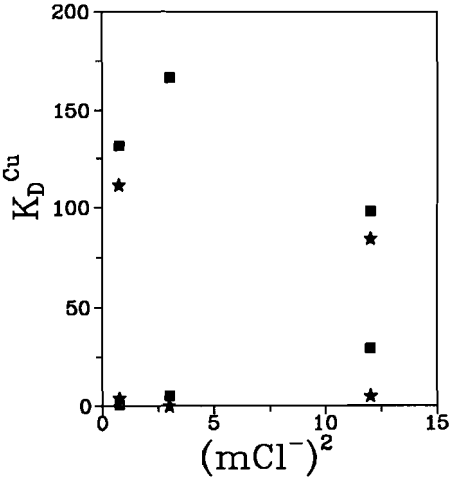

Figure 7.7. *K_D^{Cu} versus the squared chloride molality. K_D definition and symbols are in Figure 7.1.*

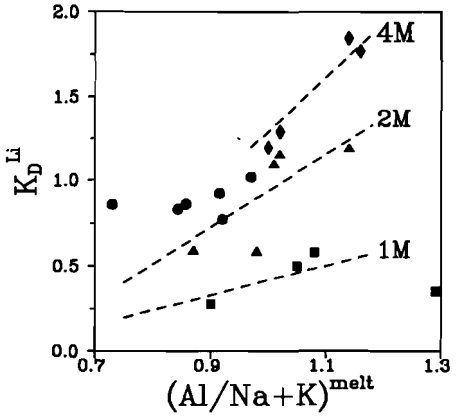

Figure 7.8. *K_D^{Li} versus the (Al/Na+K)-ratio in the melt. The symbols indicate the data points for the 1 mCl (1M) A-series experiments (squares), the 2 mCl (2M) A-series (triangles) and B-series (circles) experiments and the 4 mCl (4M) A-series (diamonds) experiments.*

the lower chlorinities the averaged values are lower for the longer term experiments, which is according to the expectations: the K_D will start at infinity at the beginning of the experiment, and will decrease until equilibrium has been attained. For the highest chlorinity however, the values for the 4 days experiments are higher than for the two days experiments. An explication other than analytical error cannot be given at the moment. If the linear relations of K_D versus mCl^- of the different alkali ions are compared with each other, the results are consistent with the results of the 5kb experiments (see Chapter 6). For these experiments the K_D slopes for Na and K were 0.40 and 0.26, with the value for Li of 0.33 in between. The values for the 2kb experiments for Na and K are 0.51 and 0.32, while the value for Li is 0.47. The $K_D^{Na/K}$-ratio for the 2kb and 750°C experiments is 0.63, which is almost equal to the ratio at 5kb and 850°C (= 0.65: see Chapter 6), but again much lower than the ratio (= 0.74), obtained by Holland (1972) for his experiments at 2kb and 850°C.

The divalent cations Zn, Pb and Cu demonstrate very clearly a non-equilibrium situation. For Zn and Pb the K_D's for the runs starting with these elements in the melt phase, the distribution is zero or very close to zero for all experiments even after 4 days. A linear relationship for the reversal runs is also absent, although the results for the 2 and 4 days experiments in many cases are not far apart. The loss of Pb and Zn during the experimental run is limited, but the loss of Cu is again tremendous: the yield of Cu averages 20% and a higher yield than 50% is not obtained. The yields for Zn vary between 60 and 137% with 89% as average value. The analytical error for this element appears to be large, but the loss seems to be restricted. For Pb the average yield is 83%, but the extremes are less far apart than for Zn, with a minimum of 61% and 100% as a maximum. Obviously the oxygen fugacity is low enough to produce metallic Cu, which is absorbed by the platinum capsule wall, but too high to produce large amounts of metallic Zn and Pb.

Equilibrium and melt composition. If the results for the distribution coefficients are compared with each other and with the 5kb results, it must be concluded that the conditions of 750°C and 2kb are insufficient to produce equilibrium results within the experimental time of 4 days. A difference is obvious between the monovalent alkali elements and the divalent ions. The monovalent elements are in general closer to equilibrium. The observation that Li in the reversed experiments is farther away from equilibrium than the larger alkali ions Na and K may be attributed to the fact, that Na and K were added in all cases to both the melt and the vapour phase in a presumed close-to-equilibrium ratio, whereas Li was added to one of these phases only. Moreover the Li removal from or addition to the melt may be inhibited by the structural coupling of Li to Al. For the divalent ions it must be concluded, that equilibrium is far away for all experiments, and that the results are partly clouded by analytical problems and uncertainties. In Chapter 6 it was suggested, that beside the experimental temperature and pressure the composition of the melt is of great importance for the distribution of the elements. Temperature, pressure and composition of the melt determine to a large extent the structure and thus the viscosity. Mysen and Kushiro (1978) observed a strong pressure dependence of the distribution coefficient of Ni between olivine and liquid. Kushiro (1980) assumes a relationship with the melt structure, but experimental evidence was not available. The Al/(Na+K)-ratio of the melt gives information on the viscosity of the high-silica melts (Brückner, 1983). In a series of experiments performed by Hunold and Brückner (1980) it was shown, that in the system Na_2O-Al_2O_3-SiO_2 the viscosity of melts with a constant SiO_2 content of 66.7 mole% increases with increasing Al/Na-ratio

up to a ratio of 1.17. If the Al/Na-ratio increases above this value, the viscosity decreases again. Hunold and Brückner (1983) explain this effect by the role of Al in the formation of the melt structure. Below the Al/Na value of 1.17 the Al increase reduces the number of non-bridging oxygens, resulting in a more stable network. Above this value another (unknown?) mechanism, related to the solution of Al destabilizes the melt again. In Figure 7.8 the K_D values for Li of the A-series are plotted versus the Al/(Na+K)-ratio of the melt. Tentatively the lines of equal chloride molality are drawn in this Figure. An optimum in K_D seems to be present at an Al/(Na+K)-ratio of 1.12. An increase in the chloride molality also produces a K_D increase, whereas an effect of the experimental time seems to be absent. The following mechanism is proposed in explaining the relations in Figure 7.8. The Al concentration in the high silica melt is an important factor in the stability of the network of the melt. An increase of Al below the Al/(Na+K)-ratio value of 1.12 produces an increase in the stability of the network and also a decrease in the alkali concentration of the melt. A result is a reduction in the ionic conductivity of the melt, which causes a decrease in the ionic diffusion rate. Increasing the ratio above 1.12 destabilizes the melt and results in an increase of the ionic diffusion rate, producing a value closer to equilibrium. The somewhat lower value of 1.12, if compared to the value of 1.17 obtained by Hunold and Brückner (1980), may originate from a slightly different structure, as K is present beside Na. In this proposition it is assumed, that an effect of the Al/(Na+K)-ratio on the equilibrium distribution coefficient is absent, so equilibrium would result in straight K_D lines parallel to the X-axis. The K_D^{Li} will then approach equilibrium, where the ionic conductivity of the melt is highest. This is true for Al/(Na+K)-ratios much lower or higher than 1.12. The equilibrium distribution coefficient for Li will in this case be lower than calculated from relation (7.3) and approach the lowest values at each chloride molality.

Conclusions

The distribution coefficient of the alkali ions Li, Na, K and Rb increase linearly with chloride molality at the experimental conditions used.

The distribution coefficient of Na and K result in an average distribution coefficient ratio $K_D^{Na/K}$ of 0.62.

The K_D^{Na} (= 0.51 x mCl^-) and K_D^{K} (= 0.32 x mCl^-) are higher than at the experimental conditions of 850°C and 5kb (= 0.40 and 0.26 x mCl^- respectively; Chapter 6), but result in an almost equal $K_D^{Na/K}$ of 0.63 (vs 0.65).

The calculated K_D^{Rb} (= 0.28 x mCl^-) agrees with the common observation, that an increase in ionic size favours partitioning in the hydrothermal solution.

The K_D^{Li} (= 0.47 x mCl^-) deviates from the observation, mentioned in the previous conclusion, as is also observed at 850°C and 5kb.

Li distributions between solution and melt generally show a linear increase with increasing Al/(Na+K)-ratio of the melt, suggesting a relation with the polymeric melt structure.

Under the experimental conditions the diffusivities for the divalent ions are too low to attain equilibrium within the experimental run time of 4 days.

References

Brückner R. (1983) Structure and properties of silicate melts. Bull. Minéral. **106,** 9-22.

Candela P. A. and Holland H. D. (1984) The partitioning of copper and molybdenum between silicate melts and aqueous fluids. Geochim. Cosmochim. Acta **48,** 373-380.

Hamilton D. L. and Henderson C. M. B. (1968) The preparation of silicate compositions by a gelling method. Mineral. Mag. **36,** 832-838.

Holland H. D. (1972) Granites, solutions and base-metal deposits. Econ. Geol. **67,** 281-301.

Hunold K. and Brückner R. (1980) Physikalische Eigenschaften und struktureller Feinbau von Natrium-Alumosilicatgläsern und -schmelzen. Glastechn. Ber. **53,** 149-161.

Khitarov N. I., Malinin S. P., Lebedev Ye. B. and Shibayeva N. P. (1982) The distribution of Zn, Cu, Pb, and Mo between a fluid phase and a silicate melt of granitic composition at high temperatures and pressures. Geochem. Intern. **19/4,** 123-136.

Kushiro I. (1980) Viscosity, density, and structure of silicate melts at high pressures, and their petrological applications. In: R. B. Hargraves (ed.) Physics of magmatic processes. Princeton University Press.

Long P. E. (1978) Experimental determination of partition coefficients for Rb, Sr, and Ba between alkali feldspar and silicate liquid. Geochim Cosmochim. Acta **42,** 833-846.

Mysen B. O. and Kushiro I. (1978) Pressure dependence of nickel partitioning between forsterite and aluminous silicate melts. Earth Planet. Sci. Letters **42,** 383-388.

Pierozynski W. J. and Henderson C. M. B. (1978) Distribution of Sr, Ba and Rb between alkali feldspar and silicate melt. N.E.R.C. 4th progress report, ser. D. no. 11, 40-46.

Platen H. von (1965) Kristallisation granitischer Schmelze. Beitr. z. Mineral. u. Petrogr. **11,** 334-381.

Rhyabchikov I. D., Orlova G. P., Yefimov A. S. and Kalenchuk G. Ye. (1981) Copper in a granite-fluid system. Geoch. Int. **18,** 29-34.

Urabe T. (1985) Aluminous granite as a source magma of hydrothermal ore deposits: an experimental study. Econ. Geol. **80,** 148-157.

Chapter 8

The effect of fluorine on the distribution of elements between a granitic melt and a hydrothermal solution

Abstract

The effect of fluorine on the distribution of the major elements Na, K and Al and of the trace elements Li, Zn and Pb between a hydrothermal solution and a eutectic granitic melt in the system Na_2O-K_2O-Al_2O_3-SiO_2-H_2O was studied. The distribution coefficients of the major elements Na, K and the trace element Li all show a positive linear relation with increasing initial fluorine content of the hydrothermal solution. For the K_D^{Al} a relation with the cubed fluorine molality is assumed. Zn and Pb exhibit no relation with fluoride molality. The distribution coefficients for Na, K and Li are lower than for the chloride-bearing systems, studied in the Chapters 6 and 7. However for Al the K_D is substantially higher. The K_D for Zn and Pb is equal to the 1 molal chlorine experiments. Fluorine contents of the melt up to 2 wt% were measured. In the high fluorine experiments quench phases such as quartz and chiolite ($Na_5Al_3F_{14}$) were abundant.

Introduction

Fluorine belongs to the most important complexing anions in hydrothermal solutions related to granitic intrusions, and is important in the melting and the crystallization relations, in geothermometry and in geochemical prospecting (Bailey, 1977). The fluorine activity during hydrothermal processes, associated with granite intrusions is reflected in the widespread occurrence of fluorite in ore deposits. The solubility of fluorite in different rock systems under hydrothermal conditions was studied by Richardson and Holland (1979a, 1979b). Fluorine has a large influence on the liquidus relations of compositions in the system Na_2O-K_2O-Al_2O_3-SiO_2, lowering the minimum melting temperature of pure albite by almost 200°C at 2750 bars (Wyllie and Tuttle, 1961) and of granitic compositions by 65°C at 2750 bars (Wyllie and Tuttle, 1961) to 100°C at 1000 bars (Manning, 1981). Another effect is the expansion of the quartz liquidus field relative to the feldspar field. Contrary to chlorine, fluorine is very soluble in the melt. Fluorine distributions between hydrothermal solution and granitic melt were determined by Hards (1976) to be 0.18 at 850°C and 0.12 at 680°C and 1 kb. The solubility mechanism of fluorine in sodium aluminosilicate melts was studied by Mysen and Virgo (1985). Fluorine strongly depolymerizes the melt, which results in very low melt viscosities and relatively high cationic diffusivities. The distribution of elements between a fluorine

Table 8.1. *ICP analyses of the starting glasses. The concentrations for the major oxides are in weight percent, for the trace elements in ppm.*

	Glass 25	Glass 36
SiO_2	75.1	76.1
Al_2O_3	14.0	12.5
K_2O	4.0	3.7
Na_2O	5.7	5.7
Li	-	100.0
Zn	-	552
Pb	-	1170
Cu	-	500

Table 8.2. *Experimental conditions of the runs. All runs were performed at 850°C and 5000 bars.*

Run no.	Starting glass		Starting solution		Run time (hrs)
	no.	wt (mgs)	mF^-	wt (mgs)	
A31	25	107.0	0.95	98.4	48
A33	36	112.5	0.95	100.4	48
A34	36	120.7	1.90	101.4	48
A34-2	36	128.2	1.90	114.8	48
A32	25	111.8	3.80	101.5	48
A35	36	142.7	3.80	101.6	48

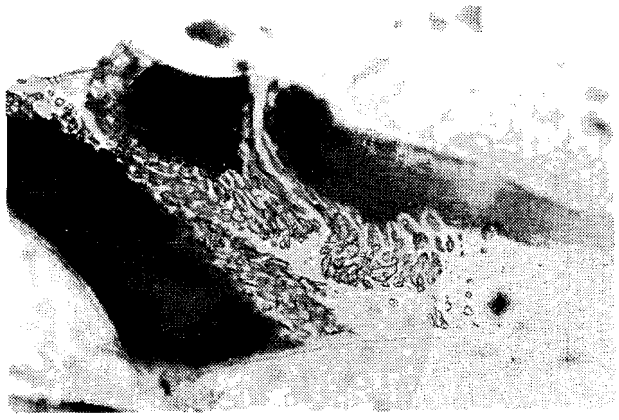

Figure 8.1. *Deformed fluid inclusions in fluorine-rich glass (A32). Bar = 100μm.*

containing hydrothermal solution and a melt of granitic composition is reported only by few authors. Candela and Holland (1984) determined the distribution of Mo as a function of fluorine content of a high silica melt, but observed no relation with fluorine concentration. Hards (1976) reported distribution coefficients between a 2M HF solution and two different granitic compositions at temperatures of ca 700°C and at 850°C, and a pressure of 1 kb. Although these experiments were not sufficient in number to determine actual relations, distribution coefficients appeared to be low compared to the corresponding distribution coefficients in the case of chlorine containing solutions. Flynn and Burnham (1978), however, observed an increase in the distribution coefficients for some Ce, Eu, Gd and Yb between melt and aqueous solution, if fluorine instead of chlorine was present.

In this chapter the effect of fluorine concentration on the distribution of Na, K, Al as major elememts and Li, Zn, Pb and Cu as trace elements between a hydrothermal solution and a granitic melt was studied. Ca and thus fluorite was not present in the experiments. The results are compared with identical experiments with chloride containing hydrothermal solutions (Chapter 6 and 7).

Experimental procedures

For the experiments synthetic glass compositions were prepared, following a gel preparation procedure by Hamilton and Henderson (1968). After preparation of the gels, they were vitrified within 30 minutes at 1200°C. The resulting glass was crushed in an achate mortar and stored in a desiccator until use. Two different glasses were used: glass 25, without trace elements, and glass 36, with traces of Li, Cu, Zn and Pb. An ICP analysis of these glasses is given in Table 8.1. Ca 100 mg of glass were added to a gold capsule, together with ca 100 μl of a 1, 2 or 4 molal hydrofluoric acid (HF) solution. The HF solution never contained trace elements. The capsules were welded shut with a carbon arc under continuous cooling in a waterbath. Capsules with a weight difference of more than 0.2 mgs before and after welding were discarded. The run capsule contents are reported in Table 8.2. The experimental conditions for all experiments were 850°C and 5000 bars during 48 hours.

The experiments were performed in a internally heated 10 kb pressure vessel, manufactured by Tempress. The pressure medium was argon gas. Pressures were monitored with a manganin cell, calibrated against a Heise precision gauge. Pressure accuracy was ±20 bars at the experimental pressure of 5 kb. The heating was applied with a double-wound Kanthal furnace. The samples were placed in a molybdenum sampleholder. Temperatures were recorded with three 90Pt10Rh thermocouples at 2cm intervals. The vessel, which could be rotated, was positioned such, that the temperature gradient over the sample capsules was less than 5°C. The accuracy of the temperature measurements was ±3°C.

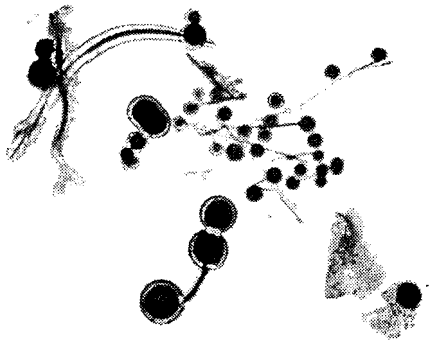

Figure 8.2. *Glass fragments, glass spheres and glass fibres in A32. Note the inclusion-free rim. Bar = 200μm.*

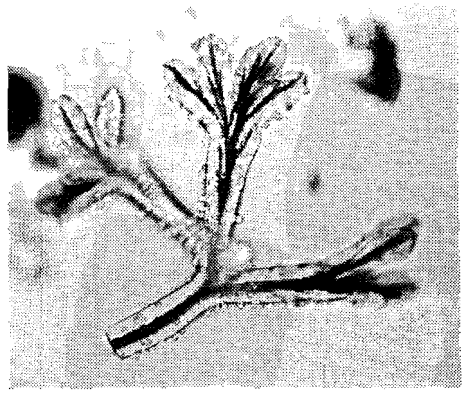

Figure 8.3. *Glass 'tree' (A32). The core of the glass fibers contains numerous fluid inclusions. The outside is covered with tiny glass spheres. Bar = 100μm.*

Figure 8.4. *SEM micrograph of glass spheres, interconnected by glass fibres (A32). Bar = 30μm.*

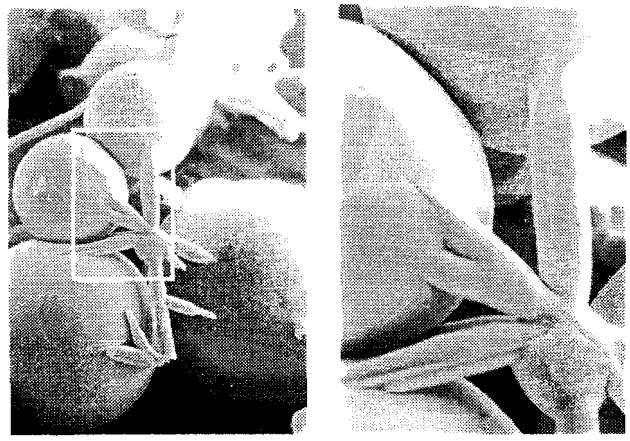

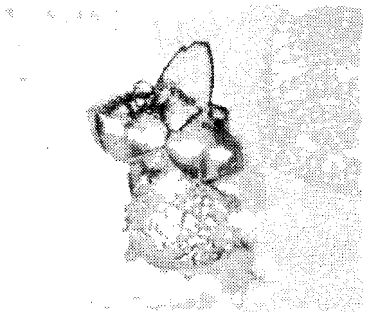

Figure 8.5. *Quartz star, nucleating at a glass sphere (A31). Bar = 50μm.*

Analytical procedures

After the experiment the capsules were thoroughly cleaned and opened with a sharp knife. The solute contents of the capsule were carefully separated from the solid contents, washed into volumetric flasks, diluted and analyzed with ICP. The glasses were also analyzed with ICP. For these analyses only the larger fragments were used. The fragments were dissolved in concentrated HF solutions at 80°C, followed by evaporating to dryness, dissolving the residu in 1:1 HCl and diluting. The F^- content of the solution was determined with a ion-selective electrode. The F^- content of the glasses of experiments A31 and A32 were analyzed with a JEOL 8600 Superprobe.

Results

The solid contents of the experiments were checked with optical microscopy and X-ray diffraction (XRD). At all fluorine molalities the glasses were optically clear, but contained enormous quantities of tiny fluid inclusions. The glass always was rimmed by an inclusion-free zone with a maximum thickness of 10μm. Also numerous tiny, inclusion-free glass spheres with diameters up to 50μm were present. The glass in the experiments with the highest fluorine concentrations provided evidence for a remarkable decrease of the viscosity of the melt. Figure 8.1 shows fluid inclusions in the melt, clearly deformed by some kind of flow pattern. Other evidence for the decreased viscosity is the development of dendritic glass structures (Fig. 8.2, 8.3), which may form an interconnective network with glass spheres (Fig. 8.4). Quartz was present in all experiments as stars, nucleating from glass spheres. The crystals are prismatic, with only three of the (1010) faces developed. Other crystal faces are not clearly developed, but the prism is terminated by a convex form of the prismatic faces (Fig. 8.5). The experiments with the highest fluorine molality further contain at least two crystalline phases. The first and most common phase is shown in Figure 8.6. It was determined by XRD to be chiolite ($Na_5Al_3F_{14}$). Optical properties could be determined on some larger crystals (optically negative with $2V_x \approx 25°$, $\delta \approx 0.020$, strong dispersion). Its tetragonal morphology can be observed, but the the small angle between the optical axes suggests a slight deviation tetragonality. The description of the crystalline phase observed by Wyllie and Tuttle (1961) in their HF containing experiments with albite corresponds with this description. The *d* spacings at 5.70 and 5.25, reported in their study, may be attributed to chiolite. Cryolite (Na_3AlF_6), which is more abundant in nature, was never observed. An unidentified phase is present as platy crystals of hexagonal habit (Fig. 8.7), which sometimes occur in hexagonally intergrown, snowflake-like structures (Fig. 8.8), but also in a more irragular, flaky habit in irragular structures (Fig. 8.9). Although the XRD patterns contain reflections, which could not be attributed to quartz or chiolite, the phase could not be identified. A complete list of XRD reflections is given in Table 8.3. In all cases the crystalline phases seem to nucleate at glass spheres (Figs. 8.5, 8.6, 8.7).

The analyses of the reacted glasses and hydrothermal solutions are given in Table 8.4. In this table the analyzed concentrations of the solution as well as the solution concentrations, calculated from the difference in composition between the initial and the final glass composition, are presented. The analyzed as well as the calculated

Table 8.3. *XRD reflections of the crystalline phases of A35, compared with literature values of chiolite and quartz.*

Observed	Chiolite			Quartz		
	d(Å)	I/I_o	hkl	d(Å)	I/I_o	hkl
5.8	5.82	20	101			
5.68 unidentified						
5.20	5.202	30	002			
3.34				3.342	100	101
2.96 unidentified						
2.915	2.909	100	202			
2.595 unidentified						
2.495 unidentified						
2.325	2.325	50	213			
2.29 unidentified						
2.225 unidentified						
2.17	2.17	20	311			
2.005	2.002	25	214			
1.995	1.996	20	105			
1.795	1.794	25	224			
1.76	1.754	23	400			
1.507 unidentified						

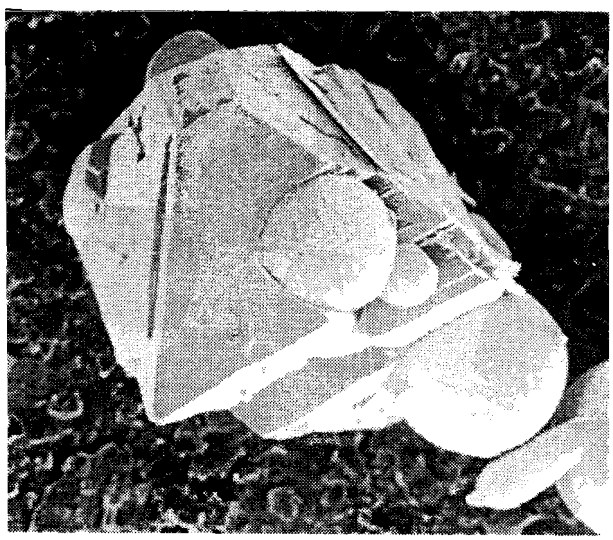

Figure 8.6. *Chiolite, nucleating at glass sphere (A32). Bar = 30μm.*

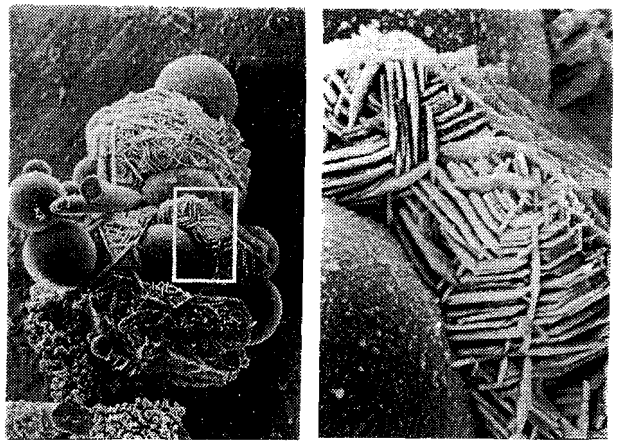

Figure 8.7. *Unidentified mica-like phase, intergrown in a regular pattern and enclosing glass spheres and fibres (A32). Bar = 100μm.*

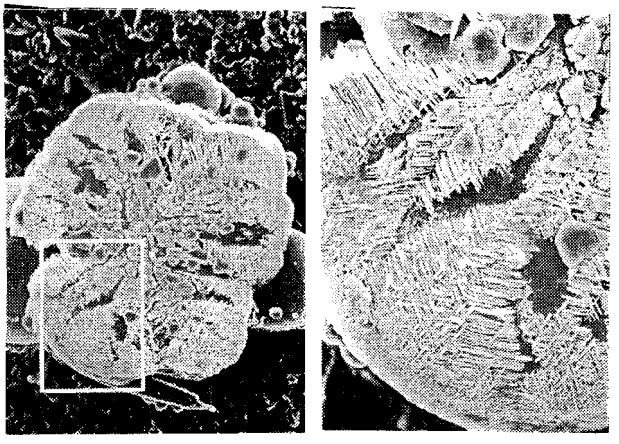

Figure 8.8. *Cross-section of a mica aggregate, showing the hexagonal intergrowth pattern (A32). Bar = 30μm.*

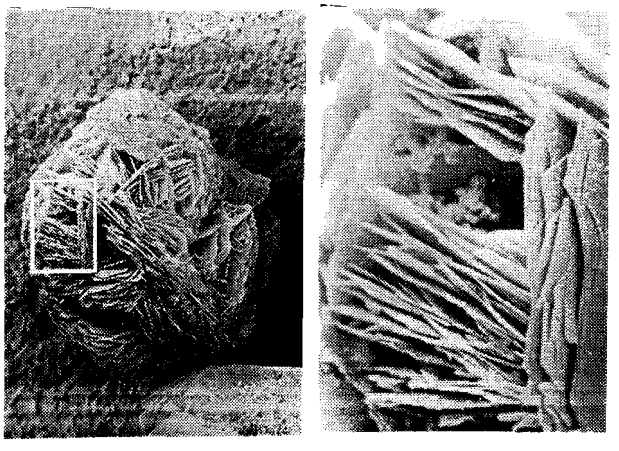

Figure 8.9. *Irregular intergrowth of probably the same mica phase as shown in Figs. 8.7 and 8.8 (A32). Bar = 100μm.*

Table 8.4. *Analyses of the reacted glasses and hydrothermal solutions. For each run the first row contains the analyzed (measured) solution concentrations, the second row the calculated solution concentrations, calculated from the difference between the initial and final glass concentration, and the third row contains the final glass concentrations. All concentration values are in ppm. Concentrations, which are below the detection limit are designated d.l.; n.a. is: not analyzed.*

	Na	K	Al	Si	Li	Cu	Zn	Pb	F
A31	1186	128	566	1507	-	-	-	-	918
	3997	3081	4009	-	-	-	-	-	8644
	38614	30377	64487	n.a.	-	-	-	-	8650
A33	2670	390	194	1456	14	20	11	22	775
	4055	1365	1875	-	11	†)	125	216	-
	38671	29502	70413	n.a.	90	1	440	977	n.a.
A34	301	96	129	1504	6	1	5	d.l.	275
	5854	2043	8259	-	14	†)	170	143	-
	37372	29004	59222	n.a.	88	1	409	950	n.a.
A34-2	solution lost after the experiment								
	5775	6406	4284	-	27	†)	202	489	-
	37119	24984	62324	n.a.	76	d.l.	371	732	n.a.
A32	1728	824	1807	4151	-	-	-	-	2277
	8079	4487	14531	-	-	-	-	-	52131
	34211	28723	59569	n.a.	-	-	-	-	18220
A35	613	340	1297	2722	10	1	31	d.l.	693
	8435	1140	6591	-	16	†)	185	246	-
	33855	29580	56234	n.a.	88	3	420	995.0	n.a.

†)Expected concentration in the fluid not calculated because of the very low glass concentration

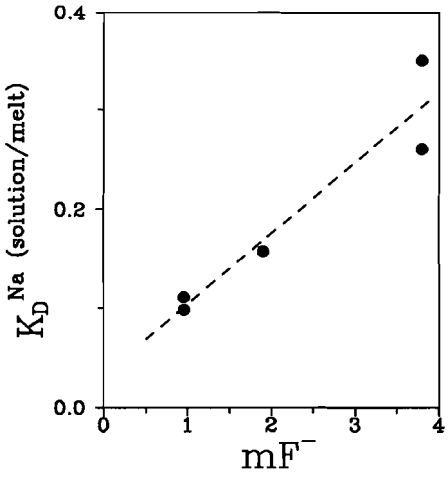

Figure 8.10. *K_D^{Na} vs. mF⁻ of the initial solution.*

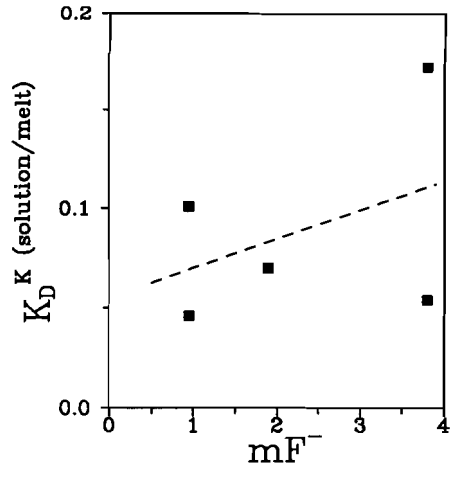

Figure 8.11. *K_D^{K} vs. mF⁻ of the initial solution.*

concentration values are used to calculate the distribution coefficients, presented in Table 8.5. For the alkali elements Na, K and Li, and for Al the distribution coefficients were also normalized by dividing the concentrations by (Na+K).

Discussion

The behaviour of fluorine versus chlorine. The appearance of large amounts of crystalline phases and the low analyzed fluorine concentrations in the quenched hydrothermal solutions point at a rather different behaviour of the fluorine ion from that of the chlorine ion. In the first place fluorine is far more soluble in the melt than chlorine. Fluorine concentrations in the melt may reach values of 2 wt% (A32), while measured chlorine solubilities do not exceed 2200 ppm (A14, Chapter 6). In the second place, increasing fluorine concentration in the hydrothermal solution increases the solubility of the silicate melt in the solution. This dissoved melt precipitates upon quenching (Webster, 1990). In the third place fluorine forms stable mineral phases in the high-fluorine experiments. These crystalline fluorine-rich phases are probably formed during the quench procedure of the experiments. As a consequence the analysis of the hydrothermal solution after the experiment will produce results, which in most cases will not represent the equilibrium composition of the solution during the experiment. It is not possible to separate the crystalline phases from the many tiny glass spheres, which may have the equilibrium glass composition of the experimental conditions. The quench phases should be added quantitatively to the hydrothermal solution, to obtain the true equilibrium composition. In Table 8.4 the composition of the hydrothermal solution has been calculated on basis of the difference between the initial and the final composition of the glass. Cu has been excluded because of the very strong absorption by the capsule wall. As the absorbed amount of Cu is unknown, it is not possible to estimate the final amount in the hydrothermal solution. Remarkable is the difference between the measured and calculated K content of the solution, suggesting that K must have been incorporated in a quench phase. A logical assumption would be the unidentified mica-like phase.

The melt structure. The tree-like structures of the melt in the high-fluorine experiments point at the very low viscosity of the melt. Fluorine acts here even stronger than H_2O as a depolymerizer of the silicate structures within the melt by the formation of non-bridging oxygens (Mysen and Virgo, 1985). As a result aluminum and alkalies react to form fluoride complexes. Probably this change in the melt structure explains the high solubility of especially aluminum in the hydrothermal solution in the high-fluorine runs. The large amount of fluid inclusions are undoubtedly also caused by the very low viscosity of the melt. During quenching and before solidifying of the melt, part of the dissolved H_2O can still exsolve due to the low viscosity.

The fluid inclusions point at another analytical problem. Although part of the inclusions may originate during quenching, part of the inclusions is formed by the entrapment of hydrothermal solution during melting of the glass, which was added to the capsule as crushed fragments. A method to separate the different inclusion generations is not available. As the glass is dissolved for analysis without crushing, some analytical error is introduced, but it is expected that the total amount of solution present within the

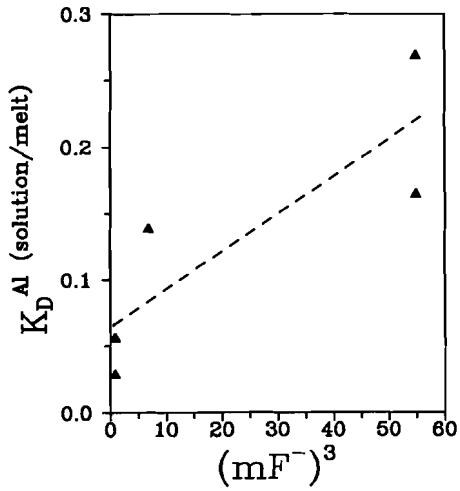

Figure 8.12. *K_D^{Al} vs. $(mF^-)^3$ of the initial solution.*

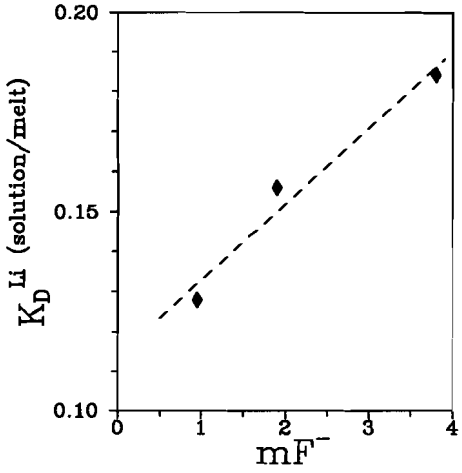

Figure 8.13. *K_D^{Li} vs. mF^- of the initial solution.*

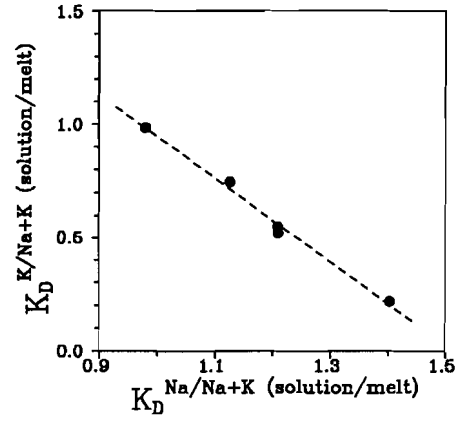

Figure 8.14. *Normalized distribution coefficients for K vs. Na.*

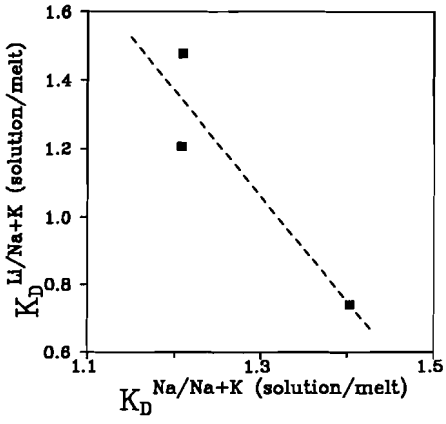

Figure 8.15. *Normalized distribution coefficients for Li vs. Na.*

inclusions is low compared to the total amount of solution present in the capsule.

The distribution coefficients. The distributions calculated on the basis of the measured glass composition and the calculated composition of the hydrothermal solution produce a good positive linear relation with initial fluorine content of the solution for Na (Fig. 8.10) and a less well, but still evidently positive linear relationship for Li (Fig. 8.13). For K (Fig. 8.11) the trend is less evident but a very low distribution coefficient is apparent. For Al (Fig. 8.12) a relation with $(mF^-)^3$ is assumed, on the basis of the considerations for trivalent ions, given in Chapter 6. The linear relations between the distribution coefficients and the fluorine molality for Na, K, Al and Li are calculated as

Table 8.5. *The distribution coefficients K_D, calculated from the values of Table 3. The K_D in the first and second row is defined as K_D(solution/melt) = ppm(reaction solution)/ppm(glass). In the first row the measured solution concentrations are used, while in the second row calculated solution concentrations are used, based on the final melt composition. In the third and fourth row the K_D is calculated on normalized values of Na, K, Al and Li, where all concentration values are divided by (Na+K) in molar quantities. The third row is based on the measured quantities, the fourth row on calculated fluid quantities.*

	Na	K	Al	Li	Zn	Pb	F
A31	0.031	0.004	0.009	-	-	-	0.106
	0.104	0.101	0.057	-	-	-	1.000
	1.376	0.189	0.393	-	-	-	-
	1.006	0.986	0.602	-	-	-	-
A33	0.069	0.013	0.003	0.160	0.025	0.023	-
	0.105	0.046	0.029	0.128	0.284	0.221	-
	1.335	0.256	0.053	3.043			
	1.210	0.534	0.307	1.478			
A34	0.008	0.003	0.002	0.070	0.012	0.000	-
	0.157	0.070	0.139	0.156	0.416	0.195	-
	1.227	0.504	0.332	10.86			
	1.209	0.541	1.076	1.205			
A34-2	-	-	-	-	-	-	-
	0.156	0.256	0.069	0.354	0.544	0.668	-
	-	-	-	-			
	0.845	1.393	0.373	1.923			
A32	0.050	0.029	0.030	-	-	-	0.125
	0.260	0.172	0.269	-	-	-	2.861
	1.167	0.663	0.701	-			
	1.126	0.745	1.163	-			
A35	0.018	0.011	0.023	0.110	0.073	0.000	-
	0.350	0.054	0.165	0.184	0.440	0.247	-
	1.142	0.725	1.454	7.071			
	1.403	0.217	0.660	0.740			

$$K_D^{Na} = 0.071 \times mF^- + 0.033 \quad (8.1),$$

$$K_D^{K} = 0.015 \times mF^- + 0.055 \quad (8.2),$$

$$K_D^{Al} = 0.003 \times (mF^-)^3 - 0.065 \quad (8.3),$$

and

$$K_D^{Li} = 0.019 \times mF^- + 0.114 \quad (8.4).$$

Run A34-2 has been omitted for all plots and calculations, because of the deviating concentration values for most elements. These relations are based on the initial fluorine concentrations of the hydrothermal solution, and will change if they are corrected for the actual fluorine content. The analyzed fluorine concentrations of the melt and calculated concentration of the solution of samples A31 and A32 (Table 8.4) suggests that the actual distribution coefficients may increase by a factor 2 after correction. A correction is not performed, as only few, highly variable microprobe analyses exist on the fluorine concentrations of the melt. The relatively high Na and Al distributions between solution and melt are reflected in the presence in the high fluorine runs of the quench phase chiolite, which is composed mainly of Na, Al and F. The formation of this phase is thus also responsible for the very low Na and F contents of the analyzed hydrothermal solution. If the normalized K_D of Na is plotted versus the normalized K_D of K (Fig. 8.14) and of Li (Fig. 8.15), a negative linear correlation is evident in both plots. The linear equations can be expressed as

$$K_D^{Li/(Na+K)} = -3.10 \times K_D^{Na/(Na+K)} + 5.09 \quad (8.5)$$

and

$$K_D^{K/(Na+K)} = -1.85 \times K_D^{Na/(Na+K)} + 2.80 \quad (8.6)$$

Probably the negative correlation of $K_D^{K/Na+K)}$ and $K_D^{Li/(Na+K)}$ with $K_D^{Na/(Na+K)}$ indicate that both K and Li substitute for Na. Correlations with Al are absent. The distribution coefficients for Zn and Pb exhibit no relation with fluorine concentration and are low, varying between 0.28 and 0.54 for Zn and between 0.19 and 0.25 for Pb. These values were obtained with the calculated solution composition. If it is assumed that Zn and Pb are not incorporated in quench phases, the K_D for these elements will be even lower (Table 8.5). Certainly part of the Zn and Pb will be absorbed by the capsule wall, as suggested in the previous chapters. Cu has disappeared almost completely from the glass and the solution (as also observed in the chlorine experiments), most probably also by absorbtion by the capsule wall.

The results from this study indicate, that fluorine is less effective in complexing than chlorine. Moreover, the high solubility of fluorine in the melt decreases the available concentration of complexing anions of the hydrothermal solution. As fluorine is strongly concentrated in residual, low-temperature melts, it will become important as complexing anion only during the late stages of crystallization of granitic magmas.

Conclusions

The distribution coefficients for Na, K, Al and Li between a fluorine bearing hydrothermal solution and a eutectic melt at 850°C and 5000 bars as a function of fluorine content are determined as: $K_D^{Na} = 0.071 \times mF^- + 0.033$; $K_D^{K} = 0.015 \times mF^- + 0.055$; $K_D^{Al} = 0.003 \times (mF^-)^3 - 0.065$; $K_D^{Li} = 0.019 \times mF^- + 0.114$.

The distribution coefficients for Zn and Pb exhibit no relation with fluorine concentration and vary between 0.28 and 0.44 for Zn, and 0.22 and 0.25 for Pb.

The distribution coefficients for Na, K and Li are low if compared to the chlorine experiments at 850°C and 5000 bars (Chapter 6), but Al partitioning in the solution is much higher.

The distributions for Zn and Pb are comparable to the 1 mCl^- experiments at 850°C and 5000 bars (Chapter 6).

Fluorine is less effective as a complexing anion than chlorine at the experimental conditions of this study, partly due to its high solubility in the silicate melt.

References

Bailey D. K. (1977) Fluorine in granitic rocks and melts: A review. Chem. Geol. **19,** 1-42.

Candela P. A. and Holland H. D. (1984) The partitioning of copper and molybdenum between silicate melts and aqueous fluids. Geochim. Cosmochim. Acta **48,** 373-380.

Flynn T. R. and Burnham C. W. (1978) An experimental determination of rare earth partition coefficients between a chloride containing vapour phase and silicate melts. Geochim. Cosmochim. Acta **42,** 685-701.

Hamilton D. L. and Henderson C. M. B. (1968) The preparation of silicate compositions by a gelling method. Mineral. Mag. **103,** 571-578.

Hards N. (1976) Distribution of elements between the fluid phase and silicate melt phase of granites and nepheline syenites. In: Third N.E.R.C. Progress Report, N.E.R.C. publ. ser. D no. 6, 88-91.

Kovalenko N. I. (1977) The reactions between granite and aqueous hydrofluoric acid in relation to the origin of fluorine-bearing granites. Geoch. Int. **14,** 108-118.

Manning D. A. C. (1981) The effect of fluorine on liquidus phase relationships in the system qz-ab-or with excess water at 1 kb. Contrib. Mineral. Petrol. **76,** 206-215.

Mysen B. O. and Virgo D. (1985) Structure and properties of fluorine-bearing aluminosilicate melts: the system Na2O-Al2O3-SiO_2-F at 1 atm. Contrib. Mineral. Petrol. **91,** 205-220.

Richardson C. K. and Holland H. D. (1979a) The stability of fluorite in hydrothermal solutions, an experimental study. Geochim. Cosmochim. Acta **43,** 1313-1325.

Richardson C. K. and Holland H. D. (1979b) Fluorite deposition in hydrothermal systems. Geochim. Cosmochim. Acta **43,** 1327-1335.

Webster J. D. (1990) Partitioning of F between H_2O and CO_2 fluids and topaz rhyolite melt - Implications for mineralizing magmatic-hydrothermal fluids in F-rich granitic systems. Contrib. Mineral. Petrol. **104,** 424-438.

Wyllie P. J. and Tuttle O. F. (1961) Experimental investigation of silicate systems containing two volatile components. Part II. The effects of NH_3 and HF, in addition to H2O on the melting temperatures of albite and granite. Amer. J. Sci. **259,** 128-143.

Appendix

The characterization of ammonium-phlogopite with XRD

A structure analysis of a synthetic ammonium-phlogopite, crystallized at 650°C and 2000 bars, was performed with a Philips X-ray generator, equipped with an Enraf Nonius Guinier camera. Cu-K_α radiation (λ = 1.54178Å) was used, with Si (JCPDS 27-1401) as an internal standard. The intensity differences on the photographic negative were recorded graphically with a densitometer. In Table A.1 the calculated d-spacings, (hkl)-values and I/I_0-ratios are presented. The ammonium-phlogopite was indexed on the basis of a 1M cell structure, with the resulting space group C2/m. Twelve reflections were used for computer calculations of the cell parameters with a least squares refinement program. The other observed reflections, which were not used in the computer calculations, were in good agreement with the computer calculations. In Table A.2 the calculated cell parameters are given. Various cell parameters are compared with those of the ammonium-phlogopite, synthesized by Eugster and Munoz (1966), and with other endmember phlogopites with a simple alkali substitution. In Figure A.1 the c-axes of the different endmember phlogopites are plotted versus the ionic radii of the alkali ions. The radii were taken for NH_4^+ from Pauling (1960) and for the other ions from Shannon and Prewitt (1969). In Figure A.2 the cell volume of the endmember phlogopites is plotted versus the cubed alkali ionic radius. Both figures are after Hazen and Wones (1972). The results of Beswick (1973) for Rb-phlogopite and of the NH_4-phlogopite of this study are added. The non-linear relationship has been explained as the result of increasing effective coordination number of the interlayer cation with increasing ionic radius (Hazen and Wones, 1972). Our NH_4-phlogopite has a larger cell volume than that of Eugster and Munoz (1966) and its position in Figures A.1 and A.2 fits the theoretical line very well.

References

Beswick A. E. (1973) An experimental study of alkali metal distributions in feldspars and micas. Geochim. Cosmochim. Acta **37,** 183-208.

Carman (1969) The study of the system $NaAlSiO_4$-Mg_2SiO_4-SiO_2-H_2O from 200 to 5000 bars and 800°C to 1100°C and its petrologic application. Ph.D.Thesis, Penn. State Univ., 290pp.

Eugster H. P. and Munoz J. L. (1966) Ammonium micas: possible sources of atmospheric ammonia and nitrogen. Science **151,** 683- 686.

Hazen R. M. and Wones D. R. (1972) The effect of cation substitutions on the physical properties of trioctahedral micas. Amer. Mineral. **57,** 103-129.

Pauling L. (1960) The nature of the chemical bond, and the structure of molecules and crystals: an introduction to modern structural chemistry. 3rd ed. Cornell University Press. 644p.

Shannon R. D. and Prewitt C. T. (1969) Effective ionic radii in oxides and fluorides. Acta Cryst. **B25,** 925-946.

Table A.1. *Calculated d-spacings, (hhl)-values and I/I_o-ratios of the ammonium-phlogopite. The values, used for the cell parameter calculation are denoted with an asterisk.*

d_{calc} (Å)	d_{meas} (Å)	(hkl)	I/I_o	d_{calc} (Å)	d_{meas} (Å)	(hkl)	I/I_o
10.30	*10.38	001	100	2.196	*2.190	133	18
5.15	5.24	002	62	2.190		202	
4.62	4.61	020	78	2.061	2.042	005	9
4.56	*4.56	110	78	2.021	2.018	204	9
4.43	*4.43	111	67	2.017		133	
3.70	*3.70	112	54	1.744	1.739	311	7
3.439	*3.43	022	58	1.742		150	
3.434		003		1.742		241	
3.187	3.18	112	37	1.703	*1.696	242	7
2.966	2.96	113	27	1.702		151	
2.656	*2.65	130	22	1.702		135	
2.655		201		1.698		204	
2.627	*2.62	131	54	1.539	1.533	060	32
2.624		200		1.538		331	
2.576	2.580	004	19	1.537		045	
2.565		113		1.533		116	
2.521	*2.514	202	26	1.522	1.518	061	16
2.519		131		1.522		332	
2.449	*2.443	132	49	1.426	1.431	225	12
2.444		201		1.405	1.416	334	12
2.309	*2.305	040	11	1.405		063	
2.302		221					
2.284	2.276	203	13				
2.281		220					
2.281		132					

Table A.2. *Cell parameters for the synthetic ammonium-phlogopite A37 and a comparison with the ammonium-phlogopite, synthesized by Eugster and Munoz (1966), and with other synthetic endmember phlogopites.*

	This work	1	2	3	4	5	6
a_o (Å)	5.329±0.003	5.311	5.265	5.315	5.34	5.34	5.37
b_o (Å)	9.236±0.006	9.224	9.203	9.204	9.24	9.24	9.30
c_o (Å)	10.460±0.007	10.443	9.994	10.311	10.48	10.49	10.83
ß	99°939'	99°42	97°45	99°54	99°54	99°76	99°54
V (Å^3)	507.079±0.337	504.2	479.8	497.0	510.0	511.0	532.8
ρ (g/cc)	2.595	2.61	2.78	2.79	3.02	-*)	3.18

1: NH_4-phlogopite — Eugster and Munoz (1966)
2: Na-phlogopite — Carman (1969)
3: K-phlogopite — Hazen and Wones (1972)
4: Rb-phlogopite — ib.
5: Rb-phlogopite — Beswick (1973)
6: Cs-phlogopite — Hazen and Wones (1972)
*) calculated density not published

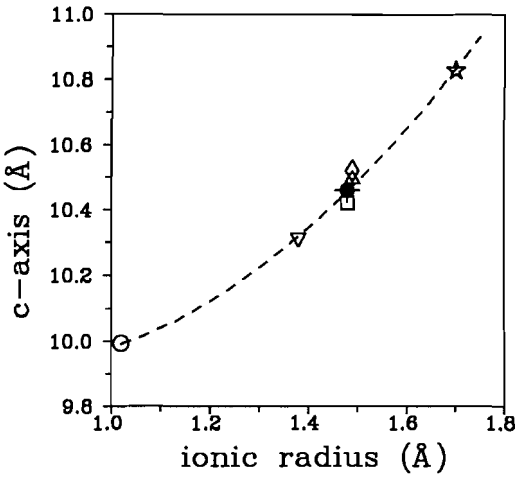

Figure A.1. *The c-axis of different endmember phlogopites vs. the ionic radius of the alkali ion. The symbols in the figure are for this work: filled circle; Carman (1969): circle (Na); Hazen and Wones (1972): down-pointed triangle (K), triangle (Rb) and star (Cs); Eugster and Munoz (1966): square (NH_4); Beswick (1973): diamond (Rb).*

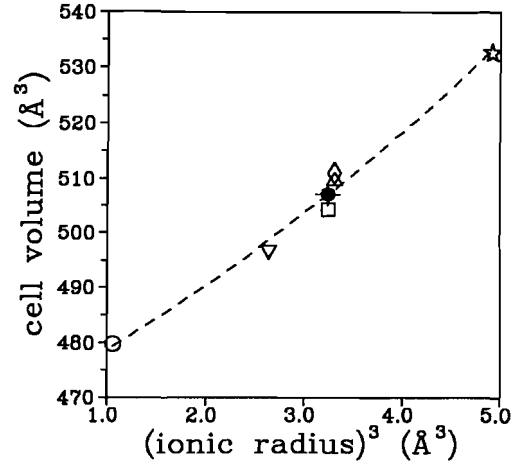

Figure A.2. *The cell volume of the different endmember phlogopites plotted vs. the cubed alkali ionic radius. The symbols are identical to the symbols used in Figure 1.*

Curriculum Vitae

Ariejan Bos werd op 2 juli 1953 geboren te Nijmegen. In 1972 behaalde hij het diploma Gymnasium β aan het Stedelijk Gymnasium te Leeuwarden. Tussen 1972 en 1975 studeerde hij Biologie aan de Rijksuniversiteit van Groningen. Vanaf mei 1975 tot september 1976 werd de dienstplicht vervuld, waarna in Utrecht een aanvang werd gemaakt met de studie Geologie aan de Rijksuniversiteit te Utrecht. In april 1980 werd hierin het kandidaatsexamen afgelegd in de richting G3. Het doctoraal examen Petrologie, met bijvakken Geochronologie en Experimentele Petrologie, werd cum laude afgelegd in april 1984. Van juni 1984 tot maart 1988 was hij in dienst van de Rijksuniversiteit Utrecht als wetenschappelijk assistent binnen de vakgroep Petrologie, Mineralogie, Kristallografie, Geochemie en Bodemkunde. Gedurende deze periode werd in het Hoge Druk en Temperatuur (HPT) Laboratorium het promotieonderzoek uitgevoerd. Vanaf maart 1988 is hij in dienst van de Stichting Energieonderzoek Centrum Nederland (ECN) te Petten. Als medewerker van de unit Materialen is hij werkzaam binnen het Centrum voor Keramiek en Katalysator Onderzoek, dat is gevestigd aan de Universiteit Twente binnen de vakgroep Anorganische Chemie, Materiaalkunde en Katalyse van de afdeling Chemische Technologie.